ADDIS ABABA UNIVERSITY
SCHOOL OF GRADUATE STUDIES
FACULTY OF TECHNOLGY
ELECTRICAL AND COMPUTERENGINEERING
DEPARTMENT

INVESTIGATION OF PERFORMANCE OF DIFFERENT KINDS OF DUAL BAND PATCH ANTENNAS FOR MOBILE PHONES

By
ESUBALLEW ABAYNEH

A thesis submitted to the school of Graduate Studies of Addis Ababa University
in partial fulfillment of the requirements for the degree of
Masters of Science
In
Electrical Engineering
Date: March 16, 2007
Addis Ababa, Ethiopia

ADDIS ABABA UNIVERSITY
SCHOOL OF GRADUATE STUDIES
FACULTY OF TECHNOLGY
ELECTRICAL AND COMPUTERENGINEERING
DEPARTMENT

INVESTIGATION OF PERFORMANCE OF DIFFERENT KINDS OF DUAL BAND PATCH ANTENNAS FOR MOBILE PHONES

By
ESUBALLEW ABAYNEH

ADVISOR
Prof. Woldeghiorgis Woldemariam

ADDIS ABABA UNIVERSITY
SCHOOL OF GRADUATE STUDIES
FACULTY OF TECHNOLGY
ELECTRICAL AND COMPUTER ENGINEERING
DEPARTMENT

INVESTIGATION OF PERFORMANCE OF DIFFERENT KINDS OF DUAL BAND PATCH ANTENNAS FOR MOBILE PHONES

BY
ESUBALLEW ABAYNEH

Approval by Board of Examiners:

Dr. Getachew Biru	_____
Chairman Dept. of Graduation Committee	Signature
Prof.Woldeghiorgis Woldemariam	_____
Advisor	Signature
_____	_____
Internal Examiner	Signature
_____	_____
External Examiner	Signature

Declaration

I, the undersigned, declare that this thesis is my original work, has not been presented for a degree in any other university and that all sources of material used for the thesis have been duly acknowledged.

Name : _____

Signature : _____

Place : _____Addis Ababa_____

Date : _____

This thesis has been submitted for examination with my approval as the university advisor.

Name : _____

Signature : _____

Place : _____Addis Ababa_____

Date : _____

ACKNOWLEDGEMENTS

I would like to thank my father and mother and all my families for their unreserved help they made to me. I am grateful to my sister, Meseret Abayneh, who managed my life.

I would like to thank Prof. Woldeghiorgis Woldemariam, my advisor, for his encouragement, patience, fast response, best effort and valuable discussion. It has been a privilege to work on the thesis under his supervision.

I am indebted to Dr:-Ing. Mohammed Abdo for sharing me his depth in microstrip patch antenna knowledge, his priceless assistance on analyzing the simulation results, creating conducive environment around the lab room and his generous treatment.

Thank you all for helping me achieve one of the major goals in my life.

TABLE OF CONTENTS

Acknowledgements……i

Table of contents……..ii

List of Tables……...iv

List of Figures……..iv

List of Symbols and Abbreviations for Wireless Communication system frequencies……v

Abstract……vi

CHAPTER 1

OVERVIEW OF MICROSTRIP PATCH ANTENNAS……1

1.1 Introduction……..…….1

1.2 Aim of Thesis……3

1.3 General Structure of Microstrip Patch Antennas……..3

1.4 Feed Techniques……..…….……4

1.4.1 Microstrip (Offset Microstrip) Line Feed1.3.2 Coaxial Feed……..5

1.4.2 Coaxial Feed……6

1.4.3 Aperture Coupled Feed……7

1.4.4 Proximity Coupled Feed……..8

1.5 Advantages and Disadvantages of Microstrip Patch Antennas……9

CHAPTER 2

NUMERIAL ANALYSIS OF MICROSTRIP PATCH ANTENNAS AND PERFORMANCES……. 11

2.1 General Description……..……..11

2.2 Models of Microstrip Patch Antenna……..……....14

A. Transmission Line Model……..14

B. Cavity Model……..15

C. Full-Wave Solutions-Method of Moment..……19

2.3 Performance Parameters of Microstrip Patch Antennas……..……..…….22

CHAPTER 3

DUAL BAND PATCH ANTENNA STRUCTURES ……..…… 32

3.1 General Features of Mobile Communication…….…….. 32
3.2 Types Dual Band Patch Antenna Structures…….…….....34
3.3 Design Considerations …….....36
CHAPTER 4
PERFORMANCE OF TRANSMITTER-RECEIVER
CELLULAR ANTENNAS……...43
4.1 Overview…….…..…...43
4.2 Simulations and Results……..……45
A. Single Input (Feed) Circular Disc Patch Antenna……..46
B. Two Input Stacked Discs……49
C. Stacked Rings…….……52
D. Planar Dual Band Patch Antenna…….....56
E. Aperture Coupled Microstrip Antenna Loaded With Two Slots…….…...59
F. Shorting Pins Loaded Patch Antenna….……62
G. Stub Loaded Patch Antenna……...65
H. Probe Fed Slot Loaded Microstrip Patch Antenna……..……...68
I. Notch Loaded Patch Antenna……..……...…….……71
J. Patches Loaded With Adjustable Air Gaps……..…….……..……74
4.3 Discussion.…….…….…77
CHAPTER 5
CONCLUSIONS AND FUTURE WORKS …….……..80
5.1 Conclusions and Recommendations…….……....80
5.2 Recommendations for Future Works……..……..82
References…….…….……...83

LIST OF TABLES

1.1 Summary of key features of microstrip patch antennas……9
3.1 Classification of patch antennas……..34

LIST OF FIGURES

1.1 Structure of microstrip patch antenna……...3
1.2 Common shapes of microstrip patch antennas……..4
1.3 Microstrip line feed and offset microstrip feed…...……..5
1.4 Probe feed of microstrip patch……..6
1.5 Aperture-coupled feed of microstrip antenna……...7
1.6 Proximity coupled feed…….……8
2.1 The three in homogeneities of microstrip patch antenna…….11
2.2 Geometries of microstrip patch antenna……..12
2.3 Transmission line of model of microstrip antenna……..14
2.4 Geometry of cavity model……...16
2.5 Field configurations and current densities for microstrip patch antenna……19
2.6 Example of Yee cell with field calculations……21
2.7 Radiation from an antenna……...23
2.8 Radiation pattern of a generic directional antenna……..25
3.1 General structure of mobile phone……..32
3.2 Dual band antenna structure……33
3.3 Classification of dual band patch antennas…….35
3.4 Flow chart based on the usual design procedure for rectangular and circular Patch antennas…….38
4.1 The different views of integrated mobile phone……..44
4.2 – 4.11 Figures of simulation results…….……..46-77
4.12 Standard monoblock and rectangular forms of mobile phone……..78
4.13 Returnloss graph for standard monoblock form and rectangular form…….78

List of symbols and abbreviations for wireless communication system frequencies.

Advanced Mobile Phone Service (AMPS)	Tx: 824–849MHz Rx: 869–894MHz	70 MHz (8.1 %)
Global System for Mobile Communications (GSM900)	Tx: 890–915MHz Rx: 925–960MHz	80MHz (8.7 %)
Personal Communications Service (PCS)	Tx: 1710–1785MHz Rx: 1805–1880MHz	170MHz (9.5 %)
GSM1800 (Digital Communication Systems, DCS)	Tx: 1850–1910MHz Rx: 1930–1990MHz	140MHz (7.3 %)
Wideband Code Division Multiple Access (WCDMA)	Tx: 1920–1980MHz Rx: 2110–2170MHz	250MHz (12.2 %)
Universal Mobile Telecommunication Systems (UMTS)	Tx: 1920–1980MHz Rx: 2110–2170MHz	250MHz (10.2 %)
IMT2000 (International Mobile Telecommunications	1885 – 2200 MHz	315MHz (15.5%)
Bluetooth	2400 – 2500MHz	100MHZ (100%)
Ultra-wideband (UWB) for Communications and measurement	3100–10 600MHz EIRP: <–41.3 dBm	7500MHz (109 %)

ABSTRACT

Mobile communications handsets with internal antennas become more popular every day. These integrated antennas must be designed to fit into a small volume, with an arbitrary shape. Indeed, the design of modern handsets is mostly fashion-oriented, and the antennas must be adapted to these requisites, without detriment to their matching or radiating performance [12]. The present study focuses on how a change in some of the antenna geometric parameters, such as its height, may affect its actual performance.

Dual band antennas are defined as:" Antennas that are useful in situations where the antenna is required to operate in two distinct frequencies which may be too far apart for a single antenna to perform efficiently at both frequencies. [8] In this thesis work different dual band patch antennas for mobile phones are designed, simulated (using the EMPIRE software) and the performance of which is compared based on the standard performance measures.

The antenna put into consideration is said to be dual band if it operates on any two of the bands: GSM, DCS, PCS, IMT2000 and Bluetooth bands. A total of 10 patch antenna types: 5 from multiresonator and 5 from reactively loaded patch antennas are considered. Of these the pins loaded patch antenna and a patch loaded with adjustable air gap have better performance as they are closer to the regulatory performance measurement standards compared to the rest. For pins loaded patch antenna the BW is 4.94% around GSM1800 ($f_c = 1800MHz$), 3.04% around IMT ($f_c = 2170MHz$) and 4.08% around Bluetooth ($f_c = 2450MHz$). For the patch loaded with adjustable air gap the BW is 10% around GSM900 ($f_c = 900MHz$) and 2.33% around GSM1800 (DCS) ($f_c = 1800MHz$). In both cases the BW is measured for $S_{11} \leq -9dB$ which is the regulatory standard for measuring impedance bandwidth. As these two antenna structures are closer to the regulatory standards of antenna performance measurement, they are suitable for dual band mobile communication handsets except that in the former case the shorting pins complicate the fabrication process.

CHAPTER 1 OVERVIEW OF MICROSTRIP PATCH ANTENNAS

1.1 Introduction

This chapter highlights the importance of microstrip patch antennas to the present day communication world. After defining the aim of this thesis, chapter one closes with an overview of the thesis.

Importance

Communication can be broadly defined as the transfer of information from one point to another. A communication system is usually required when the information is to be conveyed over a distance. The transfer of information within the communication system is commonly achieved by superimposing or modulating the information onto an electromagnetic wave which acts as a carrier for the information signal. At the required destination, the modulated carrier is then received and the original information signal can be recovered by demodulation. Over the years, sophisticated techniques have been developed for this process using electromagnetic carrier waves operating at radio frequencies as well as microwave and millimeter wave frequencies.

In today's modern communication industry, antennas are the most important components required to create a communication link. Through the years, microstrip antenna structures are the most common option used to realize millimeter wave monolithic integrated circuits for microwave, radar and communication purposes. Due to its many advantages over the conventional antenna, the microstrip antenna have achieved importance and generated interest to antenna designers for many years. In fact, active microstrip antenna arrays and active apertures are increasingly present in phased-array radar applications. In addition, these devices also serve as potentially efficient power combiners. Hence, active microstrip antennas arrays are often used in spatial or "quasi-optical" combining schemes for creating high-power and high frequency components. Furthermore, microstrip antennas are often used in military aircraft, missiles, rockets and satellite [42].

Aim of Thesis

The aim of this thesis is to investigate performance of different dual band patch antennas for mobile phones. The performance comparison is based on radiation pattern, directivity, gain, bandwidth, returnloss between standard dual band patch antennas: multiresonator (aperture coupled, two input stacked discs, single input stacked discs, stacked rings, planar dual band) patch antennas and reactively loaded (shorting pins loadede, stub loaded,probe slot loaded, notch loaded adjustable air gap loaded) patch antennas.

Outline of Thesis

Chapter 1 begins with the importance of microstrip patch antennas to the communications industry. Both the significance and the applications of microstrip antennas are given. Moreover, the general structure, feeding techniques, and advantages and disadvantages of microstrip patch antennas including aim of the thesis is also discussed.

Chapter 2 will review numerical analysis of microstrip patch antennas. Along with the general description of microstrip patch antennas this chapter briefly discusses models of microstrip patch antennas: Transmission line model, Cavity model, Full-wave solutions (Method of Moments). It also indetail discusses about the performance measures of patch antennas.

Chapter 3 in detail discusses on the structure of dual band patch antennas for mobile phones. The basic outlines of the classifications of dual band patch antennas for mobile phones (multiresonator antennas and reactively loaded antennas) will be stated. Here design considerations using the essential parameters along with flow charts for dual band patch antennas will be discussed [39].

Chapter 4 will cover performance of transmitter-receiver cellular antennas. On the simulations and results part, for each antenna simulated, this chapter in detail discusses about directivity, radiation pattern, gain, input impedance band width,

return loss.Then performance comparison of the different dual band microstrip patch antennas will be given.

Chapter 5 concludes this thesis with a discussion results obtained for the transmitter-receiver cellular antennas and the future prospects for dual band microstrip patch antennas for mobile phones.

1.2 General Structure of Microstrip Patch Antennas

In its most basic form, a microstrip patch antenna consists of a radiating patch on one side of a dielectric substrate which has a ground plane on the other side as shown in Figure 1.1. The patch is generally made of conducting material such as copper or gold and can take any possible shape. The radiating patch and the feed lines are usually photo etched on the dielectric substrate.

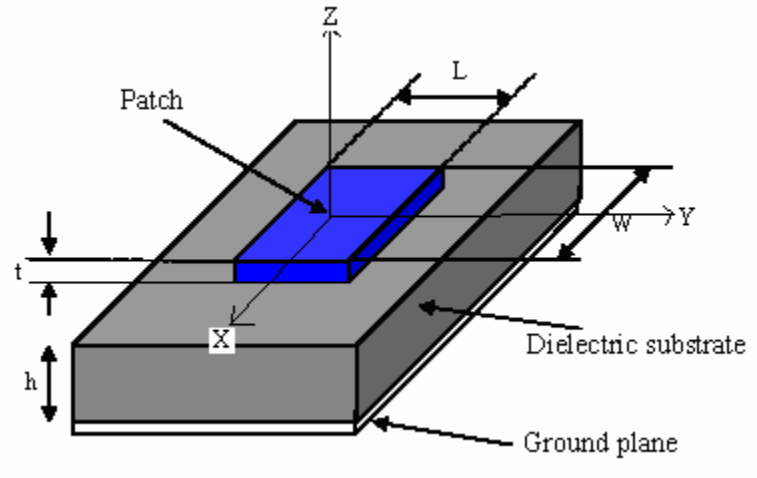

Figure 1.1 Structure of a Microstrip Patch Antenna

In order to simplify analysis and performance prediction, the patch is generally square, rectangular, circular, triangular, and elliptical or some other common shape as shown in figure 1.2. For a rectangular patch, the length L of the patch is usually in the range of: $0.3333\lambda_0 < L < 0.5\lambda_0$, where λ_0 is the free-space wavelength. The patch is selected to be very thin such that t << λ_0 (where *t* is the patch thickness). The

height h of the dielectric substrate is usually $0.003\lambda_0 \leq h \leq 0.05\lambda_0$. The dielectric constant of the substrate (ε_r) is typically in the range $2.2 \leq \varepsilon_r \leq 12$.[1]

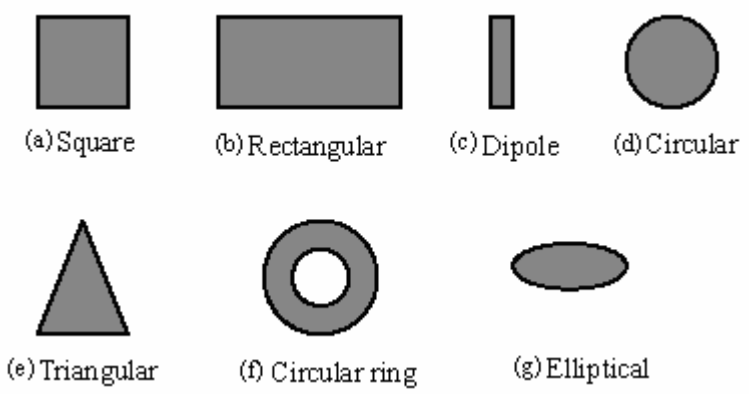

Figure 1.2 Common shapes of microstrip patch elements [1].

Microstrip patch antennas radiate primarily because of the fringing fields between the patch edge and the ground plane. For good antenna performance, a thick dielectric substrate having a low dielectric constant is desirable since this provides better efficiency, larger bandwidth and better radiation [1]. However, such a configuration leads to a larger antenna size. In order to design a compact microstrip patch antenna, higher dielectric constants must be used which are less efficient and result in narrower bandwidth. Hence a compromise must be reached between antenna dimensions and antenna performance.

Keeping in mind the above general structure of microstrip patch antennas the next thing to be discussed is about the feed techniques.

1.3 Feed Techniques

Microstrip patch antennas can be fed by a variety of methods. These methods can be classified into two categories: contacting and non-contacting. In the contacting method, the RF power is fed directly to the radiating patch using a connecting element such as a microstrip line. In the non-contacting scheme, electromagnetic field coupling is done to transfer power between the microstrip line and the radiating patch

[1]. The four most popular feed techniques used are the microstrip line, coaxial probe (both contacting schemes), aperture coupling and proximity coupling (both non-contacting schemes).

1.3.1 Microstrip (Offset Microstrip) Line Feed

In this type of feed technique, a conducting strip is connected directly to the edge of the microstrip patch as shown in figure 1.3. The conducting strip is smaller in width as compared to the patch and this kind of feed arrangement has the advantage that the feed can be etched on the same substrate to provide a planar structure.

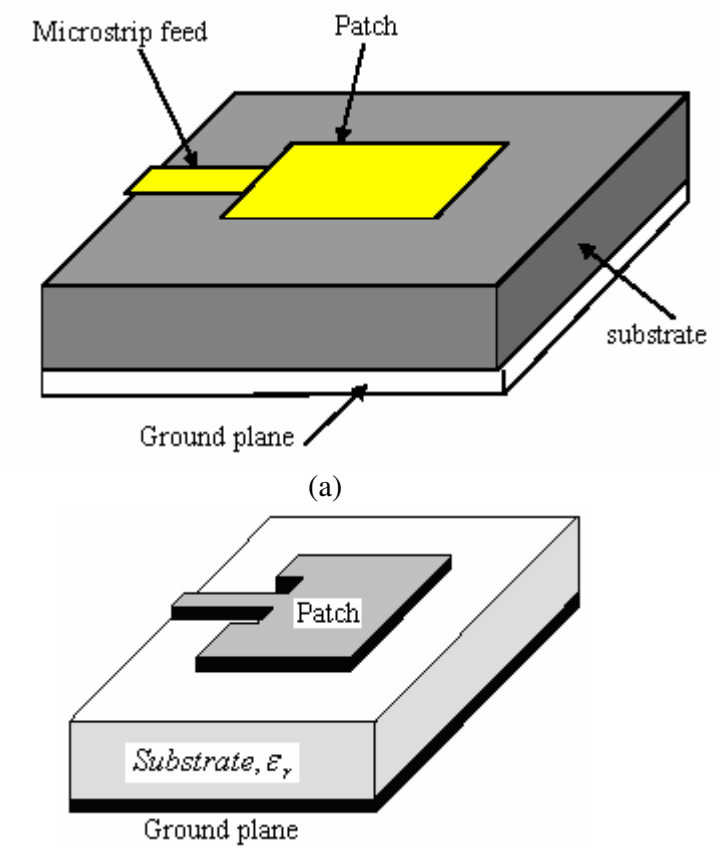

Figure 1.3 (a) Microstrip line feed (b) Offset microstrip line feed

The purpose of the inset cut, as in fig 1.3b, in the patch is to match the impedance of the feed line to the patch without the need for any additional matching element. This is achieved by properly controlling the inset position. Hence this is an easy feeding

scheme, since it provides ease of fabrication and simplicity in modeling as well as impedance matching. However as the thickness of the dielectric substrate being used, increases, surface waves and spurious feed radiation also increases, which hampers the bandwidth of the antenna [1]. The feed radiation also leads to undesired cross-polarized radiation.

1.3.2 Coaxial Feed

The Coaxial feed or probe feed is a very common technique used for feeding microstrip patch antennas. As seen from figure 1.4, the inner conductor of the coaxial connector extends through the dielectric and is soldered to the radiating patch, while the outer conductor is connected to the ground plane.

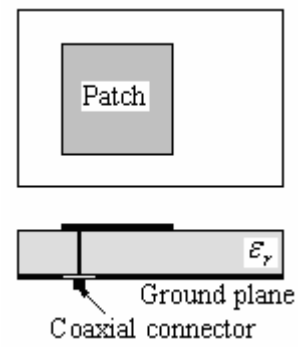

Figure 1.4 Probe Feed of a Microstrip Patch

The main advantage of this type of feeding scheme is that the feed can be placed at any desired location inside the patch in order to match with its input impedance. This feed method is easy to fabricate and has low spurious radiation. However, its major disadvantage is that it provides narrow bandwidth and is difficult to model since a hole has to be drilled in the substrate and the connector protrudes outside the ground plane, thus not making it completely planar for thick substrates ($h > 0.02\lambda_0$). Also, for thicker substrates, the increased probe length makes the input impedance more inductive, leading to matching problems [3]. It is seen above that for a thick dielectric substrate, which provides broad bandwidth, the microstrip line feed and the coaxial feed suffer from numerous disadvantages such as spurious feed radiation and

matching problem. The non-contacting feed techniques which have been discussed below, solve these problems.

1.3.3 Aperture Coupled Feed

Figure 1.5 shows the geometry of the basic aperture coupled patch antenna. The radiating microstrip patch element is etched on the top of the antenna substrate, and the microstrip feed line is etched on the bottom of the feed substrate. The thickness and dielectric constants of these two substrates may thus be chosen independently to optimize the distinct electrical functions of radiation and circuitry. Although the original prototype antenna used a circular coupling aperture, it was quickly realized that the use of a rectangular slot would improve the coupling, for a given aperture area, due to its increased magnetic polarizability [4].

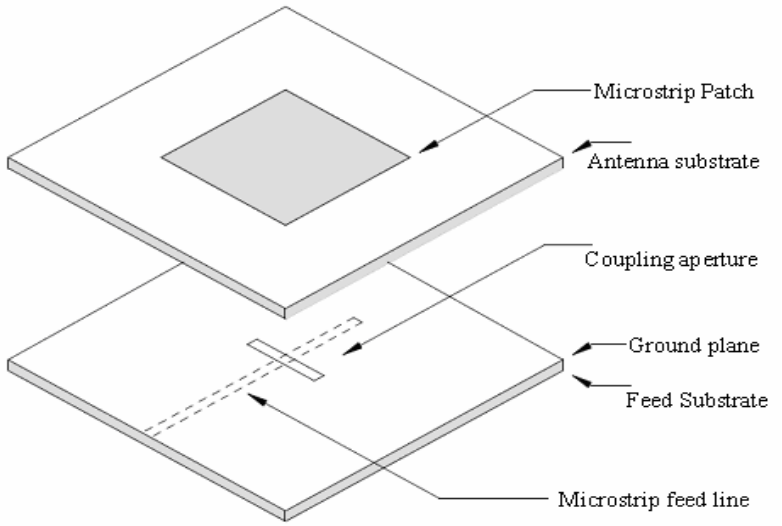

Figure 1.5 Aperture-coupled feed of a microstrip antenna

Most aperture coupled microstrip antennas now use rectangular slots, or variations thereof. The aperture coupled microstrip antenna involves over a dozen material and dimensional parameters that determine its performance are: substrate dielectric constant, substrate thickness, microstrip patch length, microstrip patch width, feed substrate dielectric constant, feed substrate thickness, slot length, slot width, feed line

width, feed line position relative to slot, position of the patch relative to the slot and length of tuning stub. The major disadvantage of this feed technique is that it is difficult to fabricate due to multiple layers, which also increases the antenna thickness. This feeding scheme also provides narrow bandwidth.

1.3.4 Proximity Coupled Feed

This type of feed technique is also called as the electromagnetic coupling scheme. As shown in figure 1.6, two dielectric substrates are used such that the feed line is between the two substrates and the radiating patch is on top of the upper substrate. The main advantage of this feed technique is that it eliminates spurious feed radiation and provides very high bandwidth (as high as 13%) [1], due to overall increase in the thickness of the microstrip patch antenna. This scheme also provides choices between two different dielectric media, one for the patch and one for the feed line to optimize the individual performances.

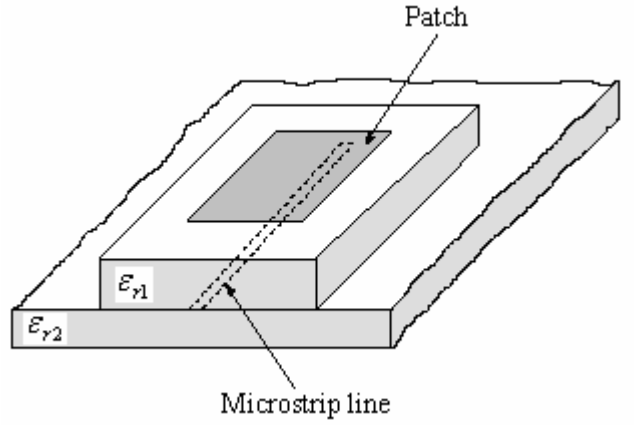

Figure 1.6 Proximity-coupled feed

Matching can be achieved by controlling the length of the feed line and the width-to-line ratio of the patch. The major disadvantage of this feed scheme is that it is difficult to fabricate because of the two dielectric layers that need proper alignment. Also, there is an increase in the overall thickness of the antenna. Comparison among these different feed techniques is shown in the table below.

Table 1.1 Summary of key features of a microstrip antenna [6]

Characteristics	Microstrip Line Feed	Coaxial Feed	Aperture coupled Feed	Proximity coupled Feed
Spurious feed radiation	More	More	Less	Minimum
Reliability	Better	Poor due to soldering	Good	Good
Ease of Fabrication	Easy	Soldering and drilling needed	Alignment Required	Alignment Required
Impedance Matching	Easy	Easy	Easy	Easy
Bandwidth (achieved with impedance matching)	2 – 5%	2-5%	2-5%	13%

The general structure along with the feed techniques give us full information about what microstrip patch antennas are. Compared to other types of antennas what are the advantages and the disadvantages of microsrtrip patch antennas?

1.4 Advantages and Disadvantages of Microstrip Patch Antennas

Microstrip patch antennas are increasing in popularity for use in wireless applications due to their low-profile structure. Therefore they are extremely compatible for embedded antennas in handheld wireless devices such as cellular phones, pagers etc. The telemetry and communication antennas on missiles need to be thin and conformal and are often microstrip patch antennas. Another area where they have been used successfully is in satellite communication. Some of their principal advantages discussed by [1] and Kumar and Ray [3] are given below:

- Light weight and low volume.
- Low profile planar configuration which can be easily made conformal to host surfaces.
- Low fabrication cost, hence can be manufactured in large quantities.
- Supports both, linear as well as circular polarization.
- Can be easily integrated with microwave integrated circuits (MICs).
- Capable of dual and triple frequency operations.
- Mechanically robust when mounted on rigid surfaces.

Microstrip patch antennas suffer from a number of disadvantages as compared to conventional antennas. Some of their major disadvantages discussed by [3] and Garg et al [5] are given below:

- Narrow bandwidth
- Low efficiency
- Low Gain
- Extraneous radiation from feeds and junctions
- Poor end fire radiator except tapered slot antennas
- Low power handling capacity.
- Surface wave excitation

Microstrip patch antennas have a very high antenna quality factor (Q). Q represents the losses associated with the antenna and a large Q leads to narrow bandwidth and low efficiency. Increasing the thickness of the dielectric substrate can reduce Q. But as the thickness increases, an increasing fraction of the total power delivered by the source goes into a surface wave. This surface wave contribution can be counted as an unwanted power loss since it is ultimately scattered at the dielectric bends and causes degradation of the antenna characteristics. However, surface waves can be minimized by use of photonic band gap structures as discussed by Qian et al [7]. Other problems such as lower gain and lower power handling capacity can be overcome by using an array configuration for the elements.

In addition to what we have seen above about microstrip patch antennas they must also be analyzed numerically, which will be discussed on the next chapter.

CHAPTER 2 NUMERICAL ANALYSIS OF MICROSTRIP PATCH ANTENNAS AND PERFORMANCES

2.1 General Description

Microstrip patch antennas are thin and lightweight radiating elements, formed by a substrate, including one or several dielectric layers, backed by a metallic sheet (the ground plane). Thin metallic patches (the radiating elements) are located on air-substrate interface and, possibly, between the dielectric layers. Microstrip antennas are manufactured by the photolithographic process developed for printed circuits. Their low profile low weight and mechanical ruggedness make them an ideal choice for aerospace applications. They can be mass-produced, and could thus provide inexpensive receiver antennas for direct reception of microwave signals from satellites (television, mobile communications). Finally, they are ideally suited to be combined in large arrays, the individual patches sharing the same substrate. Thus directive antennas can be obtained in spite of the inherent low directivity of a single patch. The remarkable practical advantages offered by microstrip antennas are offset, to some extent, by their inhomogeneous nature, and a rigorous analysis was long considered to be a hopeless task. An accurate model should take into account the three inhomogeneities of a microstrip structure:

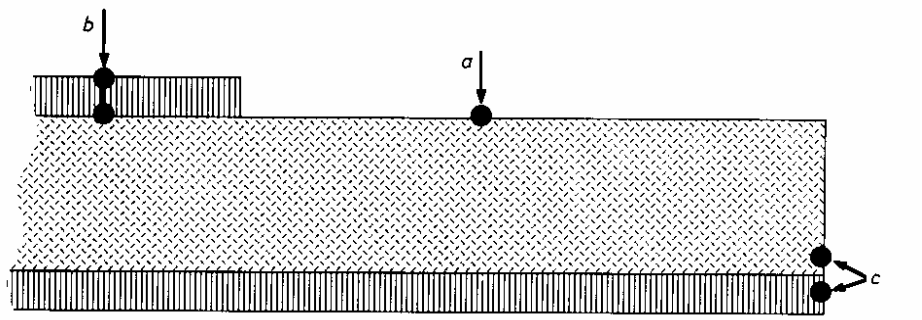

Figure 2.1 The three inhomogeneities of a microstrip structure: (a) dielectric media of unequal permittivity, (b) infinitely thin conductors introducing surface current between the dielectric media, (c) finite transverse dimensions of substrate and ground plane.

(a) The presence of at least two dielectrics (often air and substrate)

(b) The boundary conditions on the interfaces between different layers are inhomogeneous since thin metallic plates making up the radiating elements and feeding the structure can partially fill the interfaces.

(c) Any microstrip structure is finite in dimensions; i.e. its ground plane and its dielectric substrate are bounded in the transverse directions. The edges may, however, be located at a very large distance, in which case this third inhomogeneity may be neglected (the structure is then assumed, mathematically, to extend to infinity).

Models used to study microstrip patch antennas range from very simplified ones, such as the transmission-line model, through cavity models, planar circuit analysis, segmentation techniques, and up to quite sophisticated approaches based on an integral-equation formulation. In the framework of the integral-equation model, many different approaches exist, depending on the use of spectral or space quantities and on the geometries to be included. [9].

Geometry of a Rectangular Microstrip Patch Antenna

The radiating patch of a microstrip antenna can be shaped in a variety of configurations including rectangular, circular, elliptical and triangular. The example presented in this chapter deals with a rectangular patch antenna. Figure 2.2 depicts the geometry of a rectangular microstrip patch antenna.

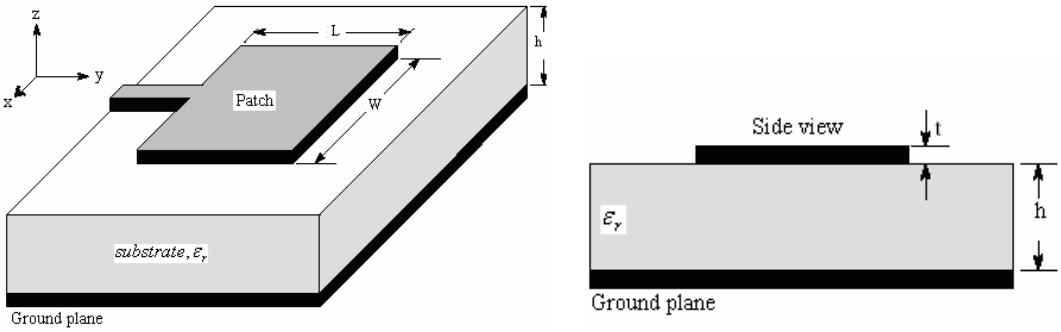

Figure 2.2 Geometry of microstrip patch antenna (not to scale)

It is seen that a microstrip antenna is made up of a metallic patch and feed line that are offset from a ground plane by a dielectric substrate material. In order to eliminate the occurrence of surface waves, the thickness of the dielectric substrate is usually kept to a small fraction of a wavelength ($0.003\lambda_0 \leq h \leq 0.05\lambda_0$). Surface waves degrade the performance of a microstrip antenna in two ways. First, they reduce the total power that is available for direct radiation, which reduces the efficiency of the antenna. Second, surface waves adversely affect the pattern and polarization characteristics of the antenna since they are scattered at surface discontinuities, namely at the edges of the substrate and ground plane. The dielectric constant of the substrate usually falls in the range of $2.2 \leq \varepsilon_r \leq 12$. This is indicative of the trade-off that exists between antenna efficiency and element size. Substrate materials with lower dielectric constants are typically low loss, which results in higher antenna efficiency. Substrates with higher dielectric constants allow size reduction of the element at the expense of antenna efficiency (due to increased losses) [1].

Photo etching is commonly used to deposit the patch and feed line on the substrate, so the thickness of the metallization is very small ($t << \lambda_0$ where λ_0 is a wavelength in free space). The length of the metallic patch, L, is selected so that the antenna resonates at a particular operating frequency ($\lambda_0/3 \leq L \leq \lambda_0/2$). As we shall see in the next section, the length of the metallic patch needs to be tuned to account for the fringing fields at the edges of the patch. Finally, the width of the patch, W, is used to adjust the input impedance of the antenna [1].

The patch element shown in figure 2.2 uses a microstrip line feed. This is one of a number of feed arrangements that can be used with microstrip antennas. Some of the most popular feed techniques are stated in *section 1.3*. Once we have defined the geometry of a rectangular microstrip patch antenna we discuss the analytical methods used to model and characterize the antenna. In the next section, three techniques will be reviewed: the transmission-line method, the cavity model, and numerical techniques.

2.2 Models Of Microstrip Patch Antenna

A. Transmission Line Model

The transmission-line model is the simplest of the three techniques we will consider and, as a result, is the least accurate. The microstrip antenna is modeled as two radiating slots that are separated by a distance L_{eff} .

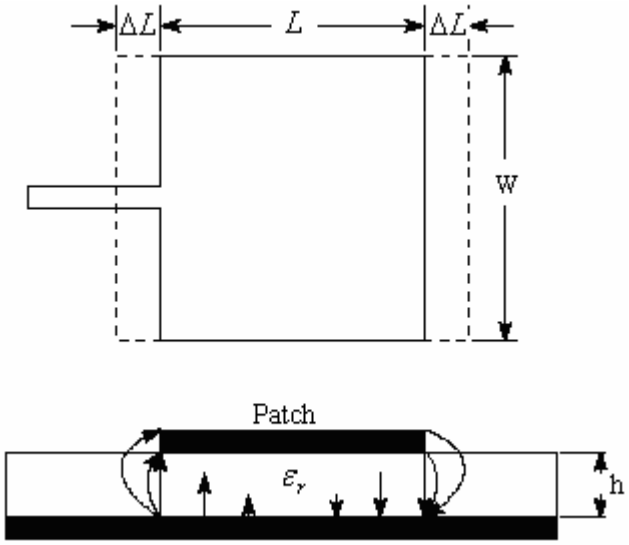

Figure 2.3 Transmission line model of microstrip antenna [1]

Referring to Figure 2.3, we can see the physical meaning of L_{eff} . It is essentially the length of the patch, L , plus an additional distance, $2\Delta L$, to account for the fact that the patch looks electrically wider due to the fringing fields. Balanis [1] provides the following formula for the added distance

$$\Delta L = 0.412h\frac{\left(\varepsilon_{reff}+0.3\right)\left(\frac{W}{h}+0.264\right)}{\left(\varepsilon_{reff}-0.258\right)\left(\frac{W}{h}+0.8\right)} \qquad (2\text{-}1)$$

In the above equation, ε_{reff} is the effective dielectric constant of a microstrip transmission line given by [2]

$$\varepsilon_{reff} = \frac{\varepsilon_r + 1}{2} \frac{\varepsilon_r - 1}{2} \left(1 + 12 \frac{h}{W} \right)^{-1/2} \tag{2-2}$$

Thus, the effective distance separating the two radiating slots becomes

$$L_{eff} = L + 2\Delta L \tag{2-3}$$

Finally, Balanis [1] uses this adjusted length to calculate the resonant frequency of the antenna

$$(f_r)_{010} = \frac{c}{2L_{eff}\sqrt{\varepsilon_{reff}}} \tag{2-4}$$

where c is the speed of light in a vacuum. Since the transmission-line model accounts for the fringing effects at the edges of the patch, it provides a good characterization of the resonant frequency. It also models the input impedance of the antenna fairly accurately. However, it does not account for the affects of a truncated dielectric substrate or a finite ground plane nor does it provide insight into the radiation patterns of the antenna. Additionally, the model breaks down as the height of the dielectric substrate, h, becomes a significant portion of a wavelength.

B. Cavity Model

In order to gain insight into the radiating mechanism of an antenna, we need to first understand the near-field quantities that are present on the structure. The cavity model aids in this pursuit since it provides a mathematical solution for the electric and magnetic fields of a microstrip antenna. It does so by using a dielectrically loaded cavity to represent the antenna. As we can see in Figure 2-4, this technique models the substrate material, but it assumes that the material is truncated at the edges of the patch. The patch and ground plane are represented with perfect electric conductors and the edges of the substrate are modeled with perfectly conducting magnetic walls. It should be noted that the cavity model does not include feed effects; the feed is shown in the figure simply for reference.

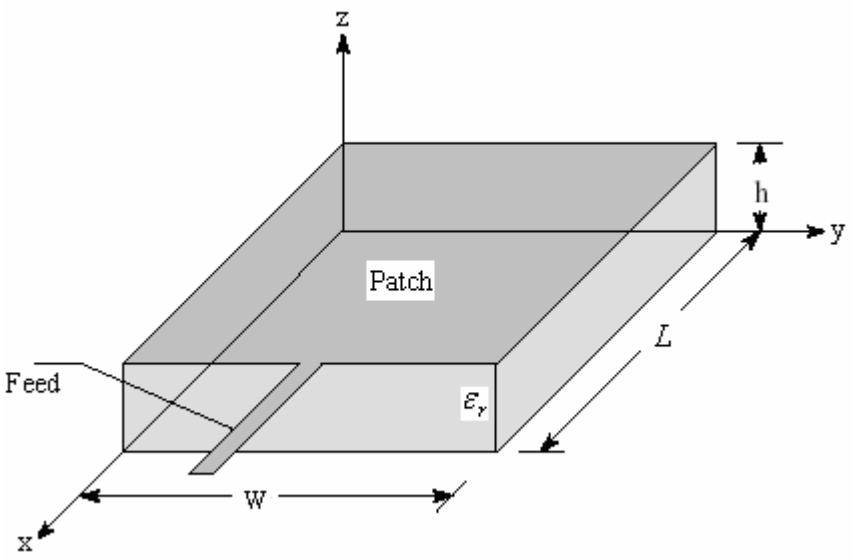

Figure 2.4 Geometry of cavity model.

Balanis formulates a solution to the above cavity problem using the vector potential approach [2] and [1]. Summarizing the technique, we begin by assuming that the dielectric is very thin, which means that the electric field is constant along the height of the substrate, h, and is nearly normal to the surface of the patch. Therefore, we only need to consider TM_z modes inside the cavity. Now, we can write an expression for the electric and magnetic fields within the cavity in terms of the vector potential A_z [2]:

$$E_x = -j\frac{1}{\omega\mu\varepsilon}\frac{\partial^2 A_z}{\partial x \partial y} \qquad H_x = \frac{1}{\mu}\frac{\partial A_z}{\partial y}$$

$$E_y = -j\frac{1}{\omega\mu\varepsilon}\frac{\partial^2 A_z}{\partial y \partial z} \qquad H_y = \frac{1}{\mu}\frac{\partial A_z}{\partial x} \qquad \text{(2-5)}$$

$$E_z = -j\frac{1}{\omega\mu\varepsilon}\left(\frac{\partial^2}{\partial z^2} + k^2\right)A_z \qquad H_z = 0$$

Since the vector potential must satisfy the homogeneous wave equation

$$\nabla^2 A_z + k^2 A_z = 0 \qquad \text{(2-6)}$$

we can use separation of variables to write the following general solution

$$A_z = \left[A_1 \cos(k_x x) + B_1 \sin(k_x x)\right] \left[A_2 \cos(k_y y) + B_2 \sin(k_y y)\right] \left[A_3 \cos(k_z z) + B_3 \sin(k_z z)\right] \tag{2-7}$$

where k_x, k_y and k_z are wave numbers. Applying the boundary conditions

$$\begin{aligned}
E_x = 0 \quad & for \quad 0 \le x \le L, 0 \le y \le W, z = 0 \\
& and \quad 0 \le x \le L, 0 \le y \le W, z = h \\
H_x = 0 \quad & for \quad 0 \le x \le L, y = 0, 0 \le z \le h \\
& and \quad 0 \le x \le L, y = W, 0 \le z \le h \\
H_y = 0 \quad & for \quad x = 0, 0 \le y \le W, 0 \le z \le h \\
& and \quad x = L, 0 \le y \le W, 0 \le z \le h
\end{aligned} \tag{2-8}$$

we obtain a solution for the electric and magnetic fields inside the cavity:

$$\begin{aligned}
E_x &= -j \frac{k_x k_z}{\omega \mu \varepsilon} A_{mnp} \sin(k_x x) \cos(k_y y) \sin(k_z z) \\
E_y &= -j \frac{k_y k_z}{\omega \mu \varepsilon} A_{mnp} \cos(k_x x) \sin(k_y y) \sin(k_z z) \\
E_z &= -j \frac{k^2 - k_z^2}{\omega \mu \varepsilon} A_{mnp} \cos(k_x x) \cos(k_y y) \cos(k_z z) \\
H_x &= -\frac{k_y}{\mu} A_{mnp} \cos(k_x x) \sin(k_y y) \cos(k_z z) \\
H_y &= -\frac{k_x}{\mu} A_{mnp} \sin(k_x x) \cos(k_y y) \cos(k_z z) \\
H_z &= 0
\end{aligned} \tag{2-9}$$

Here,

$$\left.\begin{aligned} k_x &= \frac{m\pi}{L}, m = 0,1,2,... \\ k_y &= \frac{n\pi}{W}, n = 0,1,2,.. \\ k_z &= \frac{p\pi}{h}, p = 0,1,2,.. \end{aligned}\right\} m = n = p \neq 0 \qquad (2\text{-}10)$$

and A_{mnp} is the amplitude coefficient. Finally, the resonant frequencies for the cavity are given by

$$(f_r)_{mnp} = \frac{1}{2\pi\sqrt{\mu\varepsilon}}\sqrt{\left(\frac{m\pi}{L}\right)^2 + \left(\frac{n\pi}{W}\right)^2 + \left(\frac{p\pi}{h}\right)^2} \qquad (2\text{-}11)$$

Examining the above fields for $(TM_z)_{100}$ dominant mode excitation, we see that $k_y = k_z = 0$ and the field components reduce to

$$E_z = -j\omega A_{100}\cos\left(\frac{\pi}{L}x\right)$$

$$H_y = \frac{\pi}{\mu L}A_{100}\sin\left(\frac{\pi}{L}x\right) \qquad (2\text{-}12)$$

We can convert to equivalent electric and magnetic current densities using:

$$\vec{J} = \hat{n}\times\vec{H}$$

$$\vec{M} = -\hat{n}\times\vec{E} \qquad (2\text{-}13)$$

where $\hat{n}$ is the outward directed surface normal. The magnetic field is zero along the $X = 0$ and $X = L$ walls and is normal to the surface along the $y = 0$ and $y = W$ walls. Therefore, no equivalent electric current density flows on the walls of the cavity. The electric field results in a non-zero magnetic current density on the walls of the cavity. Figure 2.5 shows both the electric field and corresponding magnetic current densities for the microstrip antenna. The magnetic currents can be broken into a pair of radiating slots and a pair of non-radiating slots. The radiating slots are in phase so they will constructively interfere in the far-field. Thus, these two slots form the primary radiating mechanism for the microstrip antenna. On the other hand, the non-radiating slots are out

of phase so they will destructively interfere in the far-field and will not contribute to the radiated fields.

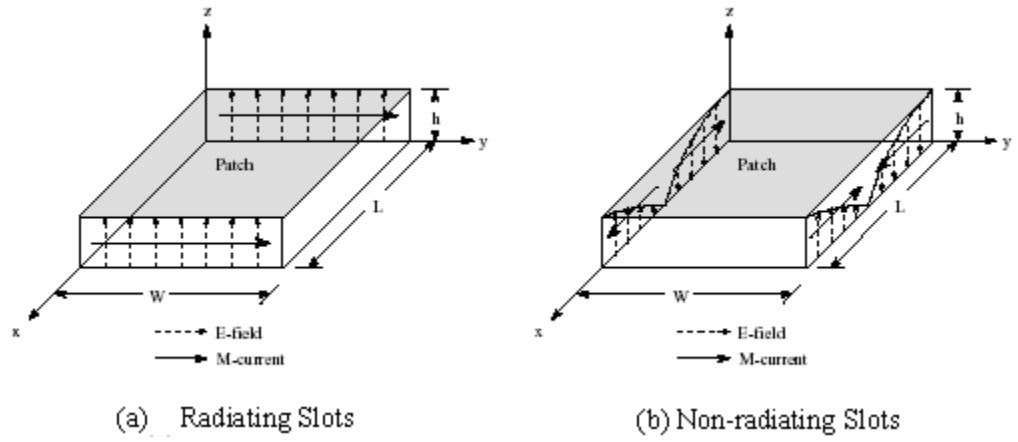

Figure 2.5 Field configurations and current densities for microstrip patch [1]

From the above results, we can see that the cavity model provides excellent insight into the radiating mechanism of a microstrip patch antenna. It provides the field configurations of the radiating and non-radiating slots that can be used to solve for the radiation patterns [1]. Since the antenna is modeled as a cavity, additional work is necessary to accurately model the input impedance. An effective loss tangent needs to be added to account for the power that is lost to radiation [1]. Alternatively, the radiated energy can be modeled using an impedance boundary condition at the walls [9].

Although the cavity model is quite adept at modeling the radiating mechanism for a microstrip antenna, it does have some limitations. First, the cavity model does not model the feed effects. Nor does it model the adverse effects introduced by a finite substrate and ground plane. One way to circumvent these limitations is to employ numerical techniques.

C. Full-Wave Solutions – Method of Moments

In some instances, we may need to understand how the behavior of an antenna is affected by its surroundings. For example, we may want to develop a model that includes the effects of a feed structure, a finite ground plane, or a case enclosure. For problems such as these, the techniques described above become highly impractical.

Fortunately, there are a variety of numerical analysis techniques that can handle these problems quite nicely, including the method of moments (MoM), the finite-element method (FEM), and the FDTD method. All three of these techniques are computationally intensive, which in the past limited the size and complexity of problems that could be approached. However, due to recent advances in computing capabilities, these techniques have become much more powerful. In addition, these techniques are somewhat generalized so they are capable of modeling a variety of antennas (not just the microstrip patch). The details of each technique are quite intricate, so we will focus on the FDTD method because it is used to generate the examples presented in this thesis.

The FDTD method uses a discretization in time and space to calculate a solution of Maxwell's curl equations directly in the time domain [10]:

$$\nabla \times \vec{E} = -\mu \frac{\partial \vec{H}}{\partial t}$$

$$\nabla \times \vec{H} = \varepsilon \frac{\partial \vec{E}}{\partial t} + \vec{J} \tag{2-14}$$

Rearranging these equations

$$\frac{\partial \vec{H}}{\partial t} = -\frac{1}{\mu} \nabla \times \vec{E}$$

$$\frac{\partial \vec{E}}{\partial t} = \frac{1}{\varepsilon} \nabla \times \vec{H} - \frac{\sigma}{\varepsilon} \vec{E} \tag{2-15}$$

Evaluating the vector curl operator ($\nabla \times \vec{A}$) and employing central differencing in both time and space to approximate the partial derivatives, we obtain six update equations (one for each component of the electric and magnetic fields). For example, the update equation for the E_x component is as follows:

$$E_x^n(i,j,k) = \left[\frac{\varepsilon}{\varepsilon + \sigma \Delta t}\right] E_x^{n-1}(i,j,k) + \left[\frac{\Delta t}{\varepsilon + \sigma \Delta t}\right] \cdot \left[\frac{H_z^{n-1/2}(i,j,k) - H_z^{n-1/2}(i,j-1,k)}{\Delta y} - \frac{H_y^{n-1/2}(i,,j,k) - H_y^{n-1/2}(i,j,k-1)}{\Delta z}\right] \tag{2-16}$$

The electromagnetic structure is modeled by approximating its geometry and composition with Yee cells of different material parameters (both conductivity and relative dielectric constant). Figure 2-6 depicts an example Yee cell along with its corresponding field calculation points.

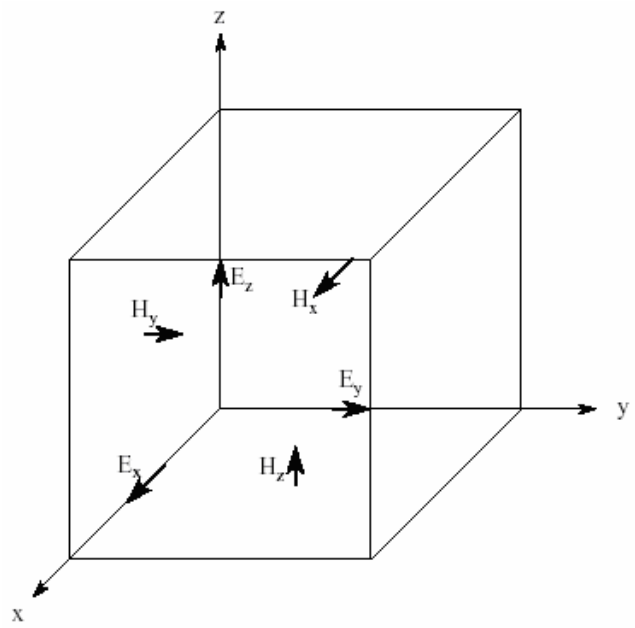

Figure 2-6 Example Yee cell with field calculation points

At the outer boundaries of the computational space an absorbing boundary condition is used to simulate free-space radiation. In order to avoid numerical instabilities in the finite-difference algorithm, the time increment must not violate the Courant stability condition [11]:

$$\Delta t \leq \frac{(\mu\varepsilon)^{1/2}}{\left[\frac{1}{\Delta x^2}+\frac{1}{\Delta y^2}+\frac{1}{\Delta z^2}\right]^{1/2}} \qquad (2\text{-}17)$$

An excitation is then applied to the computational model and the E - and H-field computations are alternately marched through time from time zero to the desired stopping point. Results can be viewed either in the time domain or in the frequency domain. In order to obtain the frequency characteristics of the antenna it is necessary to compute a fast-Fourier transform (FFT) of the transient output data.

The FDTD techniques presented above allow antennas to be modeled in fine detail. Feed lines, finite ground planes, and case enclosures can all be included in the computational model. In addition, the techniques are highly generalized so a number of antennas can be analyzed. Tirkas and Balanis [11] demonstrate the versatility of FDTD techniques by using it to model a dipole, open-ended waveguide, and horn antenna. The major drawback of numerical techniques in general is that they generate huge amounts of data. However, we can alleviate this problem greatly through the use of visualization.

2.3 Performance Parameters Of Microstrip Patch Antennas

2.3.1 Introduction

The purpose of a transmitting antenna is to radiate electromagnetic waves into "free space" (usually, but not necessarily, air). The power for this is supplied by a “feeder” (usually the feeder conveys power from a transmitter at some distance from the radiating structure, or from the antenna in receive mode to a receiver also at some distance from the structure) which is often a length of transmission line or wave guide having a well-defined characteristic impedance.

Antennas are also used in "receive mode" to collect radiation from "free space" and deliver the energy contained in the propagating wave to the feeder and receiver. Usually, antennas are reciprocal devices; their essential properties do not depend on whether they are used as transmit or receive devices. So an efficient transmit antenna can also be used as an efficient receive antenna for the same kind of signal. The directional pattern also does not depend on the transmit or receive mode usage. These properties are collected together and called reciprocity. What is the basic principle for the antenna to radiate?

A conducting wire radiates mainly because of time-varying current or acceleration (or deceleration) of charge. If there is no motion of charges in a wire, no radiation takes place, since no flow of current occurs. Radiation will not occur even if charges are moving with uniform velocity along a straight wire. However, charges moving with uniform velocity along a curved or bent wire will produce radiation. If the charge is oscillating with time, then radiation occurs even along a straight wire [1].

The radiation from an antenna can be explained with the help of Figure 2.7, which shows a voltage source connected to a two conductor transmission line. When a sinusoidal voltage is applied across the transmission line, an electric field is created which is sinusoidal in nature and this results in the creation of electric lines of force which are tangential to the electric field. The magnitude of the electric field is indicated by the bunching of the electric lines of force. The free electrons on the conductors are forcibly displaced by the electric lines of force and the movement of these charges causes the flow of current which in turn leads to the creation of a magnetic field.

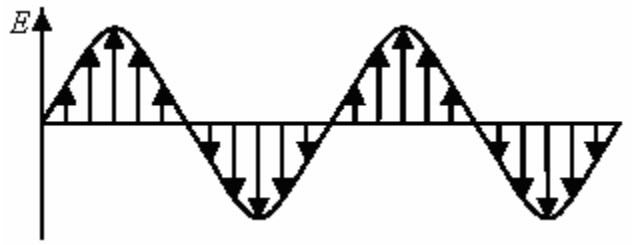

(a)

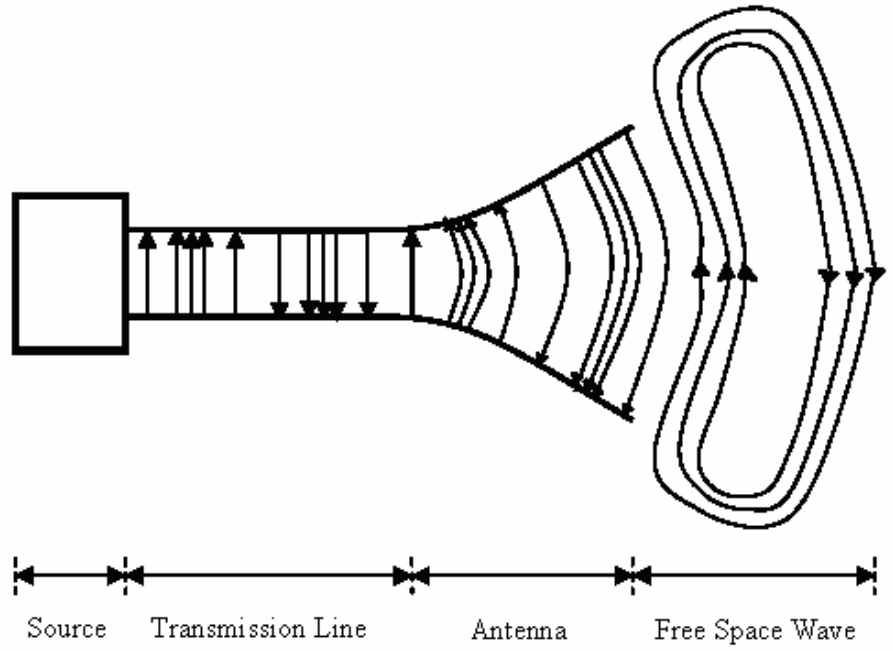

(b)

Fig. 2.7 Radiation from an antenna

Due to the time varying electric and magnetic fields, electromagnetic waves are created and these travel between the conductors. As these waves approach open space, free

space waves are formed by connecting the open ends of the electric lines. Since the sinusoidal source continuously creates the electric disturbance, electromagnetic waves are created continuously and these travel through the transmission line, through the antenna and are radiated into the free space. Inside the transmission line and the antenna, the electromagnetic waves are sustained due to the charges, but as soon as they enter the free space, they form closed loops and are radiated [1].

The field patterns, associated with an antenna, change with distance and are associated with two types of energy: - radiating energy and reactive energy. Hence, the space surrounding an antenna can be divided into three regions. These are:

(a) Reactive near-field region: In this region, the reactive field dominates. The reactive energy oscillates towards and away from the antenna, thus appearing as reactance. In this region, energy is only stored and no energy is dissipated. The outermost boundary for this region is at a distance $R_1 = 0.62\sqrt{D^3/\lambda}$ where R_1 is the distance from the antenna surface, D is the largest dimension of the antenna and λ is the wavelength.

(b) Radiating near-field region (also called Fresnel region): This is the region which lies between the reactive near-field region and the far field region. Reactive fields are smaller in this field as compared to the reactive near-field region and the radiation fields dominate. In this region, the angular field distribution is a function of the distance from the antenna. The outermost boundary for this region is at a distance $R_2 = 2D^2/\lambda$ where R_2 is the distance from the antenna surface.

(c) Far-field region (also called Fraunhofer region): The region beyond $R_2 = 2D^2/\lambda$ is the far field region. In this region, the reactive fields are absent and only the radiation fields exist. The angular field distribution is not dependent on the distance from the antenna in this region and the power density varies as the inverse square of the radial distance in this region.

The performance of an antenna is measured in effectively transmitting or receiving the radiation fields. This leads us to the next topic.

2.3.2 Performance Parameters of Patch Antennas

The performance of an antenna can be measured by a number of parameters. The followings are the critical ones.

(a) Radiation Pattern

The radiation pattern of an antenna is a plot of the far-field radiation properties of an antenna as a function of the spatial co-ordinates which are specified by the elevation angle θ and the azimuth angle ϕ. More specifically it is a plot of the power radiated from an antenna per unit solid angle which is nothing but the radiation intensity [5]. Let us consider the case of an isotropic antenna. An isotropic antenna is one which radiates equally in all directions. If the total power radiated by the isotropic antenna is P , then the power is spread over a sphere of radius r , so that the power density S at this distance in any direction is given as:

$$S = \frac{P}{area} = \frac{P}{4\pi r^2} \qquad (2\text{- }18)$$

Then the radiation intensity for this isotropic antenna U_i can be written as:

$$U_i = r^2 S = \frac{P}{4\pi} \qquad (2\text{ - }19)$$

An isotropic antenna is not possible to realize in practice and is useful only for comparison purposes. A more practical type is the directional antenna which radiates more power in some directions and less power in other directions. A special case of the directional antenna is the omnidirectional antenna whose radiation pattern may be constant in one plane (e.g. E-plane) and varies in an orthogonal plane (e.g. H-plane). The radiation pattern plot of a generic directional antenna is shown in Figure 2.8.

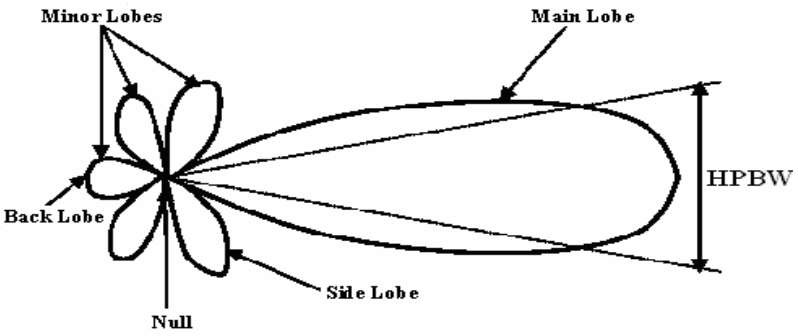

Fig 2.8 Radiation pattern of a generic directional antenna.

From the above figure we can have the following definitions.

- HPBW: The half power beamwidth (HPBW) can be defined as the angle subtended by the half power points of the main lobe.
- Main Lobe: This is the radiation lobe containing the direction of maximum radiation.
- Minor Lobe: All the lobes other then the main lobe are called the minor lobes. These lobes represent the radiation in undesired directions. The level of minor lobes is HPBW usually expressed as a ratio of the power density in the lobe in question to that of the major lobe. This ratio is called as the side lobe level (expressed in decibels).
- Back Lobe: This is the minor lobe diametrically opposite the main lobe.
- Side Lobes: These are the minor lobes adjacent to the main lobe and are separated by various nulls. Side lobes are generally the largest among the minor lobes. In most wireless systems, minor lobes are undesired. Hence a good antenna design should minimize the minor lobes.

(b) Directivity

The directivity of an antenna has been defined as "the ratio of the radiation intensity in a given direction from the antenna to the radiation intensity averaged over all directions". In other words, the directivity of a nonisotropic source is equal to the ratio of its radiation intensity in a given direction, over that of an isotropic source.

$$D = \frac{U}{U_i} = \frac{4\pi U}{P} \qquad (2 - 20)$$

where D is the directivity of the antenna

U is the radiation intensity of the antenna

U_i is the radiation intensity of an isotropic source

P is the total power radiated

Sometimes, the direction of the directivity is not specified. In this case, the direction of the maximum radiation intensity is implied and the maximum directivity is given by [1] as:

$$D_{\max} = \frac{U_{\max}}{U_i} = \frac{4\pi U_{\max}}{P} \qquad (2 - 21)$$

where $D_{\max}$ is the maximum directivity

$U_{\max}$ is the maximum radiation intensity

Directivity is a dimensionless quantity, since it is the ratio of two radiation intensities. Hence, it is generally expressed in dBi. The directivity of an antenna can be easily estimated from the radiation pattern of the antenna. An antenna that has a narrow main lobe would have better directivity, than the one which has a broad main lobe, hence it is more directive.

(c) Gain

The word antenna gain often seems to refer to some sort of mysterious signal amplification. However, one antenna with a "higher" gain doesn't amplify the signal more than another with "less" gain. Thus an antenna with greater gain simply focuses the energy of the signal differently. It is a parameter which is closely related to the directivity (how much an antenna concentrates energy in one direction in preference to radiation in other directions) of the antenna. Hence, if the antenna is 100% efficient, then the directivity would be equal to the antenna gain and the antenna would be an isotropic radiator. Since all antennas will radiate more in some direction that in others, therefore the gain is the amount of power that can be achieved in one direction at the expense of the power lost in the others . The gain is always related to the main lobe and is specified in the direction of maximum radiation unless indicated. It is given as:

$$G(\theta,\phi) = e_{cd} D(\theta,\phi) \qquad \text{(dBi)} \qquad (2 - 22)$$

where e_{cd} is the antenna radiation efficiency.

(d) Bandwidth

It is defined as "The range of usable frequencies within which the performance of the antenna, with respect to some characteristic, conforms to a specified standard." The bandwidth can be the range of frequencies on either side of the center frequency where the antenna characteristics like input impedance, radiation pattern, beamwidth, polarization, side lobe level or gain, are close to those values which have been obtained at the center frequency. The bandwidth of narrow band and broadband antennas are defined as:

$$BW_{broadband} = \frac{f_H}{f_L} \tag{2 - 23}$$

$$BW_{narrowband}(\%) = \left(\frac{f_H - f_L}{f_c} \right) 100 \tag{2 - 24}$$

where f_H is upper frequency, f_L is lower frequency and f_c is center frequency.

An antenna is said to be broadband if $\frac{f_H}{f_L} = 2$. One method of judging how efficiently an antenna is operating over the required range of frequencies is by measuring its VSWR. A $VSWR \le 2 \quad (RL \ge -9.5dB)$ ensures good performance. The VSWR is given by

$$VSWR = \frac{1 + |\Gamma|}{1 - |\Gamma|} \tag{2 - 25}$$

$$\Gamma = \frac{V_r}{V_i} = \frac{Z_{in} - Z_s}{Z_{in} + Z_s} \tag{2 - 26}$$

Where Γ is reflection coefficient, V_r is the amplitude of the reflected wave, V_i is the amplitude of the incident wave, Z_{in} is the antenna impedance at the terminals, Z_s is impedance of the transmitter.

The VSWR is basically a measure of the impedance mismatch between the transmitter and the antenna. The higher the VSWR, the greater is the mismatch. The minimum VSWR which corresponds to a perfect match is unity. A practical antenna design should

have an input impedance of either $50\,\Omega$ or $75\,\Omega$ since most radio equipment is built for this impedance.

.

The bandwidth of an antenna can be defined for impedance, radiation pattern and polarization. First, a satisfactory impedance bandwidth is the basic consideration for all antenna design, which allows most of the energy to be transmitted to an antenna from a feed or a transmission system at a transmitter, and from an antenna to its load at a receiver in a wireless communication system. Second, a designated radiation pattern ensures that maximum or minimum energy is radiated in a specific direction. Finally, a defined polarization of an antenna minimizes possible losses due to polarization mismatch within its operating bandwidth. Here we will be targeting at impedance bandwidth.

Impedance bandwidth: Since, in general, an antenna is a resonant device, its input impedance varies greatly with frequency even though the inherent impedance of its feed remains unchanged. If the antenna can be well matched to its feed across a certain frequency range, that frequency range is defined as its impedance bandwidth. The impedance bandwidth can be specified in terms of return loss (S parameter: $|S_{11}|$) or a voltage standing-wave ratio (VSWR) over a frequency range. The well-matched impedance bandwidth must totally cover the required operating frequency range for some specified level, such as VSWR = 2 or 1.5 or a return loss S_{11} of less than -10 dB or -15 dB.

The greatest disadvantage of the microstrip antenna (MSA) is its inherently low impedance bandwidth. The pattern bandwidth of the MSA is much wider than the impedance bandwidth, which can be as low as 1%. Since many wide-band applications require a low-profile conformal antenna, much work has gone into designing wide-band MSA elements or producing MSAs with a dual resonance characteristic. However, most microstrip elements that achieve greater bandwidth do so at the cost of increased height or overall volume. This leads us to the question what the broadbanding techniques are.

The followings are some of the techniques used to increase the bandwidth of a microstrip patch antenna.

a. Optimizing the substrate properties for increased bandwidth: Here to increase BW either we have to decrease the substrate's ε_r or increase its thickness *h.* If we increase ε_r, the area of the patch decreases but the bandwidth decreases. To compromise between these it is possible to modify the regular shaped patches (rectangular, circular etc) by inserting posts acting as short circuits and thereby increasing the bandwidth.
b. Use of stacked microstrip patch antennas: Since the patches are placed one on top of the other on different layers of dielectric substrates, then the total area remains unchanged. The patches are coupled electromagnetically or aperture coupled. If s stands for the separation between the stacked patch antennas, then the region $0 \le s \le 0.14\lambda$ is called the improved bandwidth region as it results in wider impedance BW. The region $0.14\lambda \le s \le 0.29\lambda$ is the region of irregular radiation pattern. The region $s \ge 0.3\lambda$ is called high gain region.
c. Use of planar multi-resonators: the patches are etched close to each other on the same layer and the gap shouldn't exceed $2h$ (where h is substrate height).

(e) Return Loss

The Return Loss (RL) is a parameter which indicates the amount of power that is "lost" to the load and does not return as a reflection. As explained in the preceding section, waves are reflected leading to the formation of standing waves, when the transmitter and antenna impedance do not match. Hence the RL is a parameter similar to the VSWR to indicate how well the matching between the transmitter and antenna has taken place. The RL is given as:

$$RL = -20\log|\Gamma| \qquad \text{(dB)} \qquad (2 - 27)$$

For perfect matching between the transmitter and the antenna, $\Gamma = 0$ and $RL = \infty$ which means no power would be reflected back, whereas as $\Gamma = 1$ has a $RL = 0$ dB, which implies that all incident power is reflected. For practical applications, a VSWR of 2 is acceptable, since this corresponds to a RL of -9.54 dB [43].

(f) Specific Absorption Rate (SAR)

When a person is exposed to the radio waves from mobile phones or base stations, most of the energy will be reflected by the body or travel around it (called diffraction). Some of the energy will however be absorbed in the tissues at the surface of the body.

Inside the body certain molecules, like water, will start to move or rotate due to the presence of the electromagnetic fields. By "friction" the energy is converted into heat. If the radio wave intensity is very high, the heating may be significant and potentially detrimental. The power used by mobile phones is very low and the tissue heating due to radio wave absorption is too small to be noticeable.

The specific absorption rate, SAR, is used to specify the amount of radio frequency (RF) energy absorbed in the body or is the value that corresponds to the relative amount of RF energy absorbed in the head of a user of a wireless handset. SAR is expressed in the unit watts per kilogram (W/kg). Since SAR is a reliable measure of its ability to cause cell damage, then the lower is the better.

Where is the location of the patch antenna on the mobile phone and how does it radiate? This is what we see in the next chapter from simulation using the EMPIRE software.

CHAPTER 3 DUAL BAND PATCH ANTENNA STRUCTURES

3.1 General Features of Mobile Communication

Mobile communications handsets with internal antennas become more popular every day. These integrated antennas must be designed to fit into a small volume, with an arbitrary shape. Indeed, the design of modern handsets is mostly fashion-oriented, and the antennas must be adapted to these requisites, without detriment to their matching or radiating performance [12]. The present study focuses on how a change in some of the antenna geometric parameters, such as its height, may affect its actual performance.

There exist some basic requirements in the design of the latest handset antennas. They must guaranty a good performance, occupy a very small volume and provide multiband operation [13], while keeping a very low fabrication cost. Different standards may be considered, namely GSM900/1800, PCS, and, more recently, UMTS. In any case, it is desirable that the different modes excited upon the antenna could be tuned separately.

Nevertheless, there are some limitations linked to the specific nature of integrated mobile handset antennas. The starting point of the design is a terminal whose size and form are already fixed, to fit fashion and marketing requirements. Some problems arise then, as the volume available to implement the radiating element is usually very small. In practical situations, the maximum dimensions allowed for the antenna are often specified in terms of volume. However, this volume has usually an irregular shape, such as in Fig.3.1, for example. This shape depends both on the outline of the handset and the position of some of its components.

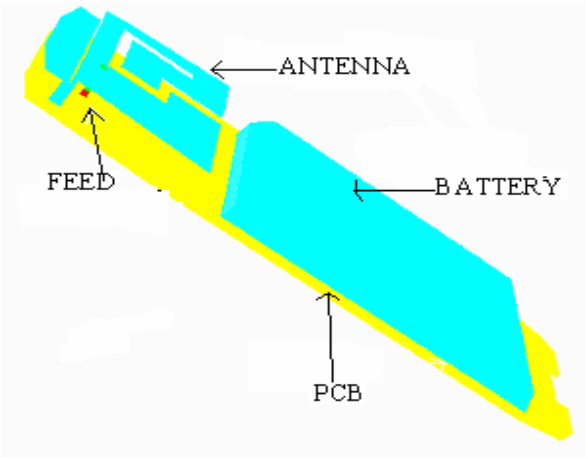

Figure 3.1 General structure of mobile phone

A microstrip antenna being basically a leaky cavity, [8] is inherently narrow band (almost 1%). Considerable research has been undertaken in order to increase the bandwidth. The approaches introduced include thickening the substrate, using lower dielectric constants [15], or adding parasitic elements to the main patch [16]. However some of these methods introduce adverse problems. For example a thick substrate supports surface waves, which will produce undesirable effects on the radiation pattern and will reduce the radiation efficiency of the antenna. Also, higher order cavity modes develop, introducing further distortions in the pattern and impedance characteristics. Instead of increasing the bandwidth, methods have been introduced to *tune* the frequency of the patch over a certain range of frequencies so it can be used for several adjacent channels [17]. In another scheme dual frequency antennas (dual band antennas) with resonant frequencies separated by a certain range have been developed.

Dual band antennas are defined as:*"Antennas that are useful in situations where the antenna is required to operate in* two *distinct frequencies which may be too far apart for a single antenna to perform efficiently at both frequencies.* [8]

A metallic patch antenna with dual-band operation, corresponding to the GSM-900 and 1800, for example, is shown below. The antenna is located at the upper part of the PCB, and occupies a 26mm x 40mm x 8mm volume. The patch was integrated upon a 100mm x 40mm ground plane, with a 50mm x 36mm x 7mm metallic box that accounts for the effect of the battery. The overall structure is presented in figure 3.2. The radiating element consists of a folded, PIFA-like patch, which operates almost as two separate, mutually coupled radiators [14].

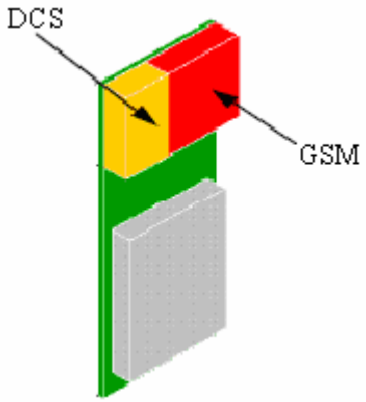

Fig. 3.2 Dual-band antenna structure

3.2 Types of Dual Band Patch Antenna Structures

As mentioned earlier, a dual band antenna is an antenna that can perform at two different assigned frequencies. In order to achieve that, several structures have been developed in the past. In this section, a quick review of some of the most commonly used configurations will be presented. These configurations can be categorized according to the number of patches used, the number of layers, the type of feed, number of feeding points, type of the parasitic loading that have been added to the main patch, etc. In general they will be classified into two main categories namely: multiresonator antennas and reactively loaded antennas.

In multiresonator antennas multifrequency behavior is obtained by means of multiple radiating elements, each supporting strong currents and radiating at resonance.

The reactive-loading patch antenna consists of a single radiating element in which the double resonant behavior is obtained by connecting stubs, shorting pins, notches, slots... etc. to the radiating element. Tabe 3.1 shows this classification.

Table 3.1 Classification of patch antennas

<table>
<tr><th colspan="3">Multi Resonator Antennas</th><th>Reactively Loaded Antennas</th></tr>
<tr><td rowspan="2">Multilayer Stacked Antennas [20,21,22,23, 24,25,31]</td><td rowspan="2">Stacked Discs</td><td>Single input [18]</td><td rowspan="3">• Shorting pins loaded PA [29]
• Stub loaded patch antenna (PA) [30]
• Slot loaded PA [17,29,31,32]
• Notch loaded PA [33]
• Patches loaded with adjustable air gaps [34]
• Patches loaded with spur-lines [32,35-38]</td></tr>
<tr><td>Two inputs [19]</td></tr>
<tr><td colspan="2">Other stacked shapes (Rectangles, Triangles etc..)</td></tr>
<tr><td colspan="3">Aperture Coupled Antennas (Different Resonators, slot loaded) [26,27,28]</td></tr>
</table>

Figure 3.3 below shows the above classified patch antennas.

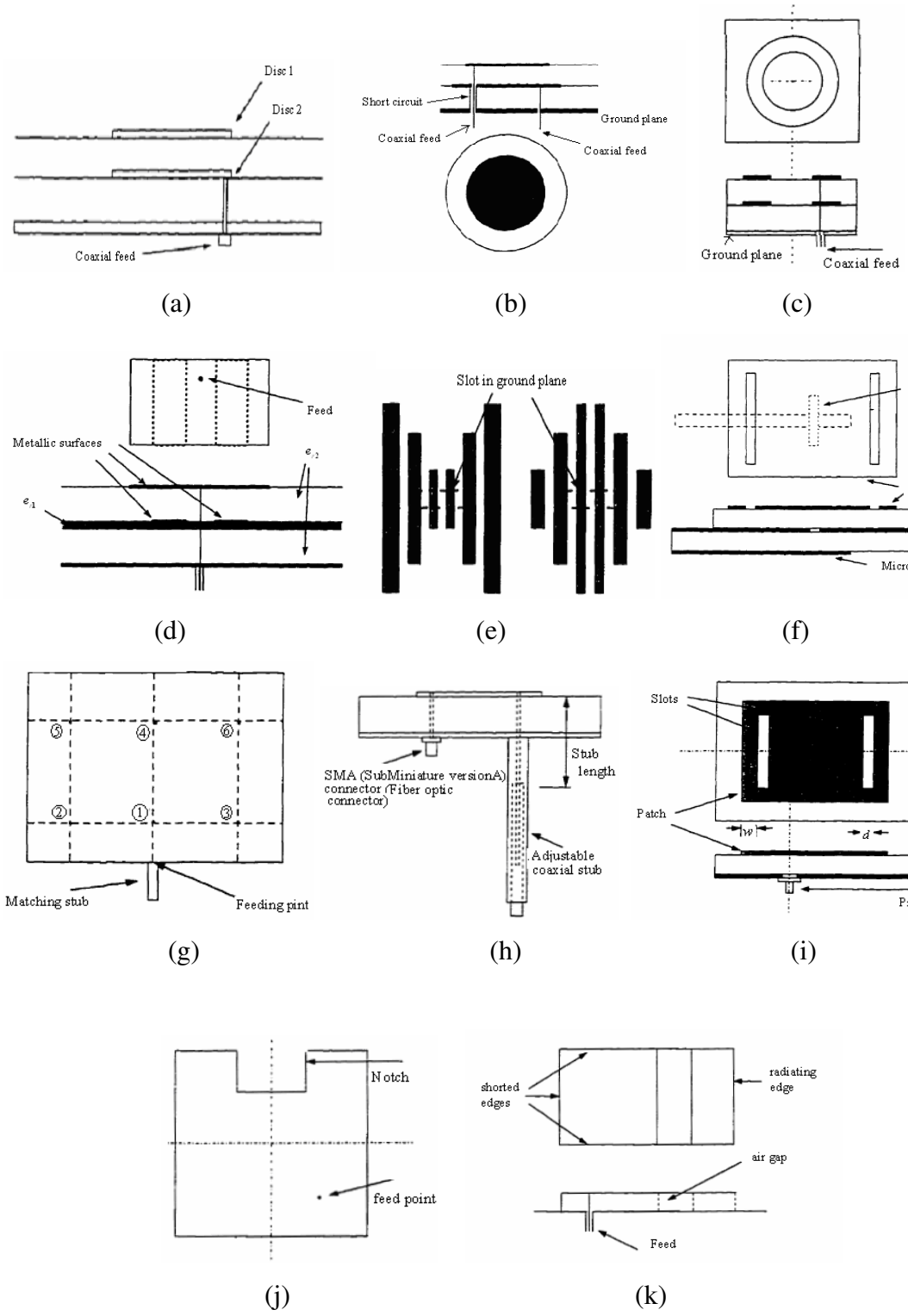

Fig 3.3 (a) Single input circular disc (b) Two input stacked discs (c) Stacked rings(d) Planar dual band microstrip antenna (e) multiresonator aperture coupled antenna (f) Aperture coupled antenna

loaded with two slots (g) Shorting pins loaded patch antenna (h) stub loaded patch antenna (i) probefed slot loaded pathc antenna (j) notch loaded patch antenna (k) Patch loaded with adjustable air gaps ,i.e, a-f are multiresonator antennas are g-k are reactively loaded patch antennas

Once we have the general classifications of dual band patch antenna structures the next thing is to design and simulate them so that we can compare their performance. This leads us to the next topic.

3.3 Design Considerations

Aesthetical design and marketing aspects have a large impact on the development of mobile phones. Therefore there is a remarkable trend to fully integrate the antenna in the mobile phone. Compared to traditional antennas it is more complicated to master the typical parameters like bandwidth, efficiency and influence of the user with in the limited antenna volume. This becomes even more critical with respect to multiband functionality that is an essential feature of modern mobile phones. To enable a rapid and efficient design some general relations concerning the physical behavior of an antenna in a small mobile have to be considered.

3.3.1 Major Design Concepts

The three essential parameters for the design of a microstrip patch antenna are:

- Frequency of operation (f_0): The resonant frequency of the antenna must be selected appropriately. The GSM band uses the frequency range from 880 – 990 MHz and the DCS/IMT (Digital Cordless System/International Communication Systems) band uses the frequency range from 1710 – 2200 MHz.
- Dielectric constant of the substrate (ε_r): If a substrate with a high dielectric constant is selected, then it reduces the dimensions of the antenna. ε_r ranges from 2.2 – 12.
- Height of dielectric substrate (h): For the microstrip patch antenna to be used in cellular phones, it is essential that the antenna is not bulky.

The main design goal for a microstrip patch antenna is to determine the substrate properties and patch dimensions necessary to satisfy the specific performance characteristics over the required frequency band. The usual design procedure, however, only takes resonant frequency into account, and does not consider the required bandwidth. The designer is forced to obtain the required bandwidth with a step-by-step, or trial-and-error, design technique. Before completing the design procedure, however, one needs to find a way to determine the location of the feed point to match to the characteristic impedance of the MSA. The feed can be easily located by using another design chart obtained by numerical calculation or experiment [39].

In the typical procedure, the thickness and the dielectric constant of the substrate are known. Then, a patch antenna that operates at the required resonant frequency can be designed by following the flow chart shown in Fig. 3-4 [39], where (a) is for rectangular MSA and (b) is for a circular one. In the rectangular case, we know that the greater the width W, the higher radiation efficiency becomes. However, excessive width is not desirable because the influence of higher order modes becomes significant and the original characteristics may suffer some degradation as a result. This implies that there exists an optimum value for the width. The ideal width for practical use can be determined from the design flow chart in Fig. 3.4, although the value may not be optimum.

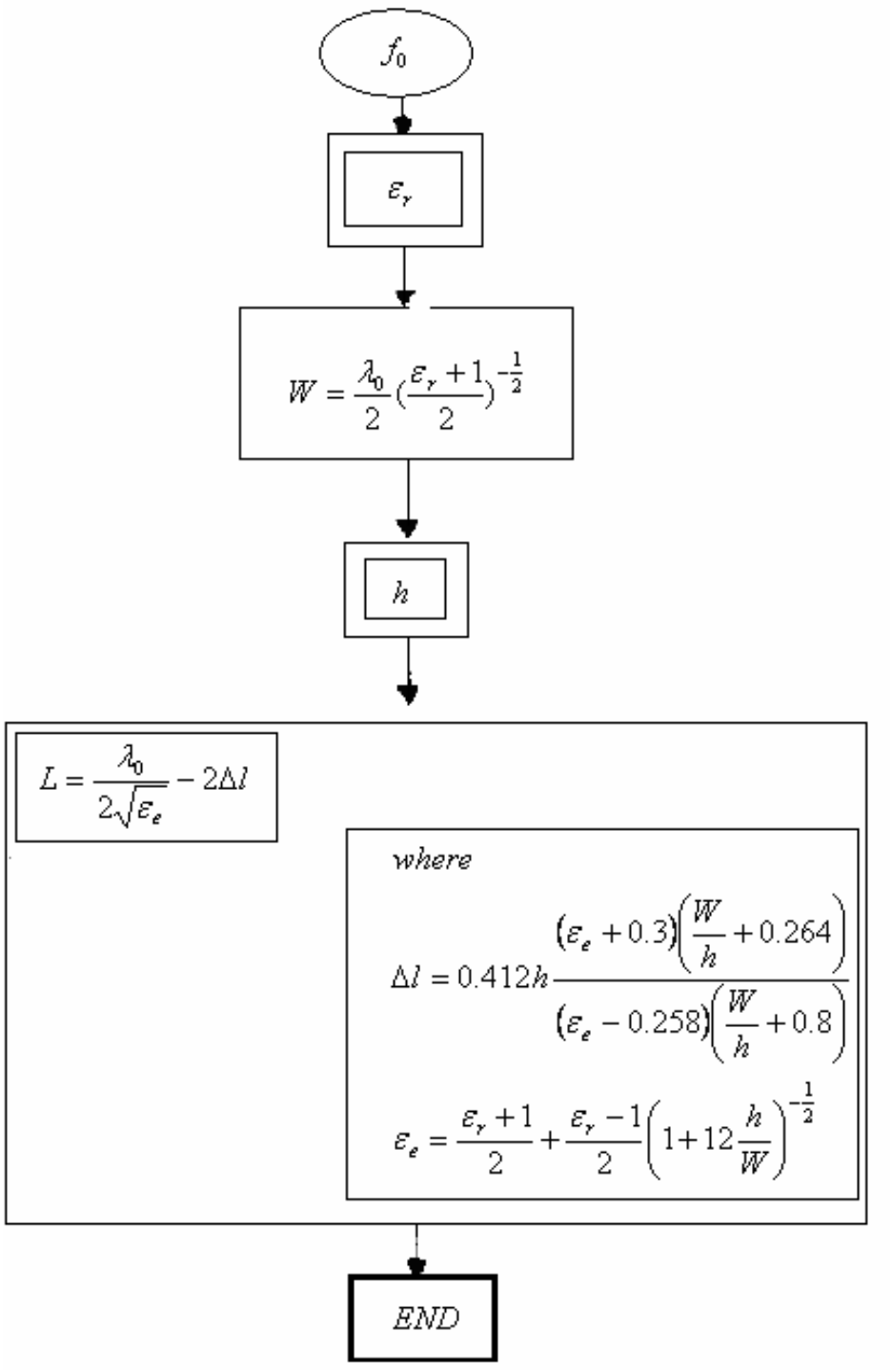

(a)

Fig 3.4 Flow chart based on the usual design procedure [39] (a) for the rectangular patch antenna (b) for a circular patch antenna.

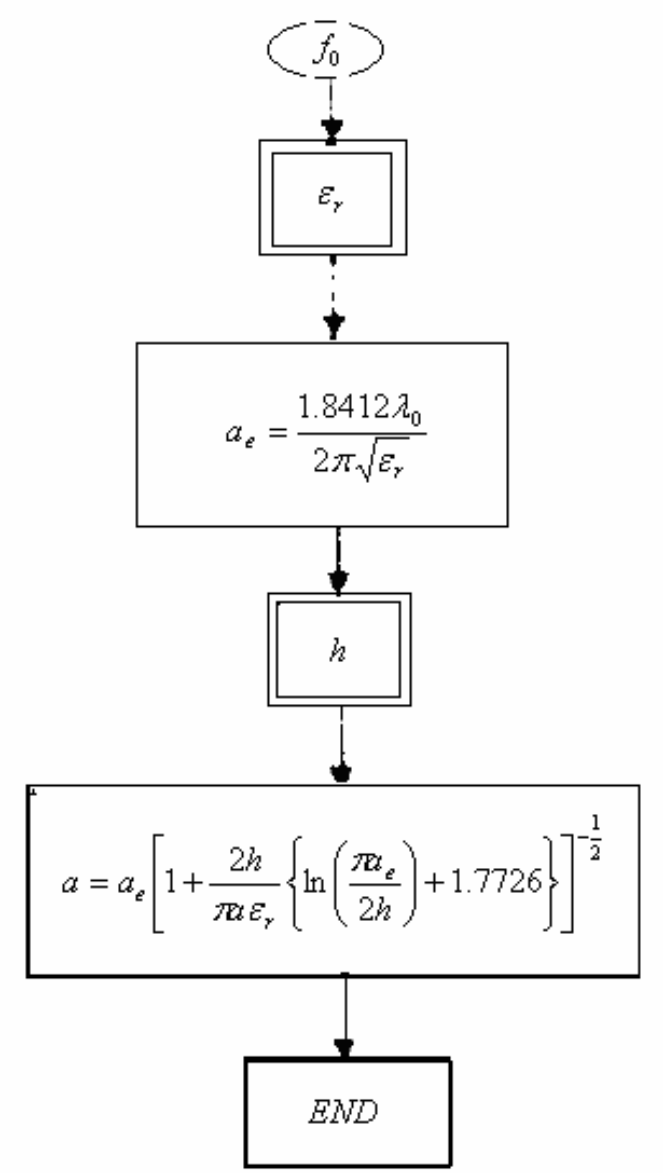

(b)

Fig 3.4 (Continued)

Another thing that must be put in to consideration as one of the design parameters is the feeding technique. Depending on the required result and the complexity of the structure it is possible to switch to one of the following methods of feeds.

Generally, the feeding methods of a microstrip antenna can be classified as microstrip feeding, probe feeding and electromagnetic coupled (EMC) feeding. The microstrip feeding is easily fabricated by connecting the microstrip to the edge of the patch

directly, but the impedance matching is not convenient compared to probe feeding and unwanted radiation can occur from the feed line. Feeding by a coaxial probe has the advantages of ease in impedance matching and low spurious radiation, and the disadvantage of having to be physically connected to the center of the patch. The coaxial- fed microstrip antenna has a narrow impedance bandwidth. The third method, known as EMC feeding is different from the other feeding methods. Spurious radiation does not occur and it has the advantage of offering a wideband characteristic without any matching circuit.

Position of the feed also plays great role in arriving at the required result. The feed point must be located at that point on the patch, where the input impedance is 50 ohms for the resonant frequency. Hence, a trial and error method is used to locate the feed point. For different locations of the feed point, the return loss (R.L) is compared and that feed point is selected where the R.L is most negative. According to [1] there exists a point along the length of the patch where the R.L is minimum. For example, starting from the center of the patch vary the point in the direction of the length or the width of the patch to locate the optimum feed point.

In general factors to consider in internal antenna design are the followings.

- Size constraints of phone housing
- Material from which phone housing is made
- Material from which the antenna is made
- Location of feedpoint
- Size of elements
- Available surface area and the freespace volume for the antenna
- Location of elements
- The means by which the ground tab connects to the counterpoise (this comprises the phone itself as well as the contributions of the hand and the head);
- Volume of antenna
- Desired bandwidth and the means by which bandwidth is specified (usually, voltage-standing-wave ratio)

- Desired performance, including peak gain, average gain, overall efficiency
- Operating bands

Having all these information at hand what are we going to use for the simulation purpose? Though there are numerous softwares available now a days on market, we will use the EMPIRE software as it is 20 times faster than any other software and also uses full-wave solutions modeling which is based on FDTD so that it enables us to model the integrated structure (antenna, feed, housing, etc…).

3.3.2 Application For Simulation

The versatile electromagnetic field simulator EMPIRE (ElectroMagnetic field simulator for the analysis of Packages, Interconnects, Radiators, Waveguide Elements) nad EMC problems are established based upon the Finite Difference Time Domain (FDTD) at the IMST GmBH. The exact knowledge of electromagnetic fields and the propagation of waves is a prerequisite for the design of radio frequency (RF) elements. In former times, RF design tasks were based on measurement and simple models, leading to time and costs consuming design procedures. Today, affordable computer hard- and software have established and simulation programs can accurately predict the electromagnetic behavior of new products. So, field simulators have become a new standard for RF calculations.

Unlike the Finite Element Method, which has long been established in computing electromagnetic fields, the FDTD method had its breakthrough in the late 80's when extensive research and development lead to a number of improvements in applying advanced boundary conditions, e.g. free space or waveguides, and, therefore, reducing significantly the area of simulation. Today, its applicability covers the whole area of three-dimensional (3D) field simulations for RF designer. Originally intended to analyze planar passive structures, the EMPIRE simulator was continuously extended to capture more and more high frequency applications. It has proven its functionality in numerous comparisons with measurements and was successfully applied in many different microwave component designs. The method is based on the most efficient algorithm

known which is very accurate and simplification is hardly necessary since it solves the discredited Maxwell's equations directly.

In general, EMPIRE is powerful and fast 3D electromagnetic field software based on 3D Finite Difference Time Domain method which includes specially modified algorithms and methods for efficient utilization of multiple points and catches to achieve ultra fast solution times and excellent accuracy. It is 15 to 20 times faster than any other 3D simulation software on the market. It is used in modeling microwave devices and antennas, body models and active and passive devices.

After having the patch antennas to be compared and the software used to design, simulate and analyze what parameters do we use to compare and contrast performance of each antenna? This will be discussed in the next chapter.

CHAPTER 4 PERFORMANCES OF TRANSMITTER-RECEIVER CELLULAR ANTENNAS

4.1 OVERVIEW

The life of the present day antenna designer is tough as he faces different challenges in arriving at the simplified, efficient, aesthetically best and integrated mobile phones. Some of the challenges are the followings.

(a) Reduce the antenna size: Perhaps the most fundamental challenge is the quest for minimizing the antenna size. Since antenna operation up to quad-or even penta-band operation is needed, network operators require better over-the-air performance from the terminals which can be achieved with sufficient antenna volume and current internal antenna designs push the fundamental performance limits of electrically small antennas, the volume of the main antenna can be reduced only by little.

In general, volume required for antennas in mobile terminals is increasing rather than decreasing due to additional antennas needed for complementary (non-cellular) systems and diversity.

(b) Meet regulatory operator demands: These include over-the-air performance, EMF safety regulations (SAR), hearing aid compatibility and EMC requirements (spurious emissions and self jamming).

(c) Supply multi radio with antennas: This refers to how to fit up to 10 radio systems, which all require at least one antenna, in small hand held device, how to design antennas for low frequency systems such as FM and AM radio and how to implement antenna diversity and MIMO.

(d) Find antenna solutions which can be used with various form factors and materials: Since phones of different size and shape (whose form factor include monoblock or candy bar, fold, slide, swivel) are in the market today, so far it has been impossible to make the universal antenna (module), because different form factors have different requirements on antenna shape and placement.

(e) Cope with user interaction: This refers to how to design antenna solutions that are insensitive to users hand and provide sufficient performance in all directions (in pocket, on table, in various orientations).

The above challenges show that there is lots of work still to be done with antennas. All mobile phones which are efficient and integrated that we see today are results of the above challenges.

The following figure fig4.1 ((a) and (b)) is an integrated generic model of a cellular phone implemented to model multi band antennas in mobile devices using the EMPIRE software. The Antenna height is the distance between the upper antenna structure and the PCB and is set to 6mm. With the two geometric parameters board length (107mm) and board width (40 mm), the total size of the device can be adopted to the dimension of interest. This template is particularly useful to setup a quick simulation for any kind of mobile devices. The position, shape and size of the Antenna structure can be rearranged and modified so to tackle customer's needs. The frequency range for this template is automatically set from 500 MHz to 2.5 GHz. And the farfield computation is done for 920 MHz. For this template the dimensions of the cell phone should be limited to 40mm < w < 100mm and 70mm < h < 150mm. The two switches model battery and model plastic casing, will generate the a phones battery (modelled as PEC) and a 1mm thick casing with a permittivity of 3, respectively.

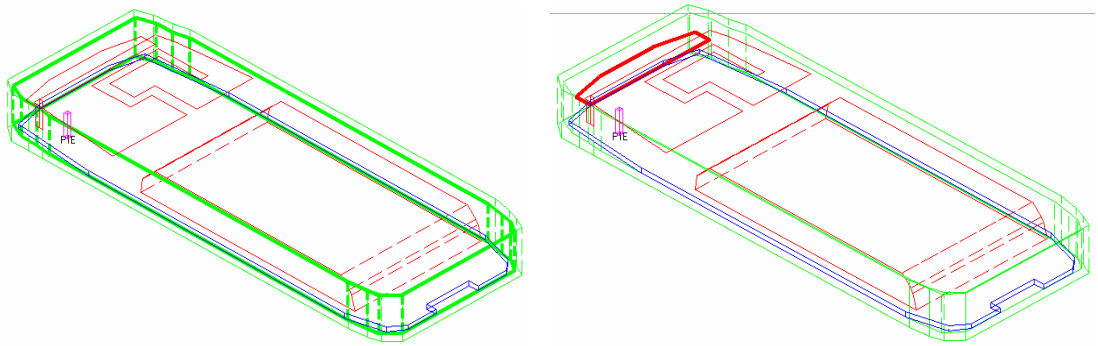

(a) (b)

Fig 4.1 (a) The 3D ISO view of the mobile phone when the antenna is bold (b) when the parasitic patch is bold (c) when the ground plane is bold (d) when the battery is bold (e) the 3D view of the integrated mobile phone without the casing .

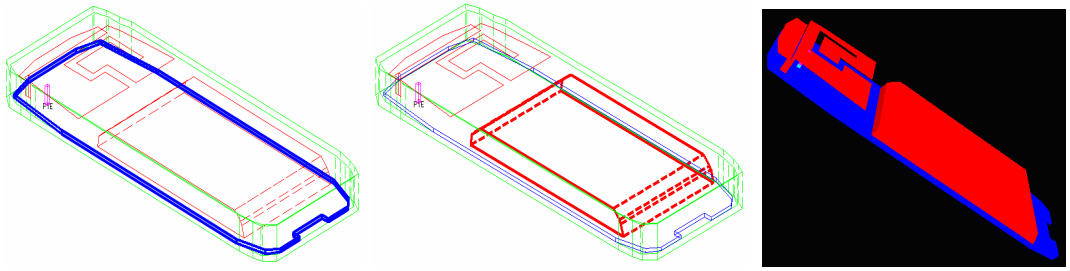

(c) (d) (e)

Figure 4.1 (Continued)

4.2 SIMULATIONS AND RESULTS

Based on the classification of dual band patch antenna structures on chapter 3 ten (10) patch antenna samples (5 from multiresonator and 5 from reactively loaded patch antenna structures) are taken that include one or combinations of square, rectangular, circular and dipole geometries. For the sake of ease of comparison of performance each antenna is confined in to an integrated mobile phone that has a total volume of 42mmx111mx12mm $42mm\ x\ 111mm\ x\ 12mm\ (l\ x\ w\ x\ h)$ that includes a 1mm thick casing. In each case the antenna, whose feed is matched to a 50Ω transmission line, is placed at the top back of the integrated mobile phone. For variety lumped, microstrip line and coax feed ports are used. Relative permitivities of materials for casing and substrate are different values for different structures. For each structure the thickness of the patch is 0.001 cm ($10\mu m$). For each integrated structure the ground plane has a thickness of $1mm$.

Performance is measured for $VSWR \le 2.6$ or $|S_{11}| \ge 7dB$. Bandwidth operation of each antenna is directly measured from the returnlosss graph. The 2D and 3D radiation patterns are also found from post process in the simulation in free space. Concerning to the SAR value of each antenna I put into consideration the following assumption. Since the SAR value of a handset is determined under laboratory conditions applying the highest possible transmission power and worst-case scenario, I assumed all mobiles into consideration have SAR value within the regulatory standard. That is at or below 1.6W/kg taken over a volume of 1g of tissue or 2W/kg over a volume of 10g of tissue. According to the simulation done using the EMPIRE software the result is as follows.

A. Single input (feed) circular disc patch antenna structure

Two separate resonances can be found and adjusted to the desired values through a proper choice of the two disc diameter and their spacing. Their centers are along the same line perpendicular to the ground plane.

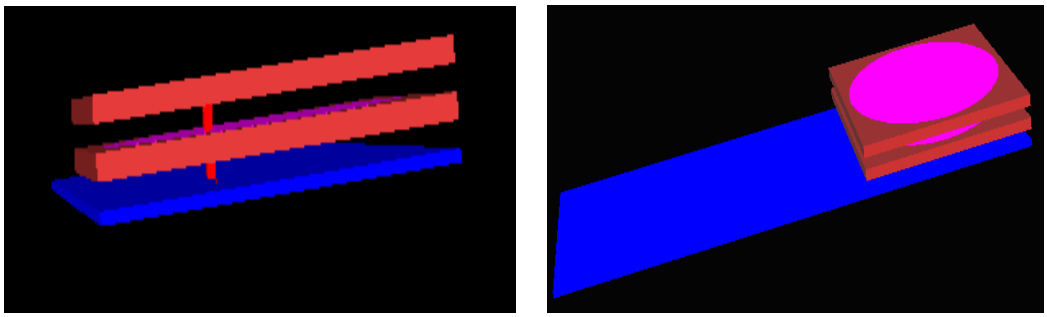

Figure 4.2 Structure of single feed circular patch antenna

Here the top patch has radius of 1.85cm and the lower patch has radius of 1.81cm and the spacing between the discs is 0.4cm and the spacing between the lower disc and the ground plane is 0.4cm. The relative permitivities of the substrates is 2.2 and that of the casing is 3.85.

Results:

(a) Voltage wave forms as seen at the input terminal of the antenna

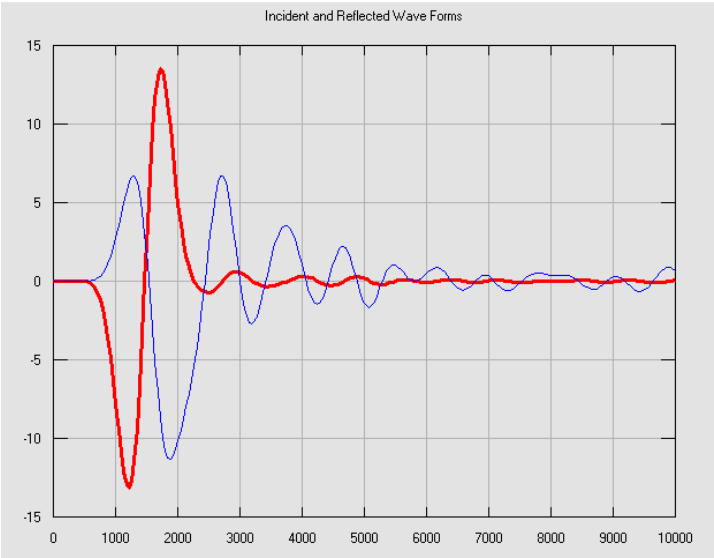

Fig 4.2a Incident and reflected wave forms

(b) Returnloss : the magnitude of the RL at 1975MHz and 2450MHz are 8.2dB and 17dB.

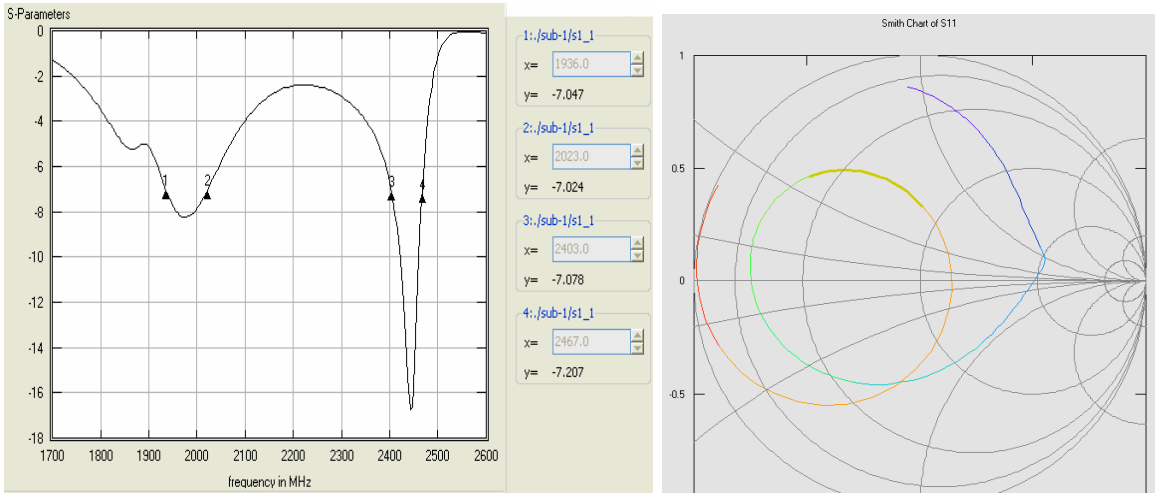

(i) (ii)

Fig 4.2b: (i) Returnloss graph and (ii) Returnloss on Smith Chart

(c) Bandwidth (for $RL \leq -7dB$): the first frequency of operation is for IMT 2000 with bandwidth of 87MHZ (1936 -2023 MHz) and the second frequency of operation is for Bluetooth service with bandwidth of 64MHz (2403 – 2467 MHz). The impedance BW is taken for the range of frequencies for which the antenna is well matched at its input. That is the BW for which $RL \leq -9dB$ or $\text{VSWR} \leq 2$. Thus this antenna structure has an impedance BW of 215MHz (2148-2463MHz) around bluetooth band. Around IMT the performance degrades and the impedance BW becomes 0. Its plot is shown below. The input impedance can be as low as 1%.

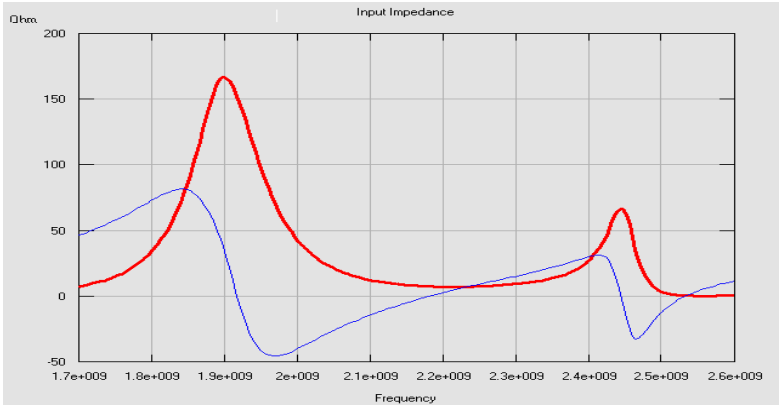

Fig 4.2c Input impedance graph (dark or red is real and light or blue is imaginary part)

(d) Radiation pattern: at 1950 MHz the radiation is almost isotropic. At 2450MHz the pattern is more directive. In both cases the pattern maximum tilts towards the positive x-axis.

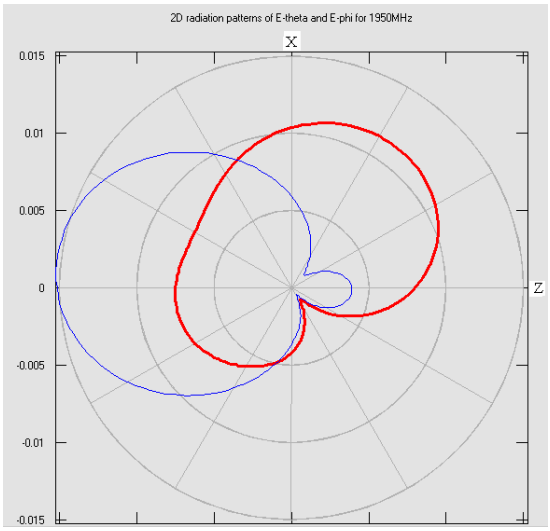

(i)

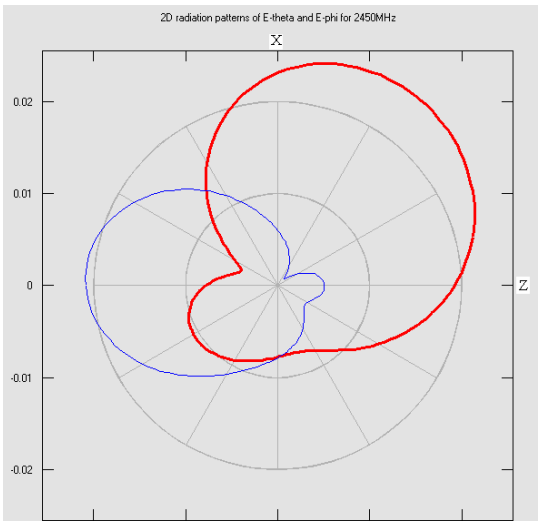

(ii)

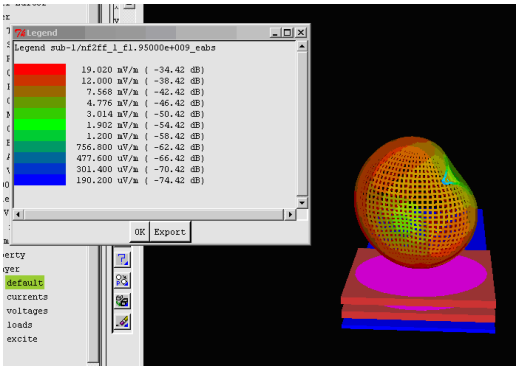

(iii)

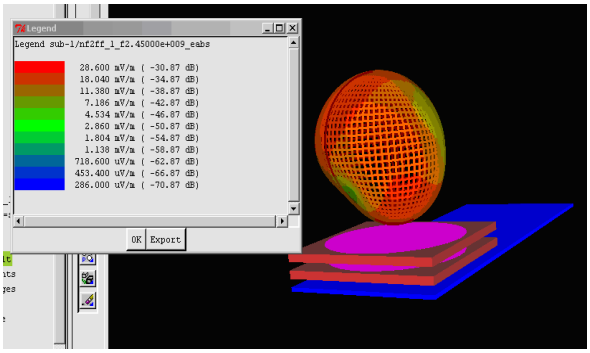

(iv)

Fig 4.2d (i) and (iii) & (ii) and (iv) are the 2D and 3D radiation patterns of 1950 MHz and 2450MHz, respectively.

General remark : Eventhough this dualband antenna structure exhibits sufficient band width around the IMT and Bluetooth service bands with good performance ($|S_{11}| \leq 7dB$) and has simple configuration, the alignment process together with the feeding mechanism is very difficult to implement.

B. Two input stacked discs

Here radius of the upper circular patch is 1.4cm and that of the lower circular patch is 1.95cm. The separation between the two patches is 0.5cm and thes eparation between between the ground plane and the lower patch is taken to be 0.3cm. The substrates have $\varepsilon_r = 3$ and the casing has $\varepsilon_r = 9.4$.

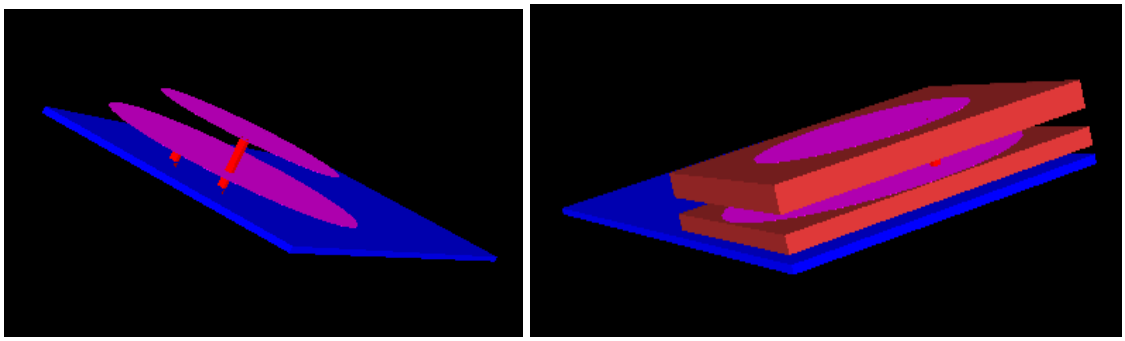

Fig 4.3 Structure of two input stacked disc patch antenna

Results:

(a) Incident and reflected voltage wave forms in time domain

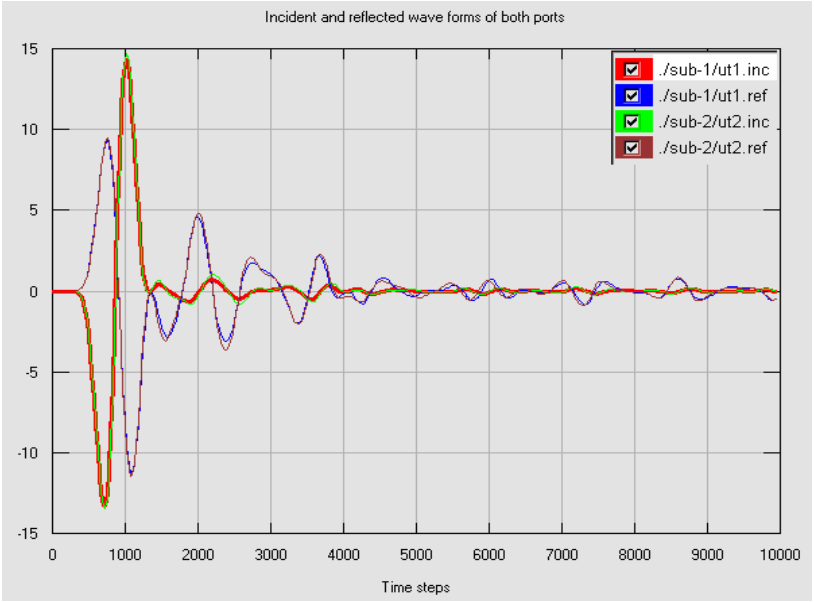

Fig 4.3a Incident and reflected wave forms at both pors.

We can see that at both inputs the incident and reflected wave forms are the same (i.e.incident waves at both inputs are the same and reflected waves at both inputs are the same). This shows that both feeds are matched to the same input impedance of a transmission line.

(b) Returnloss: The target frequency ratio for this antenna is 2:1. This antenna can operate around GSM1900 at 1944MHz, around IMT2000 at 2059MHz and around Bluetooth at 2450MHz for $RL \leq -4.5dB$, the value which is common for both ports

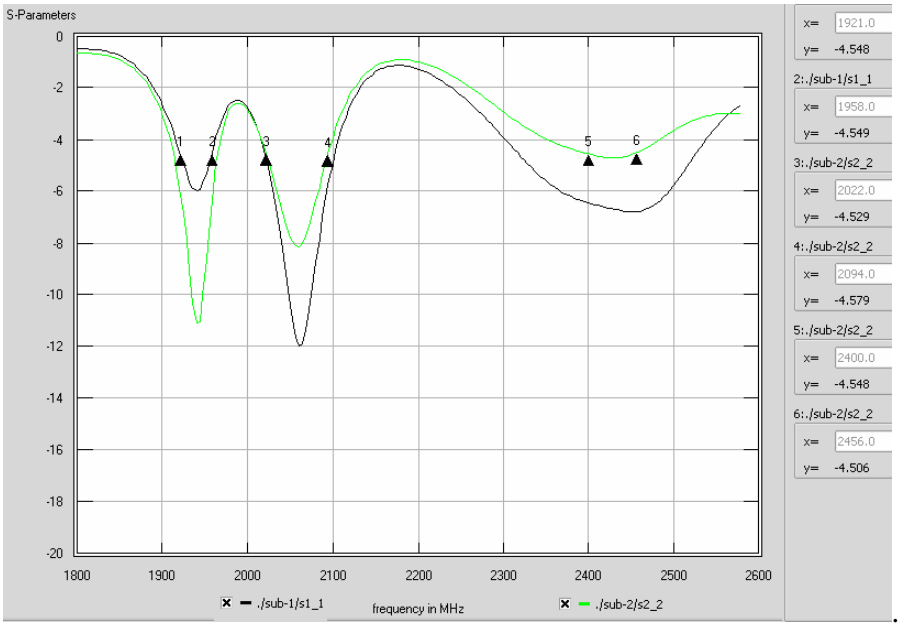

(i)

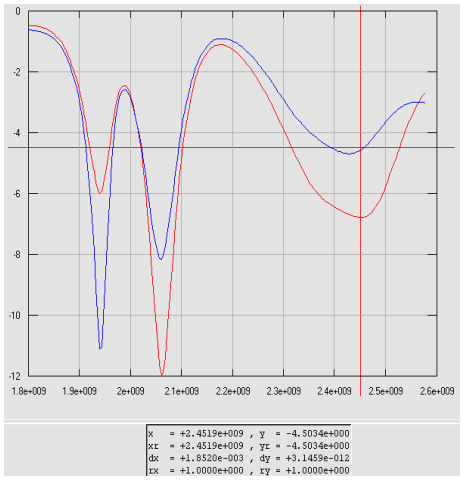

(ii)

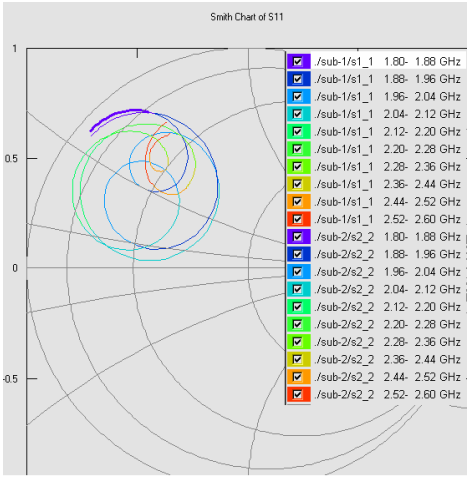

(iii)

Fig 4.3 b: (i) and (ii) returnloss graphs and (iii) returnloss on a Smith Chart.

(c) Band width and Impedance BW: for $RL \leq -4.5dB$ around GSM 1900 the BW is 37 MHz (1921 – 1958 MHz), around IMT2000 the BW is 72 MHz (2022-2094 MHz) and around bluetooth the BW is 56MHz (2400-2456MHz). Compared to the actual regulatory standards the BWs are narrow. Since the above three bands are measured for $RL \leq -4.5dB$ and doesn't meet the standard value ($RL \leq -9dB$), then the impedance BW in each band can be considered to be zero.

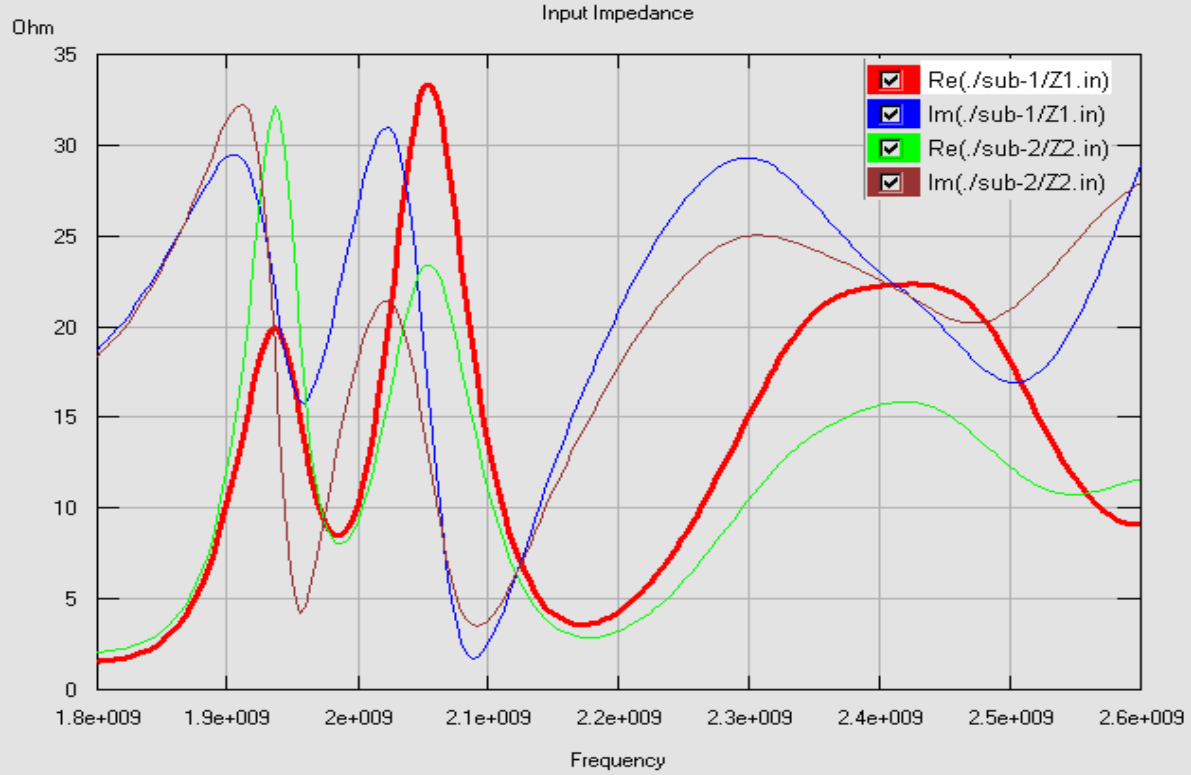

Fig 4.3d Input impedance at both ports (the black and light ones are real parts and the rest are imaginary parts)

(d) Radiation pattern: At 1944MHz the radiation pattern is somehow distorted isotropic, at 2059MHz it is almost isotropic and at 2462MHz it is somehow directive and complex whose maximum pattern alligns itself almost with the X-axis. The 2D and 3D patterns are shown below.

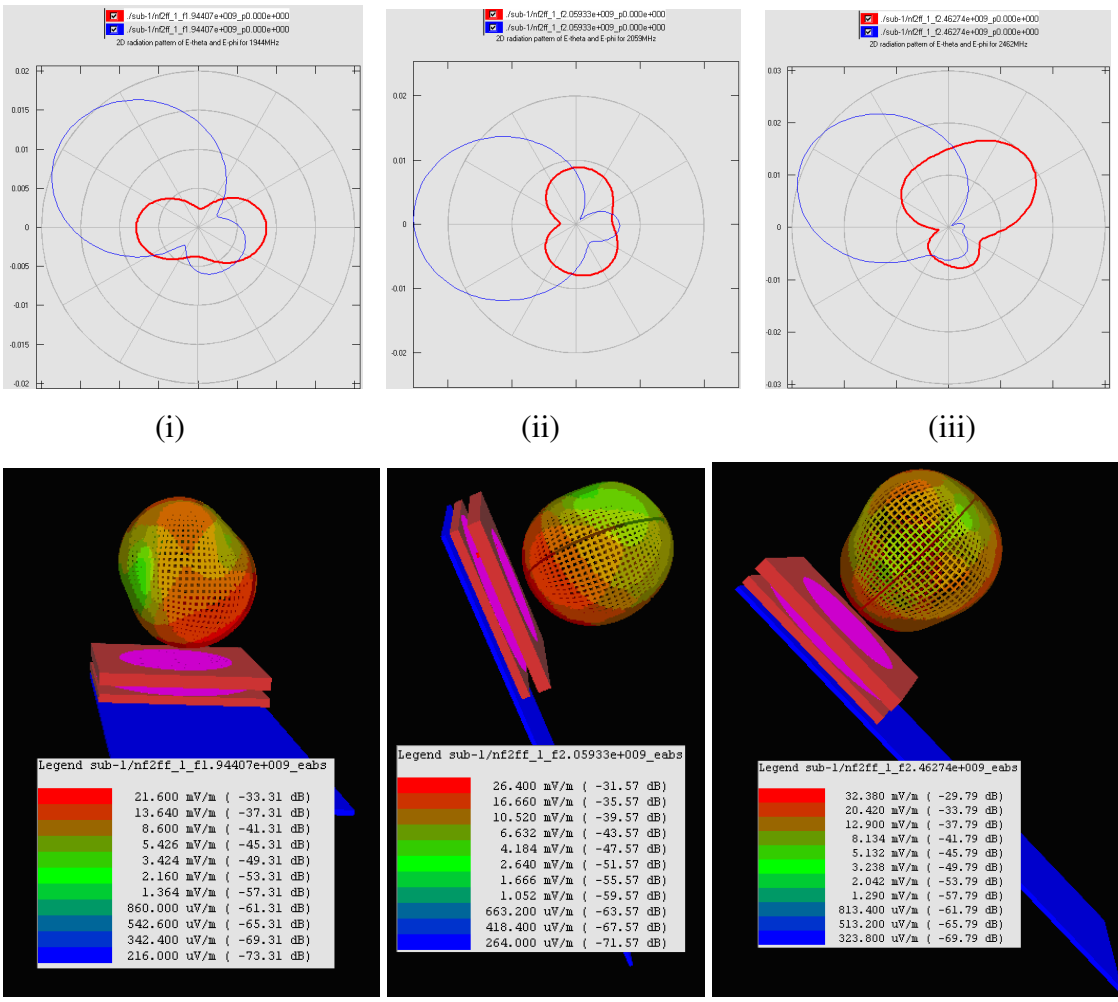

Fig 4.3d: (i)&(iv), (ii)&(v), (iii)&(vi) are the 2D and 3D radiation patterns for 1944MHz, 2059MHz, 2462MHz, respectively.

General remark: For this antenna to operate at the specified bands there is a price paid. That is its performance is decreased as the magnitude of S_{11} is decreased to 4.5dB below the regulatory standard.

(C) Stacked Rings

The overall structure can be viewed as two coupled ring cavities. The inner radius is taken to be 1cm and the outer radius to be 1.95cm. The lower and the upper rings are separated by 0.25cm. The separation between the ground plane and that of the lower ring is 0.55cm. Frequency separation can be altered by the adjustable air gap inserted between

the lower ring and the upper substrate. The antenna is feed near the inner edge of the upper disc. The substrates have $\varepsilon_r = 4.1$ and the casing has $\varepsilon_r = 16$.

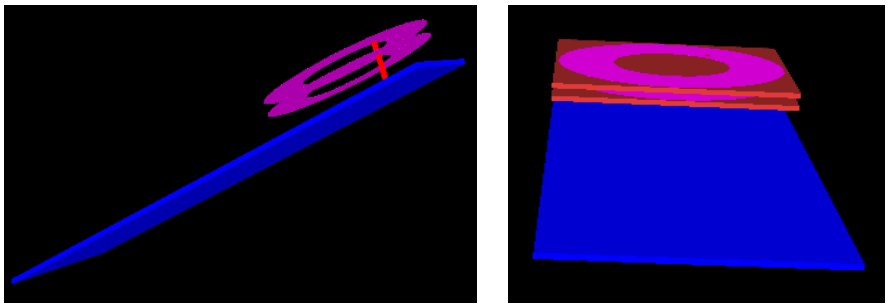

Fig 4.4 Structure of stacked rings microstrip patch antennas

Results:

(a) Incident and reflected wave forms

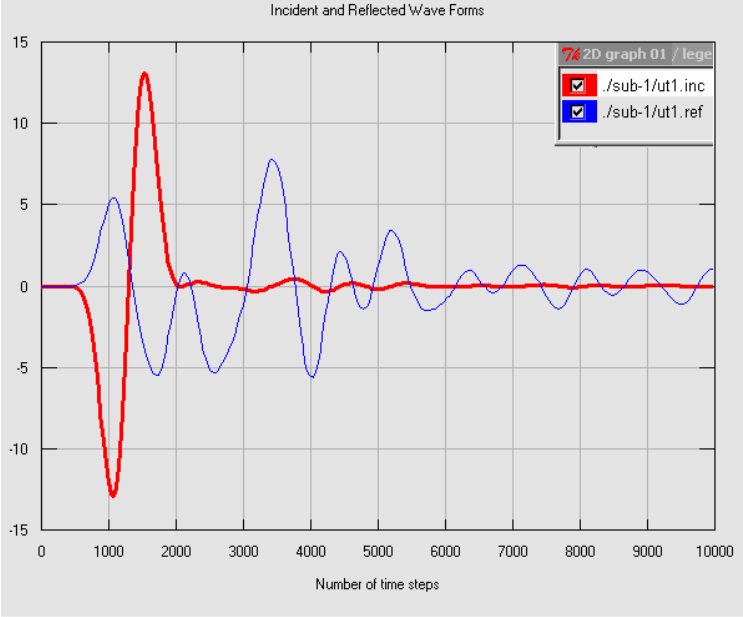

Fi g 4.4a Incident and reflected wave forms

(b) Returnloss

This antenna operates around GSM900, GSM1800 and bluetooth service bands.

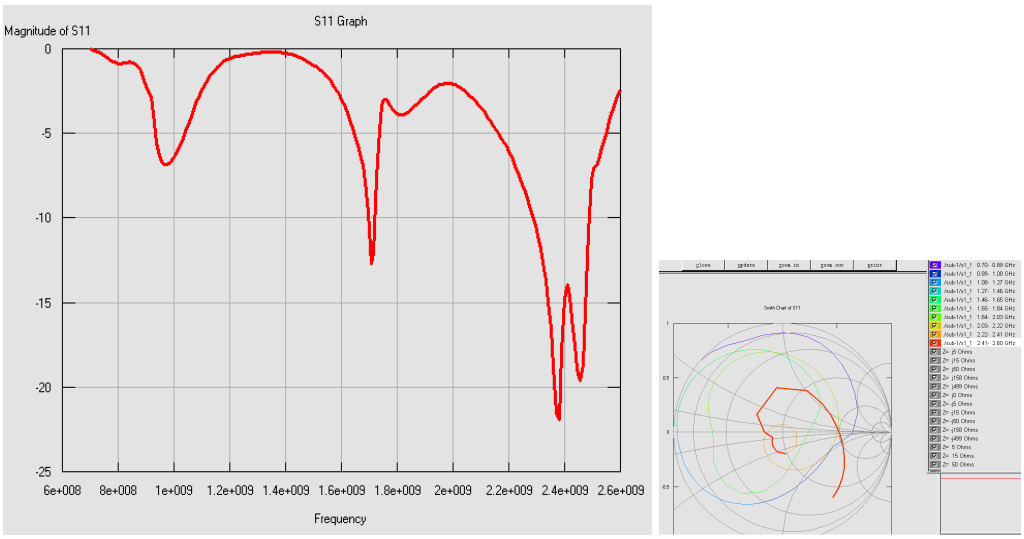

(i) (ii)

Fig 4.4b (i) Returnloss graph and (ii) Smith Chart of returnloss

(c) Band width: Around GSM900 the BW is 26MHz (934-960MHz), 26MHz around GSM1800 (1710-1726MHz) and 610MHz around bluetooth service and IMT (1885-2500MHz)band. The impedance BW for $RL \leq -9dB$ around GSM900 is zero, around GSM1800 is 13MHz (very narrow compared to the standard BW) from1710MHz to 1723MHz and around blutooth band 92MHz (2400-2492MHz) which is almost equivalent to the standard BW.

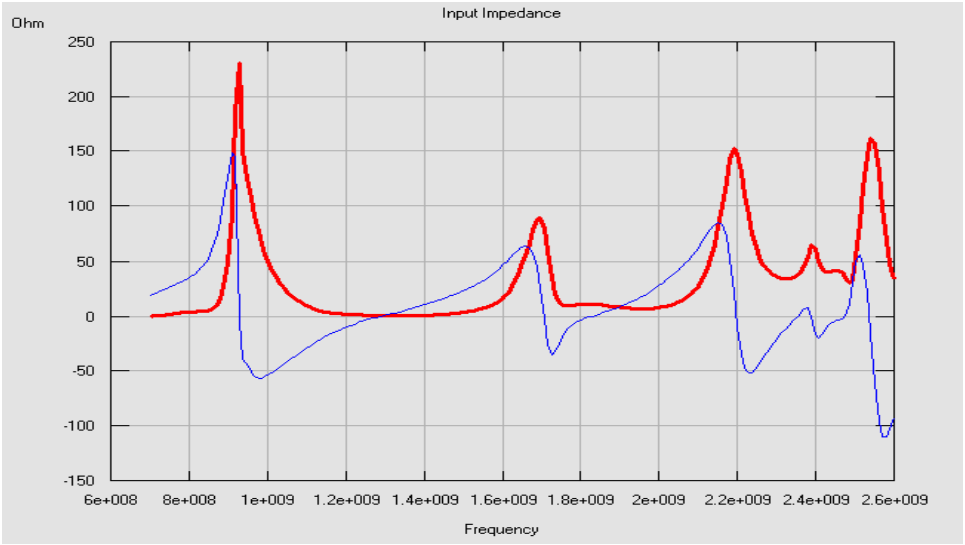

Fig 4.4c Input impedance graph

(d) Radiation Pattern: At 953MHz the pattern is directive and the pattern maximum is tilted from the negative X-axis towards the positive Z-axis. At 1713MHz the pattern is some how isotropic and at 2473MHz it is almost isotropic.

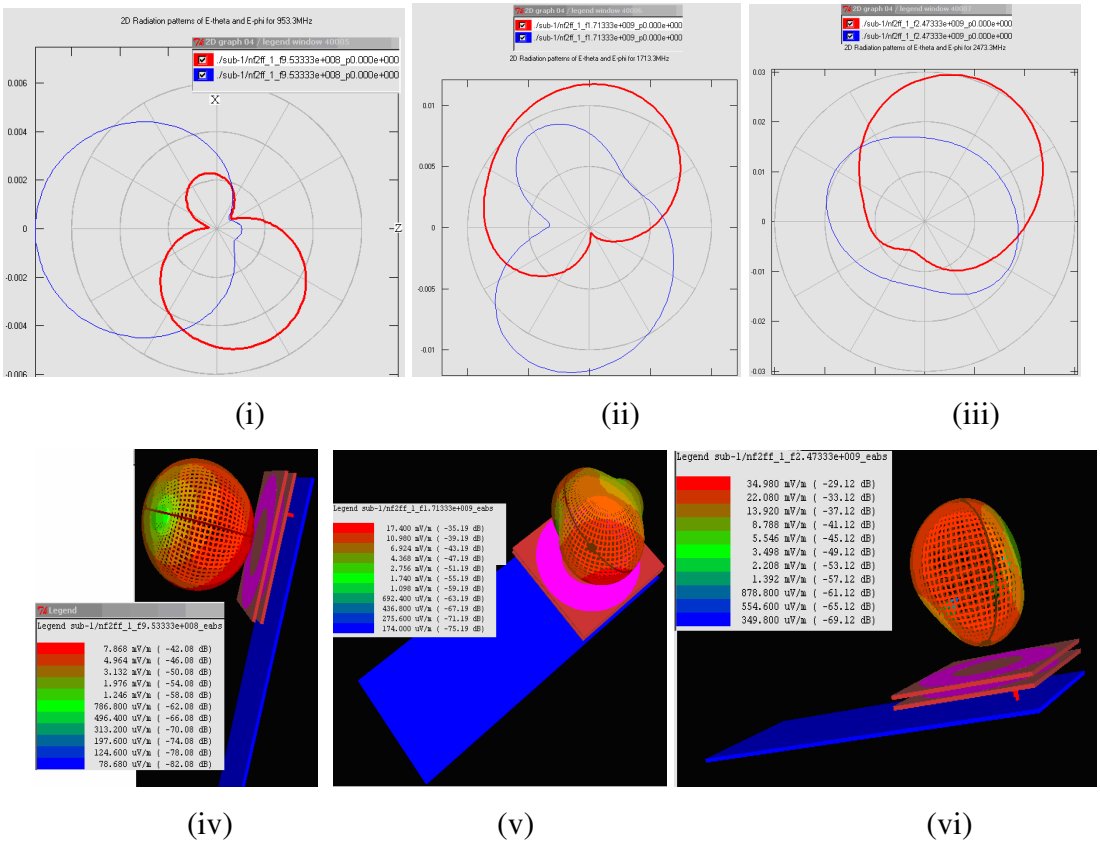

(i) (ii) (iii)

(iv) (v) (vi)

Fig 4.4d (i)&(iv), (ii)&(v), (iii)&(vi) are the 2D and 3D radiation patterns for 953MHz, 1713MHz, 2473MHz, respectively

Remark: Compared to the theoterical value of RL where antenna performs best for $RL \leq -9dB$ the performance of this structure is less around GSM900 and GSM1800 as $RL \leq -5dB$. And also in these bands the measured BWs are small compared to the regulatory BWs. But around Bluetooth band the antenna meets the regulatory BW standards. In this band the antenna has best performance as the BW can be found for $RL \leq -9dB$.

D. Planar Dual Band Patch Antenna

It consisted of multiple layers with metallic strips placed at one of the dielectric interfaces under the radiating patch. The separation between the upper main patch and the lower strips of patches is 0.45cm and the separation between the lower patches and the ground plane is 0.35cm. The dielectric constants of the upper and lower substrates are $\varepsilon_r = 6.0$ *and* $\varepsilon_r = 2.2$. The casing has $\varepsilon_r = 4.1$.

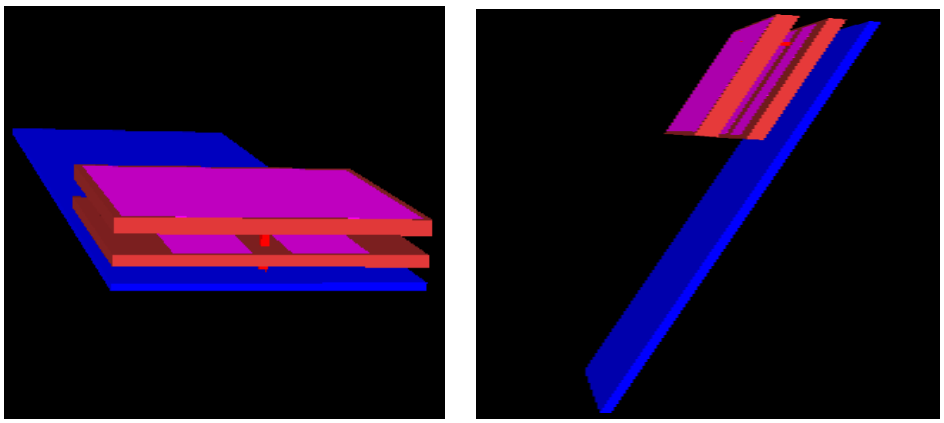

Fig 4.5 Structure of the planar dual band patch antenna.

Results:

(a) Incdent and reflected wave forms

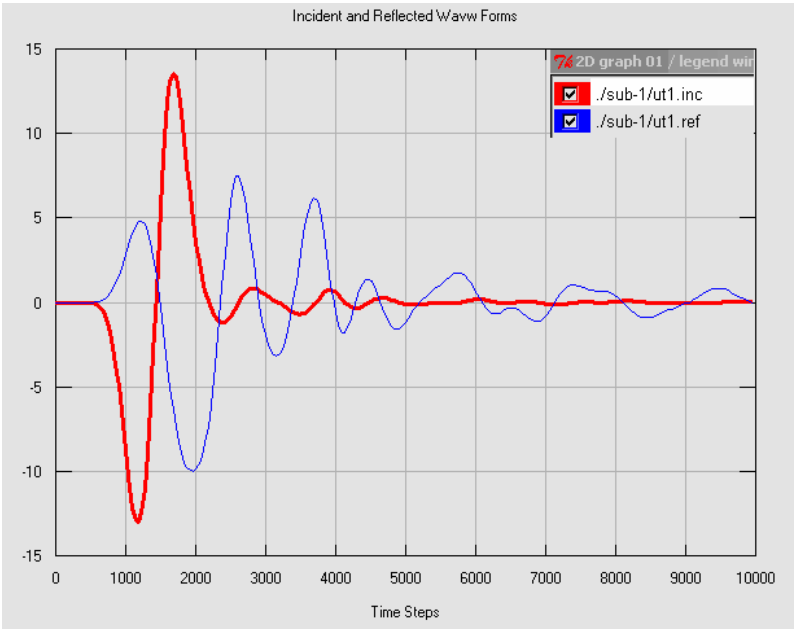

Fig 4.5a Incident and reflected wave forms.

(b) Returnloss

For this antenna resonance is occurred around GSM900 (maximum of $RL = -25dB$), IMT (maximum of $RL = -6.1dB$)and Bluetooth (maximum of $RL = -9dB$) bands.

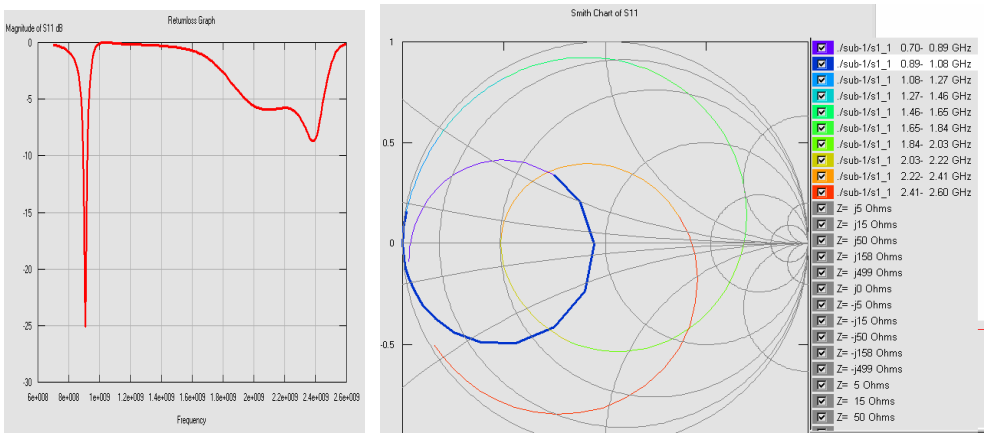

(i) (ii)

Fig 4.5b (i) Returnloss graph and (ii) Smith Chart of reurnloss

(c) Band width and Input impedance bandwidth: The band width is measured for $RL \le -5.5dB$. Around GSM900 it is 46MHz (884-930MHz), around IMT it is 204MHz (1996-2200MHz) and around Bluetooth it is 50MHz (2400-2450MHz). Since the impedance BW is defined as the frequency of band for which we can get acceptable vcalue of returnloss ($RL \le -9dB$) or VSWR (VSWR ≤ 2), then around GSM900 we have 30MHz (896-926MHz) and around IMT and Bluetooth the impedance bandwidth does not exist. This means the antenna is not verywell matched at these bands provided that its performance also degraded. The plot of impedance is also shown.

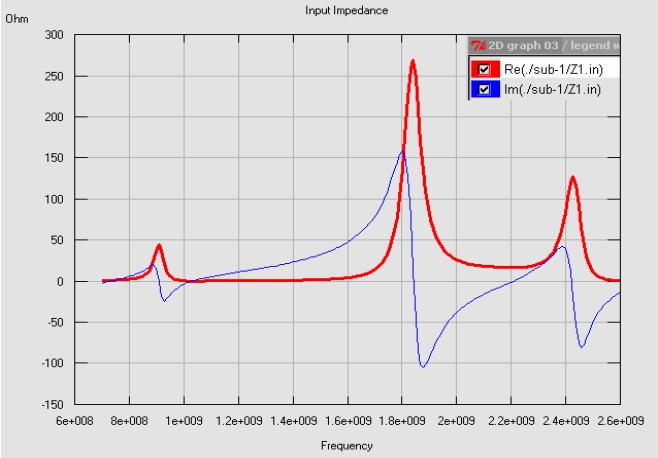

Fig 4.5 c Input impedance curve(the dark is real and the light is imaginary part)

(d) Radiation pattern: At 919MHz, 2161MHz and 2427MHz the pattern is almost omnidirectional and looks like that of a half-wave dipole.

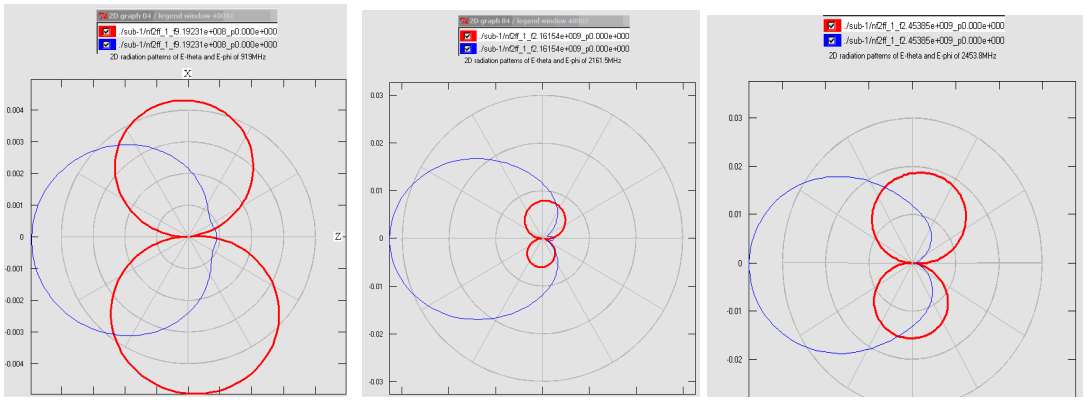

(i) (ii) (iii)

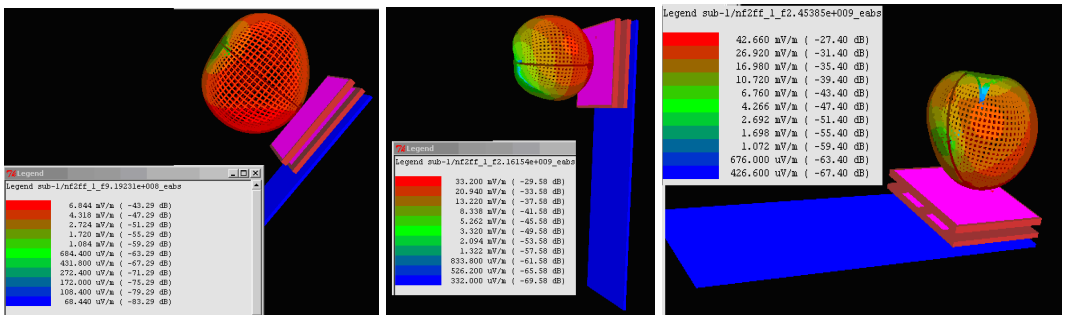

(iv) (v) (vi)

Fig 4.5d (i)&(iv), (ii)&(v), (iii)&(vi) are the 2D and 3D radition pattens for 919MHz, 2161MHz, 2427MHz, respectively.

Remark: Eventhough the impedance BW doesn't meet the regulatory standard, its performance is best around GSM900. However, its performance degrades around IMT and Bluetooth bands as $|S_{11}| < 9dB$. Compared with the stacked dualband microstrip antenna, this antenna is free from any unwanted scattering, because al1 the modification is under the main patch. Another advantage of the antenna is that bandwidths at two frequencies can be adjusted separately. The widening of the two bandwidths at each operating frequency can be achieved by increasing the corresponding layer thickness while maintaining the effective dielectric constant fixed in the region. However, the antenna design is too difficult to implement and fabricate.

E. Aperture Coupled Microstrip Antenna Loaded With Two Slots

To obtain a dual band operation two slots parallel to the coupling aperture are cut. The aperture slot has dimensions of $2.9cmx0.5cm$. The widths of the slots are 0.2cm which are extracted from a rectangular patch of dimensions $39cmx31cm$. The port here used is the stripline port coupled with te main patch through the slot on the ground plane. In this structure the substrates above and below the ground plane have $\varepsilon_r = 2.2$ and that of the casing has $\varepsilon_r = 2.615$.

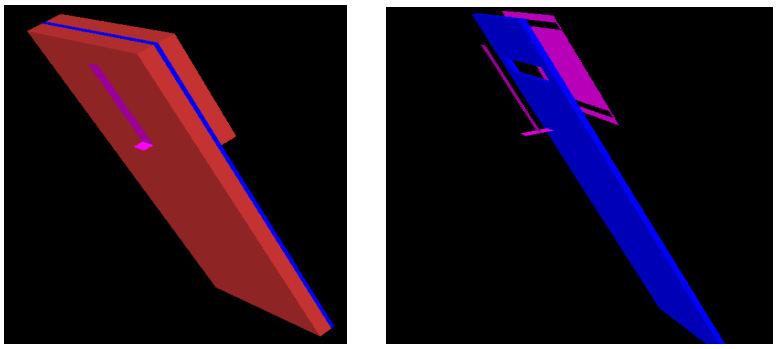

Fig 4.6 General structure of aperture coupled patch antenna

Results:

(a) Incident and reflected wave forms:

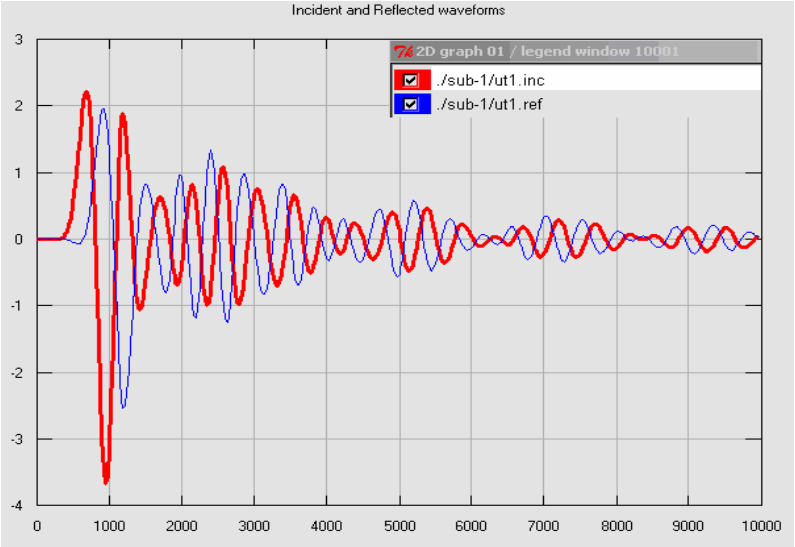

Fig 4.6a Incident and reflected wavef orms

(b) Returnloss: The frequency of operation is around GSM1800 and Bluetooth bands. At 1800MHz $|S_{11}| = 22dB$ and at 2466.67MHz $|S_{11}| = 5.73dB$.

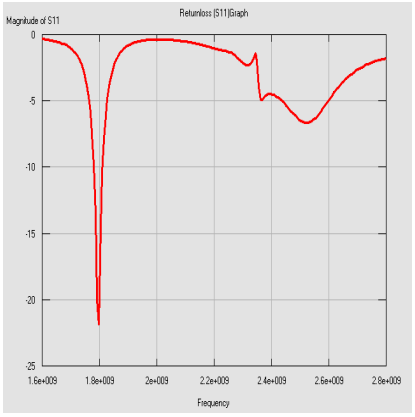

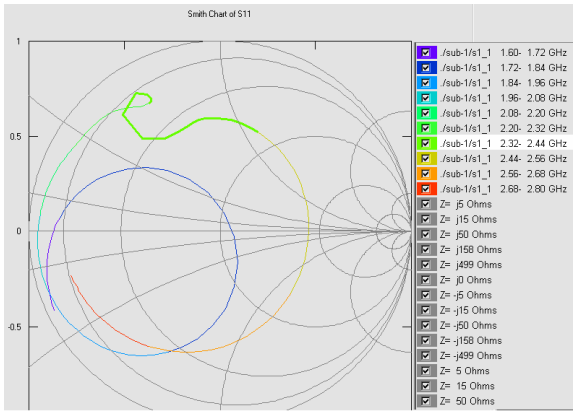

(i) (ii)

Fig 4.6b (i) Graph of returnloss (ii) Smith Chart of the returnloss

(c) Radiation Pattern: At both frequencies the radiation pattern is almost isotropic but somehow directive at 1800MHz.

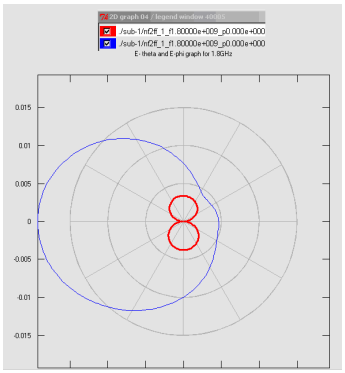

(i)

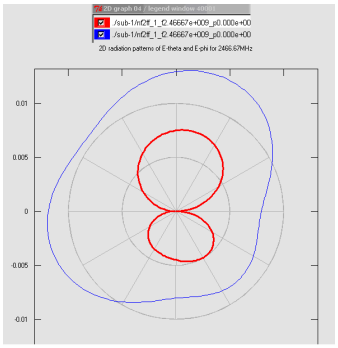

(ii)

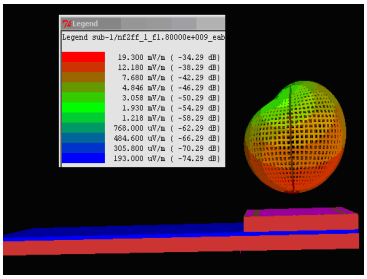

(iii)

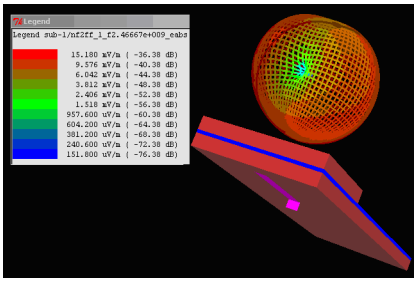

(iv)

Fig 4.6c (i)&(iii), (ii)&(Iv) are the 2D and 3D radition patterns for 1800MHz, 24667MHz, respectively.

(d) Band width and Impedance band width: around GSM1800 the bandwidth is 64MHz (1763-1827MHZ) and around blutooth the BW is 62MHz (2438-2500MHZ) for $RL \leq -5dB$. The antenna is very well matched around GSM1800 for $RL \leq -9dB$. That is the impedance BW around GSM1800 is 34Mhz (1779-1813MHz).Around Bluetooth band since the performance is degraded, then the impedance BW is zero. In both bands at the frequency of operation the real part is maximum and the imaginary part is minimum (zero).

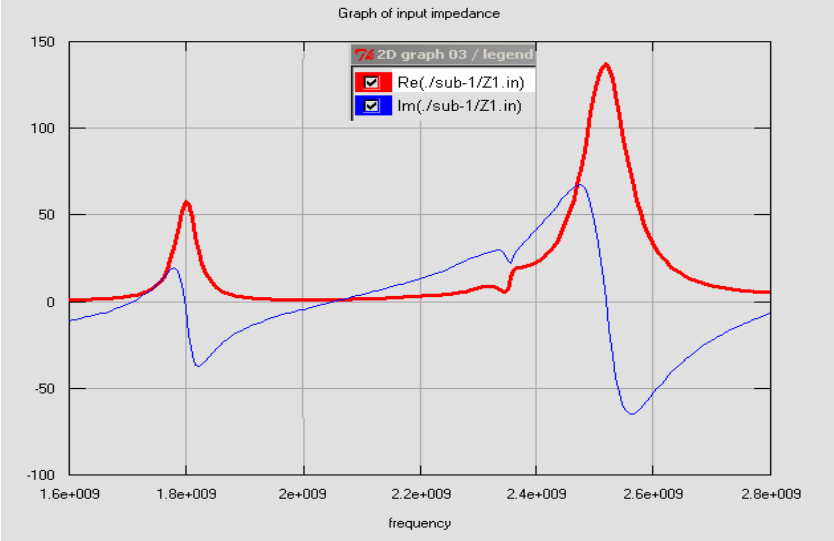

Fig 4.6d Input impedance curve (dark is real part and light is imaginary part)

Remark: The performance of this antenna around GSM1800 is good though doesn't exploit all the standard frequency range however its performance degarades around Bluetooth band as $|RL|$ is not in the accepted range of value ($RL \leq -9dB$). The main disadvantage of this design is that having the slots embedded in the radiating edges of the patch causes distortions in the radiation pattern and increases the cross polarization levels.

F. Shorting Pins Loaded Patch Antenna

A rectangular patch of dimensions $2.55cmx3.9cm$ is loaded with six shorting pins. The substrate has $\varepsilon_r = 4.4$ and that of the casing has $\varepsilon_r = 8.4$. A stripline feed which is matched to a 50Ω line is used, as shown.

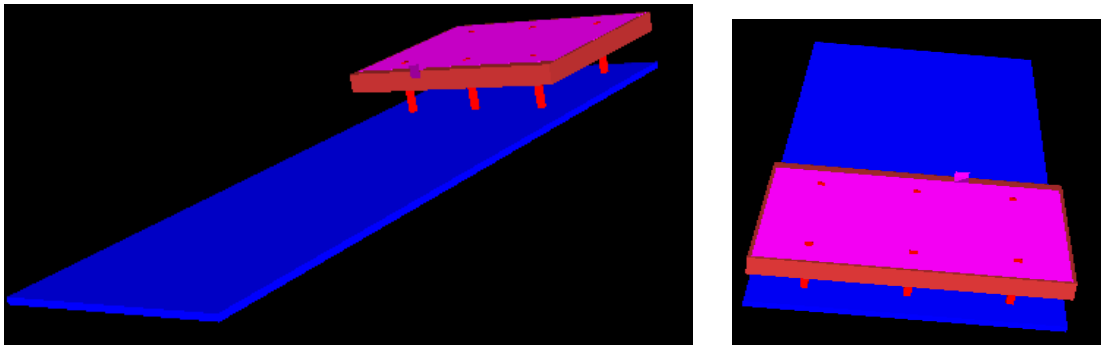

Fig 4.7 Structure shorting pins loaded patch antenna

Results:

(a) Incident and reflected wave forms:

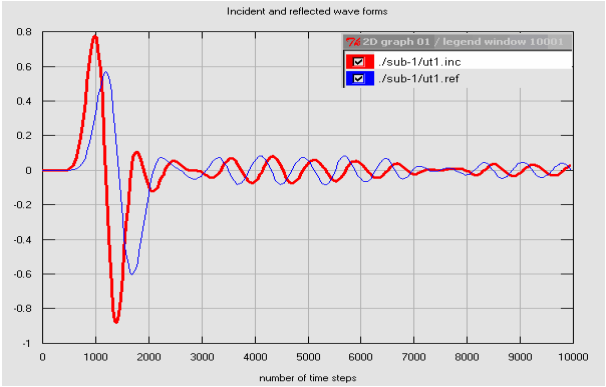

Fig 4.7a Incident and reflected wave forms

(b) Returnloss: The returnloss graph shows that the frequency operations are around GSM1800, IMT and Bluetooth bands. In each of these bands the performance of the antenna meets the standard as $RL \leq -9dB$.

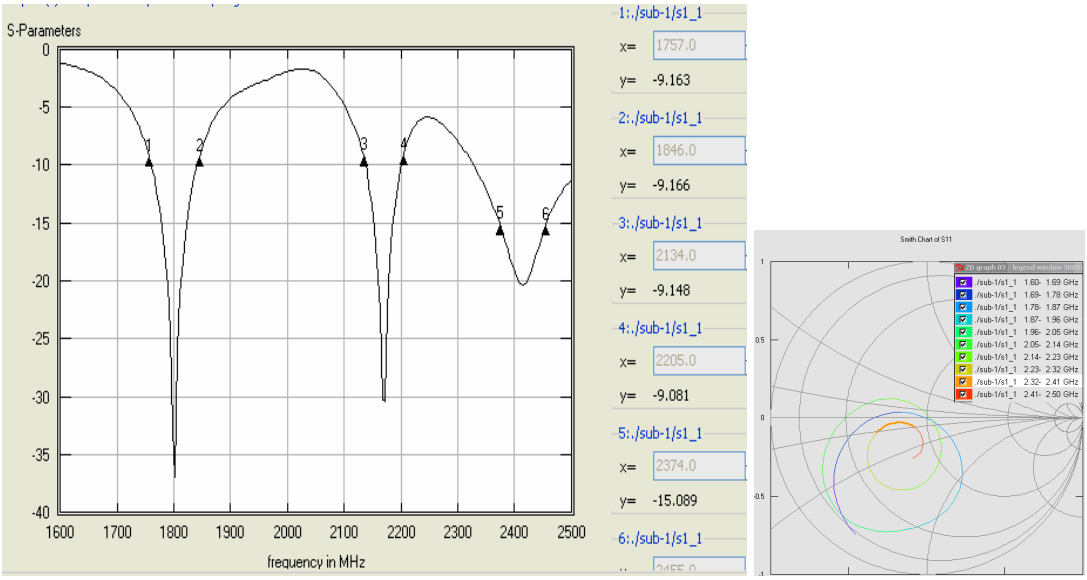

(i) (ii)

Fig 4.7b (i) Returnloss graph and (ii) Smith Chart of returnloss

(c) Radiation Pattern: At 1780MHz the pattern is almost omnidirectional except that the pattern maximum is slightly deviated from the X-axis. At 2140MHz the pattern is somehow directive whose pattern maximum is tilted from the +X-axis to the +Z-axis and at 2440MHz the pattern is almost isotropic.

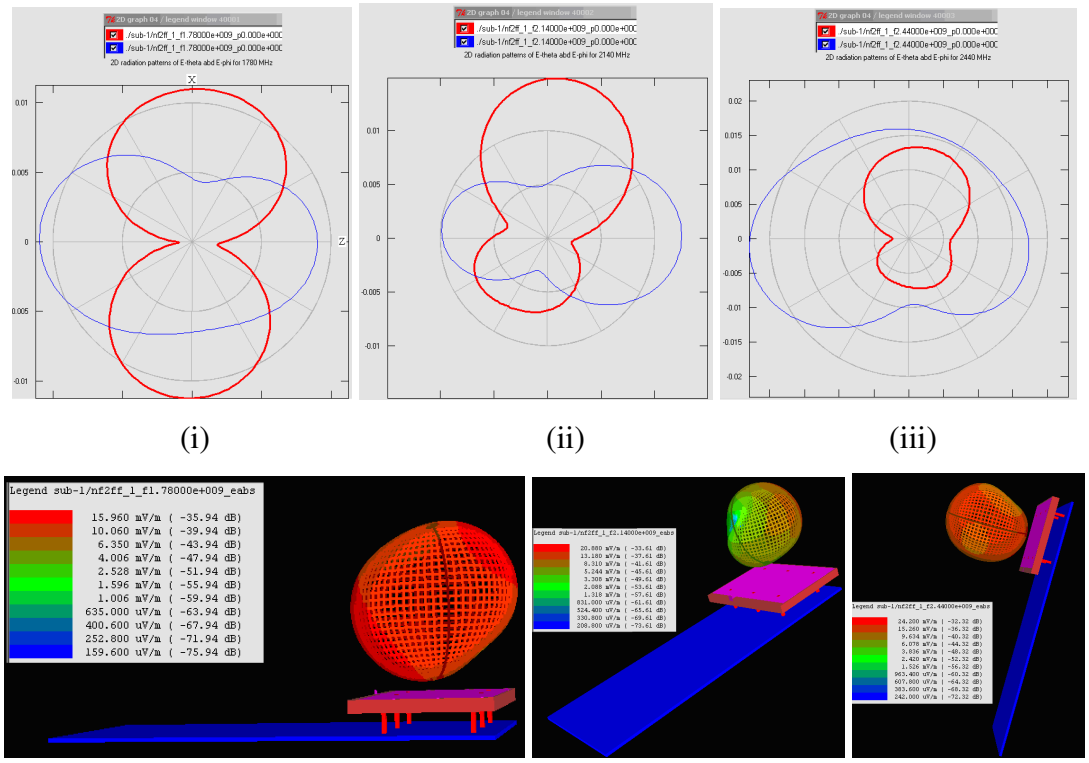

(i) (ii) (iii)

(iv) (v) (vi)

Fig 4.7c (i)&(iv), (ii)&(v), (iii)&(vi) are the 2D and 3D radiation patttens for 1780MHz, 2140MHz,2440MHz frequencies, respectively.

(d) Band width and Impedance band width: around GSM1800 the BW is 89MHz (1757-1846MHz)and around IMT the BW is 71MHz (2134-2205MHz). Around bluetooth where $RL \leq -11.5dB$ the BW is 100MHz (2400-2500MHz). The BWs found for each band can also be considered as the impedance BW as $RL \leq -9dB$.

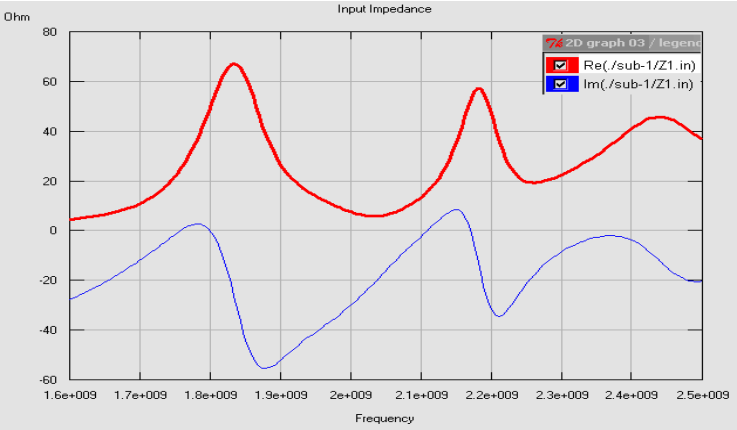

Fig 4.7d input impedance curve (dark is real part and light is imaginary part)

Remark: The antenna has good performance in each of the above bands ($RL \le -9dB$). However, the BW meets the regulatory standard value only in the bluetooth band. In GSM1800 and IMT bands compared to the regulatory standard values the BWs are narrow. The size, weight, thickness and materials used are not diiferent from the ordinary patch antennas. The difficulty is that the bands couldnot be made arbitrarily close and that the shorting pins complicate the fabrication process.

G. Stubloaded Patch Antenna

A rectangular patch antenna ($3.9cmx3.1cm$) loaded with a variable length short-circuited coaxial stub is considered. The length of the stub can be varied from 0-25cm and in this case I considered 1.6cm. The substrate has $\varepsilon_r = 2.2$ and that of the casing has $\varepsilon_r = 2.85$. The characteristic impedance of the stub is 49.81Ω.

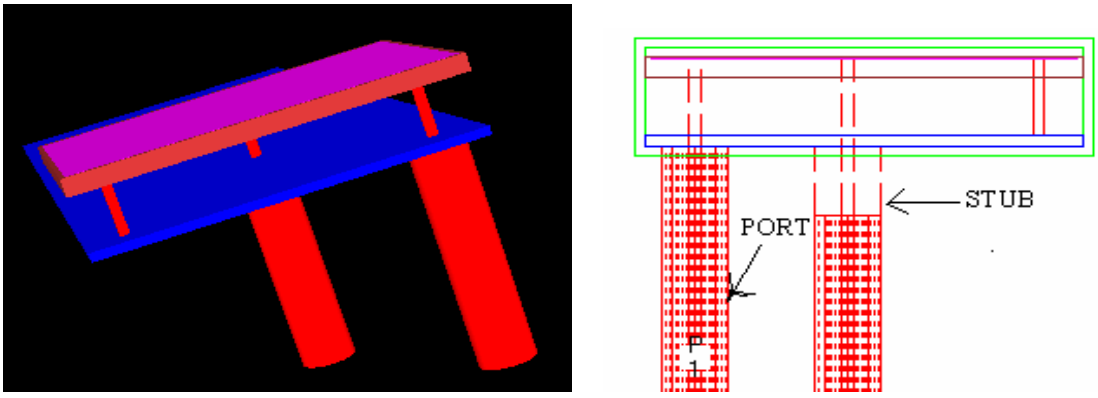

Fig 4.8 Structure of stubloaded patch antenna

Results:

(a) Incident and reflected waveforms

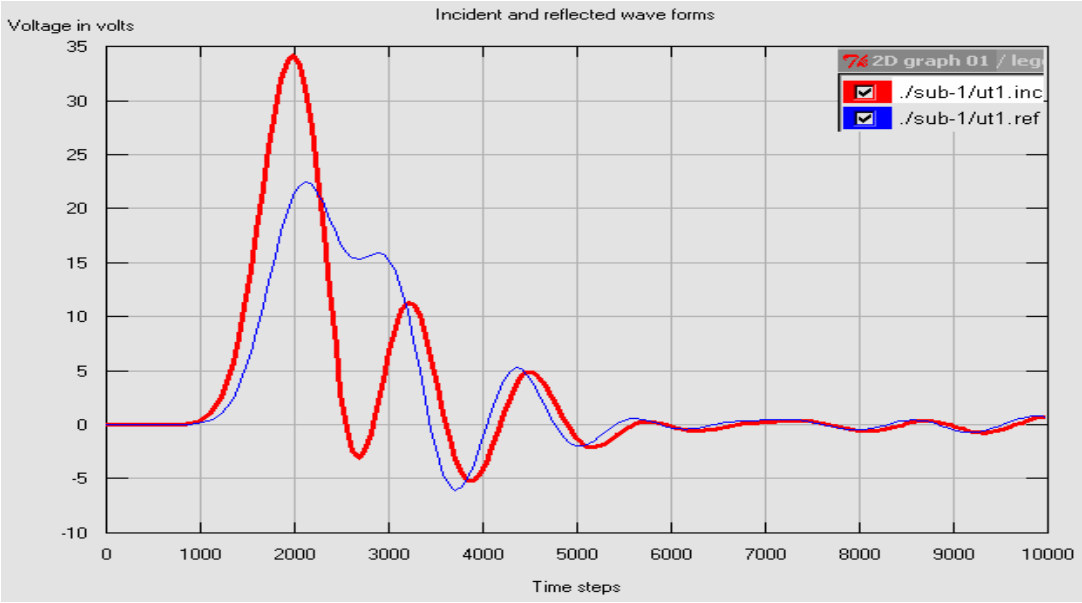

Fig 4.8a Incident and reflected wave forms at the input of the antenna

(b) Returnloss: This antenna can operate around GSM1800, GSM1900 and IMT2000. At 1800MHz $|RL| = 12.4dB$, at 1900MHz $|RL| = 9dB$ which is boarder of the graph and at 2050MHz $|RL| = 7.8dB$.

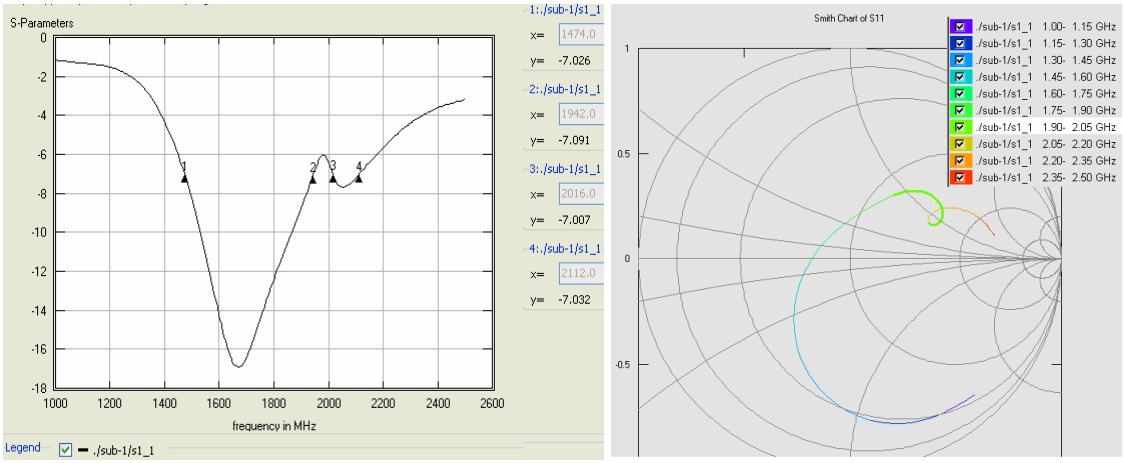

(i) (ii)

Fig 4.8b (i) Returnloss graph and (ii) Smith Chart of returnloss

(c) Bandwidth and impedance bandwidth: BW in this case is measured for $RL \leq -7dB$ so that all bands will exist. BW is 170MHz (1710-1880MHz) around GSM1800, 92MHz (1850-1942MHz) around GSM1900 and 96MHZ (2016-2112MHz) around IMT2000. The impedance bandwidth meets the standard BW (170MHz) for GSM1800 and very narrow for GSM1900 and zero for IMT2000 (measured for $RL \leq -9dB$).

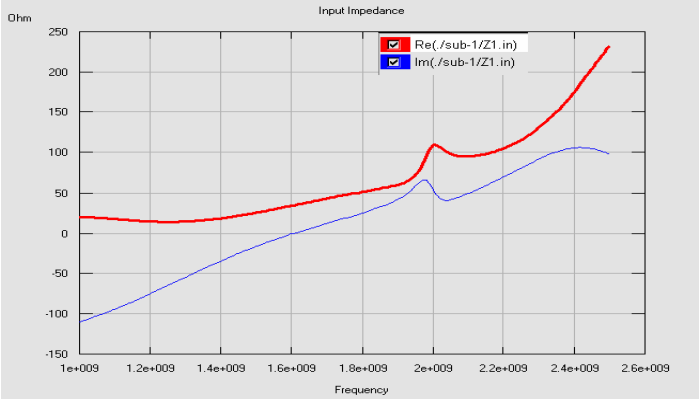

Fig 4.8c Input impedance curve (dark is real and the light one is imaginary part)

(d) Radiation patterns: The radiation pattern at 1800MHz seems omnidirectional and seems that of a half wave dipole except that the pattern maximum is slightly tilted from the -Z-axis to the +X-axis. At 1900MHz and 2050MHz the radiation patterns are almost isotropic.

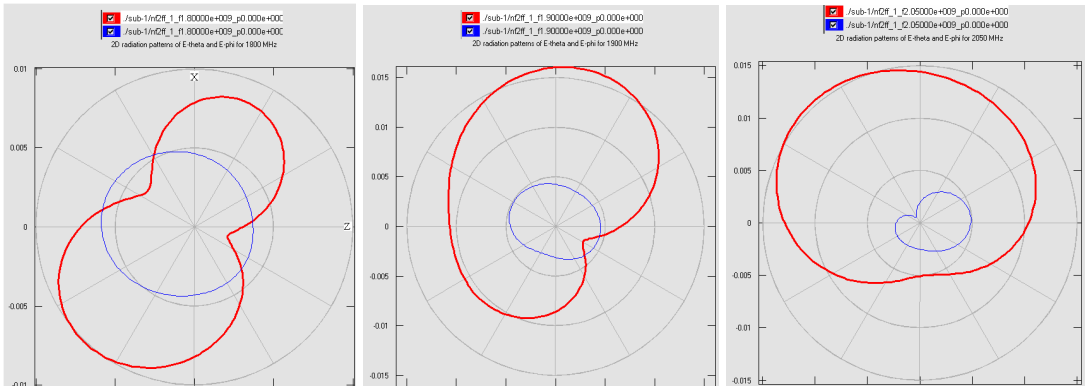

(i) (ii) (iii)

Fig 4.8d (i)&(iv), (ii)&(v), (iii)&(vi) are 2D and 3D radiation patterns at 1800MHz, 1900MHz,2050MHz, respectively.

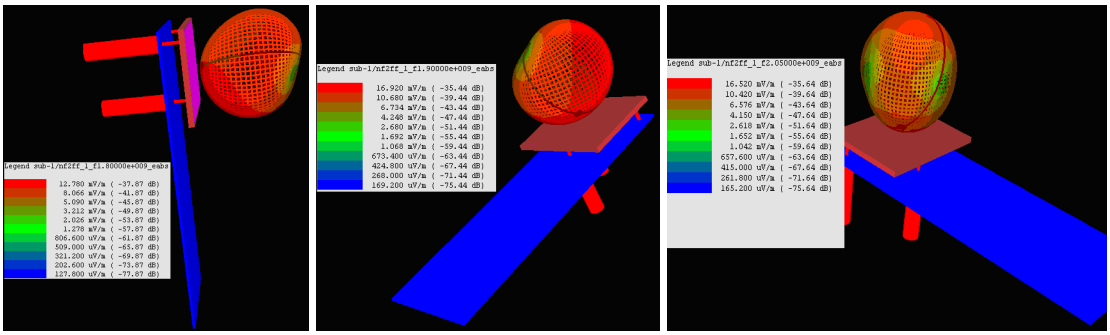

(iv) (v) (vi)

Fig 4.8d … (Continued)

Remark: Eventhough this antenna has good performance around GSM1800 and GSM1900 the antenna structure is a bit complex and impractical for integration purposes.

H. Probe Fed Slot Loaded Microstrip Patch Antenna

Dual band operation can be optained either by having a dot cut on the surface of the patch or by cutting two narrow slots close and parallel to the radiating edges of a rectangular patch. Here the main patch is $3.9cmx3.1cm$ and the slots are $0.35cmx2.7cm$. The substrate and the casing have $\varepsilon_r = 2.2 and \varepsilon_r = 11.6$, respectively.

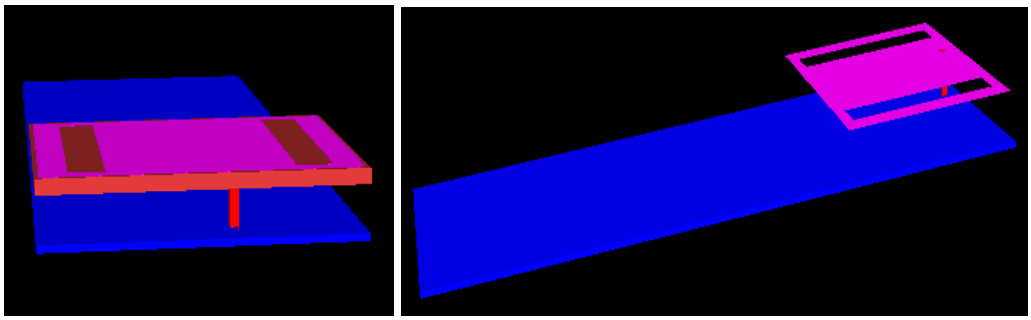

Fig 4.9 Structure of probe fed slot loaded microstrip patch antenna

Results:

(a) Incident and reflected wave forms:

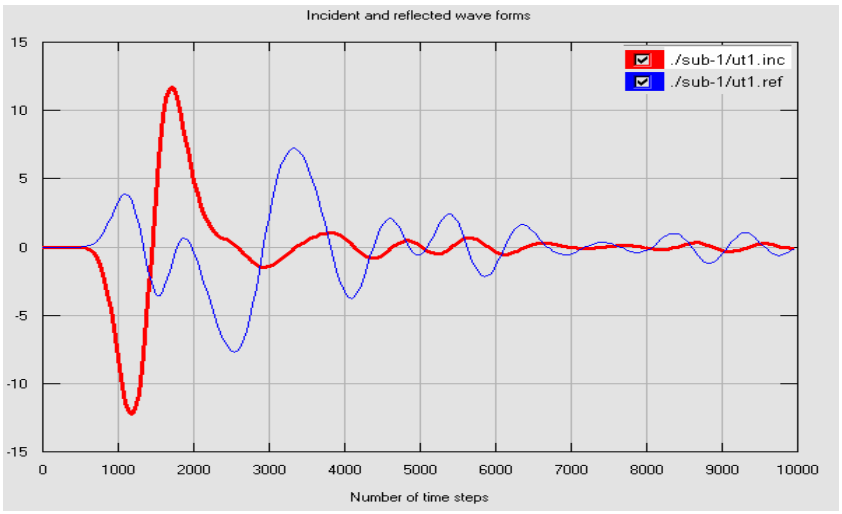

Fig 4.9a Incident and reflected wave forms at the input port

(b) Returnloss: There are two bands of frequency of operations, around GSM1800 and around IMT2000 whose $|S_{11}|$ are 9dB and 34dB, respectively.

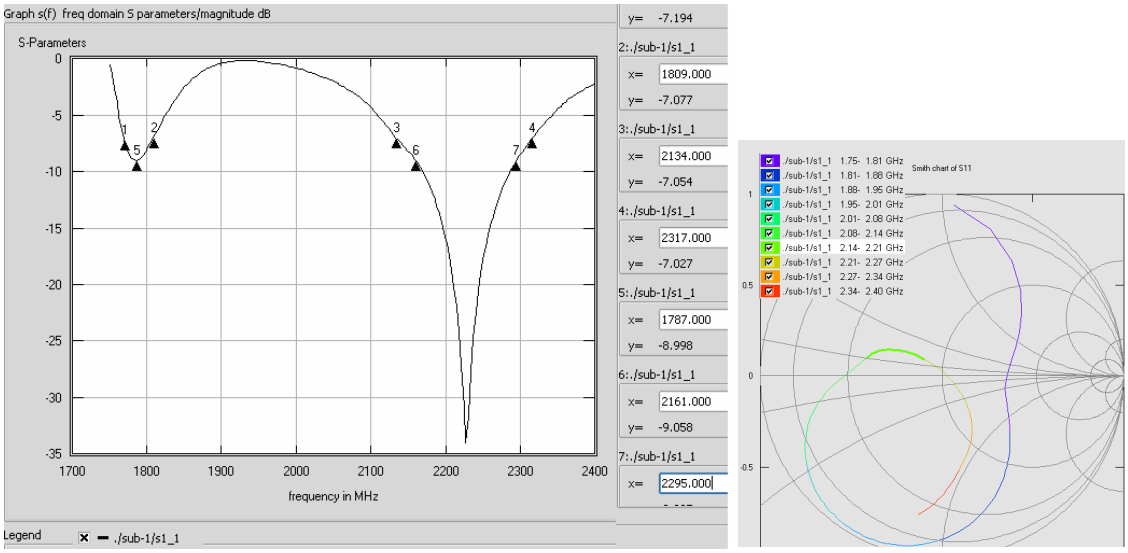

(i) (ii)

Fig 4.9b (i) Returnloss graph and (ii) Smith Chart of returnloss

(c) Band width and impedance BW: The BWs are measured for $RL \leq -7dB$. Around GSM1800 the BW is 39MHz (1770-1809MHz) and around IMT2000 the BW is 66MHz

(2134-2200MHz). The impedance BW around IMT2000 is 39MHz (2161-2200MHz) and around GSM1800 the impedance BW is almost zero.

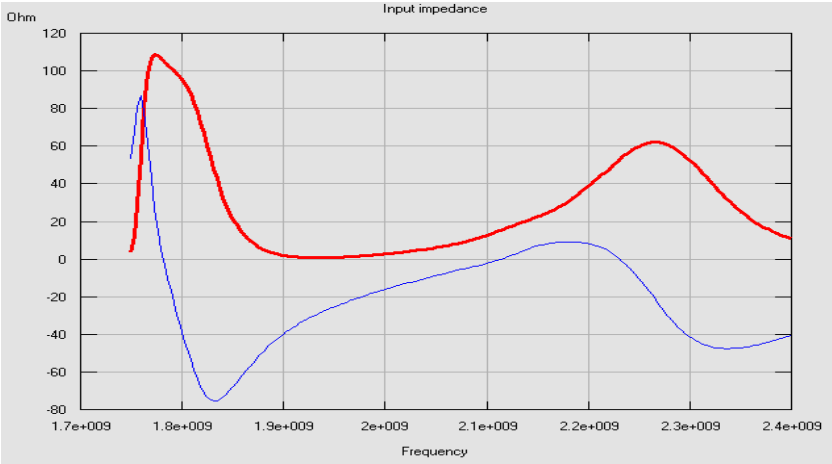

Fig 4.9c Input impedance curve

(d) Radiation pattern: At 1807.69MHz the radiation pattern is somehow directive whose maximum pattern is in the positive X-axis. At 2184.6MHz the pattern is almost isotropic.

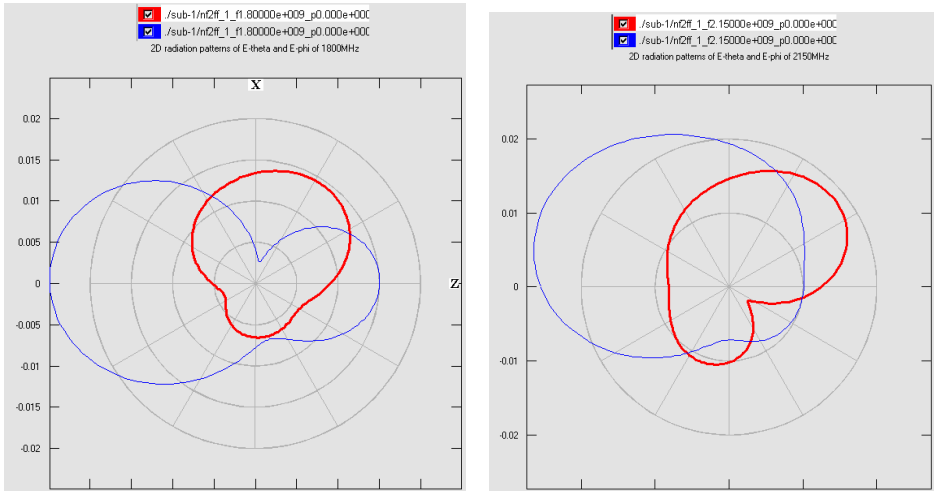

(i) (ii)

Fig 4.9d (i)&(iii), (ii)&(iv) are the 2D and 3D radiation patterns of 1807.69MHz, 2184.6MHz, respectively

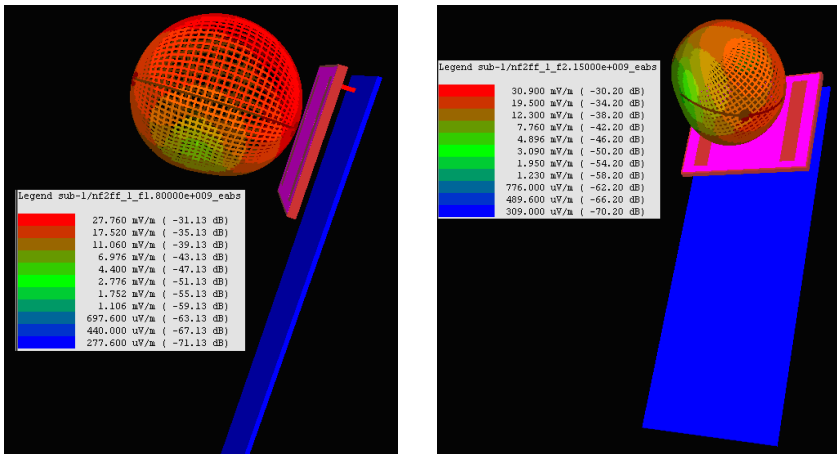

(iii) (iv)

Fig 4.9d (… Continued)

Remark: Compared to the aperture coupled feed slot loaded patch antenna this antenna structure is better to be implemented as it needs only one substrate layer.

I. Notch Loaded Patch Antenna

A square patch of side 3.5cm is considered. The feed is just on the diagonal so that we can get a dual band operation. A notch of depth 1.15cm is taken. The notch depth controls the difference between the resonant frequencies. It also controls the performance at each resonance frequency. Increasing the depth (decreasing the patch size) detunes the lower frequency and decreasing the depth (increasing the patch size) detunes the higher frequency. This in agreement with the theory. The substrate and the casing have $\varepsilon_r = 2.2 \, and \, \varepsilon_r = 4.67$, respectively. A shorting plate and an LP port is used.

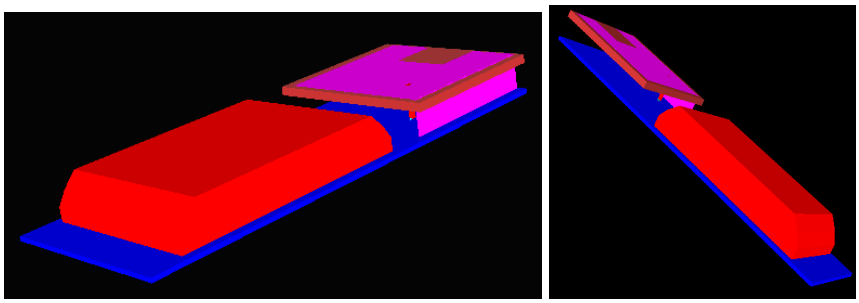

Fig 4.10 Structure of notch loaded patch antenna

Results:

(a) Incident and reflected wave forms:

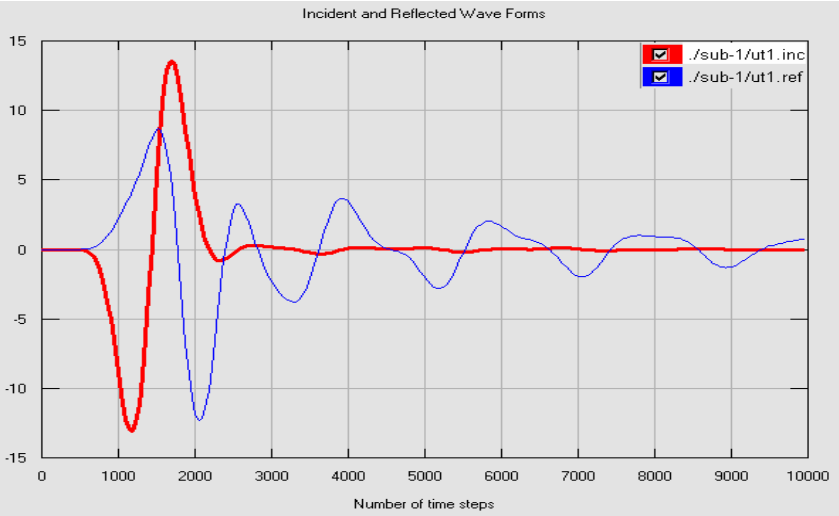

Fig 4.10a Incident and reflected wave forms at the input port

(b) Returnloss: The resonance frequencies are around GSM900 and GSM1900 whose $|RL|$ are 9dB and 8.7dB, respectively.

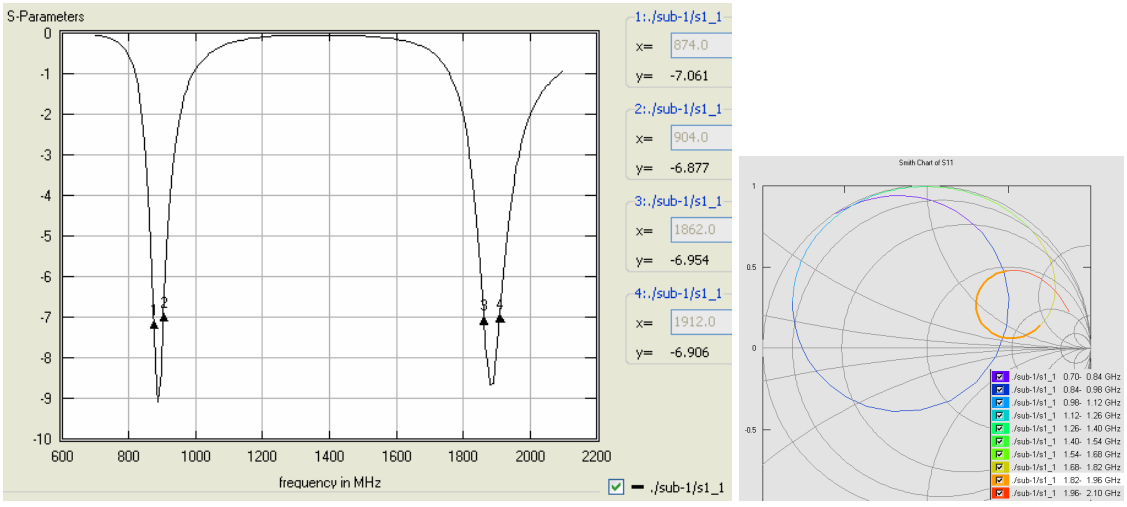

(i) (ii)

Fig 4.10b (i) Returnloss graph and (ii) Smith Chart of the returnloss curve

(c) Band width and Impedance BW: The BWs measured for $RL \leq -7dB$ are 30MHz (874-904MHz) around GSM900 and 50MHz (1812-1962MHz) around GSM1900. For both bands the impedance BW is zero.

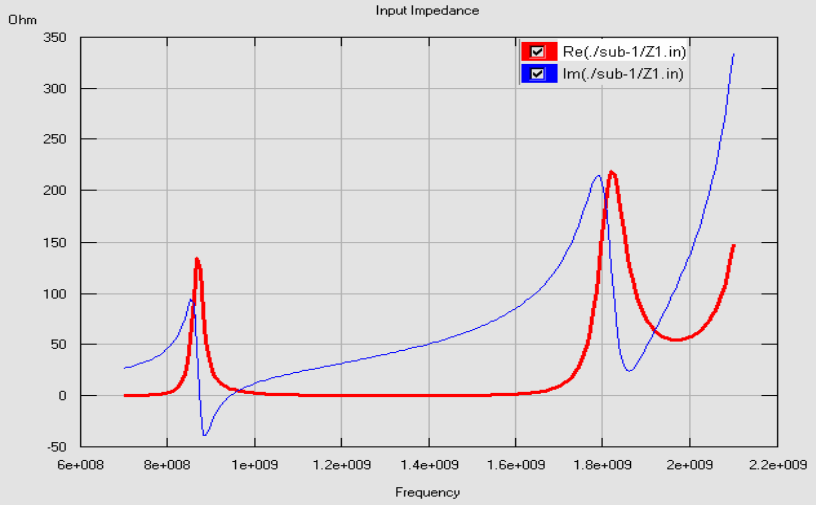

Fig 4.10c Input impedance curve (dark is real and light is imaginary part)

(d) Radiation pattern: At 900MHz the pattern is omnidirectional and resembles that of a half-wave dipole and the pattern maximum aligns itself with the X-axis. At 1900Mhz the pattern is somehow directive and the pattern maximum deviates slightly from the positive X-axis to the positive Z-axis.

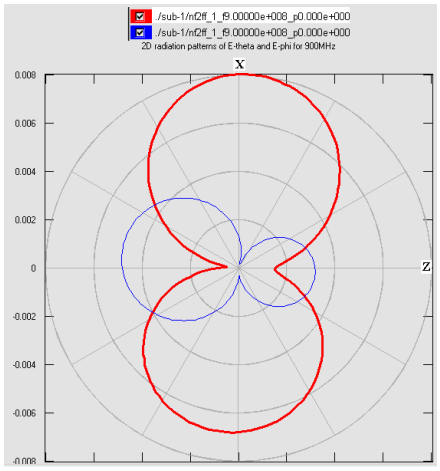

(i)

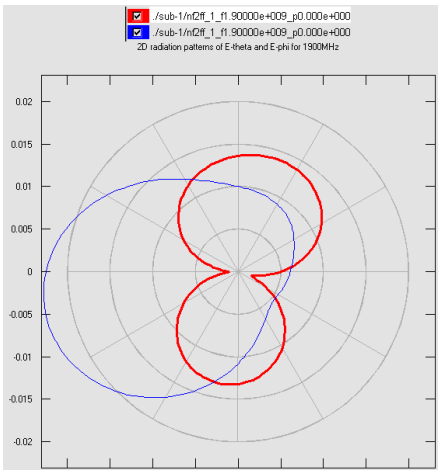

(ii)

Fig 4.10d (i)&(iii), (ii)&(iv) are the 2D and 3D radiation patterns at 900MHz, 1900MHz, respectively.

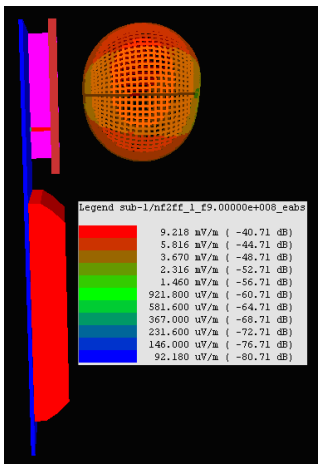

(iii)

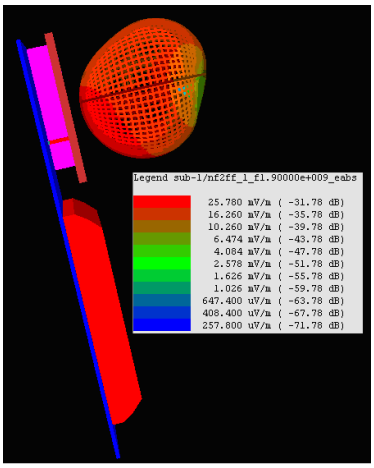

(iv)

Remark: This antenna structure is not complex and is easy to implement. But one difficulty is that there is no good theoretical prediction of the resonance frequencies and there are deformations on the radiation patterns.

J. Patches Loaded With Adjustable Air Gaps

A rectangular patch antenna $39cmx29cm$ is used. A 3.3cm air gap is considered. The separation of the resonant frequencies can be nearly zero without an upper limit. The substrate and the casing have $\varepsilon_r = 2.2 and\ \varepsilon_r = 6$, respectively. A shorting plate and an LP port are used.

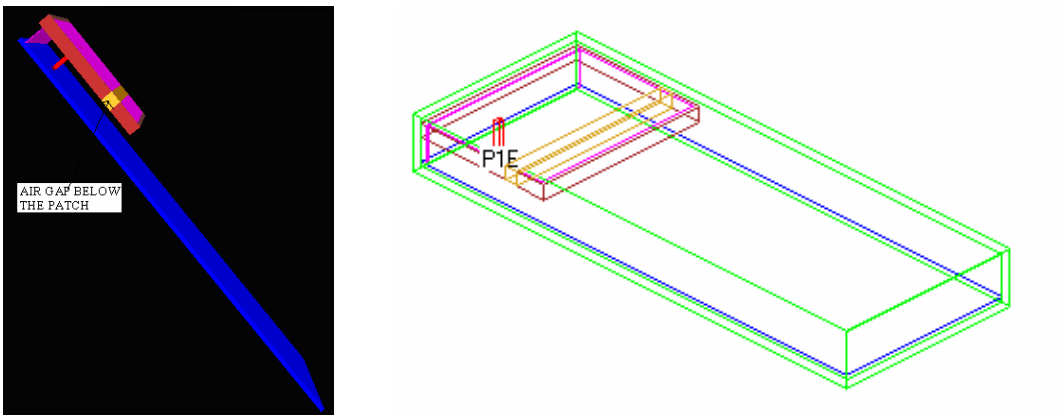

Fig 4.11 Structure of a patch loaded with adjustable air gap

Results:

(a) Incident and reflected wave forms

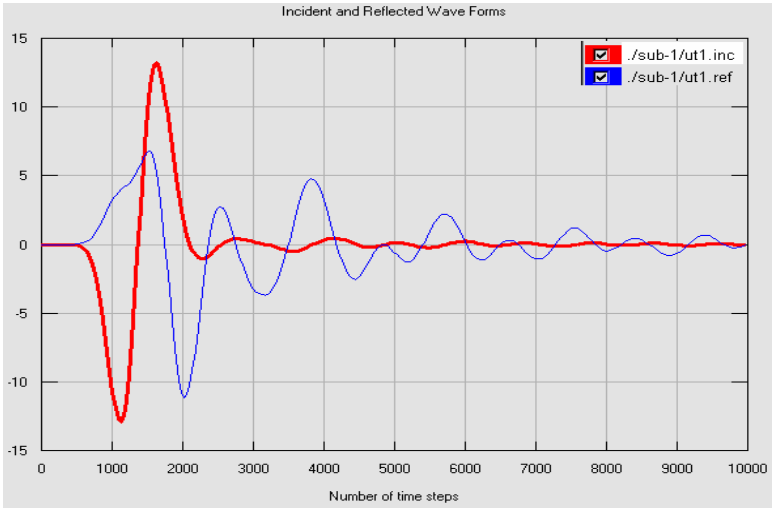

Fig 4.11a Incident and reflected wave form at the input port

(b) Returnloss: The resonant frequencies are around GSM900 and GSM1800 where the $|RL|$ is 14.6dB and 16.7dB, respectively. The graph of RL in dB and on a Smith Chart is shown below.

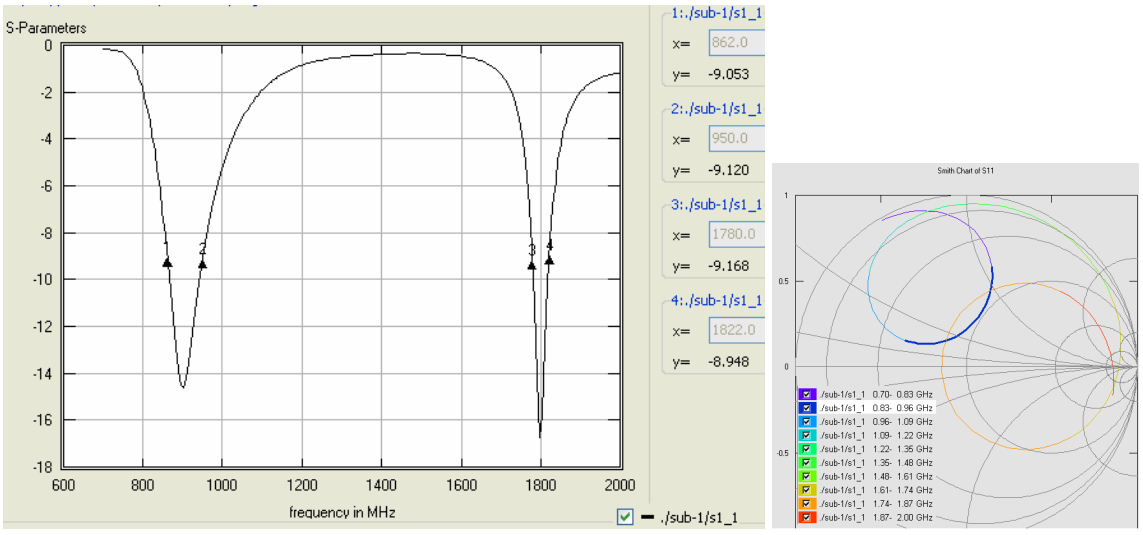

(i) (ii)

Fig 4.11b (i) Returnloss graph and (ii) Smith Chart of the returnloss curve

(c) Band width and impedance BW: The antenna is well matched at its input as in both bands $RL \leq -9dB$ at the resonant frequencies. Thus the impedance BW are 60MHz (890-950MHz) around GSM900 and 42MHz (1780-1822MHz) around GSM1800.

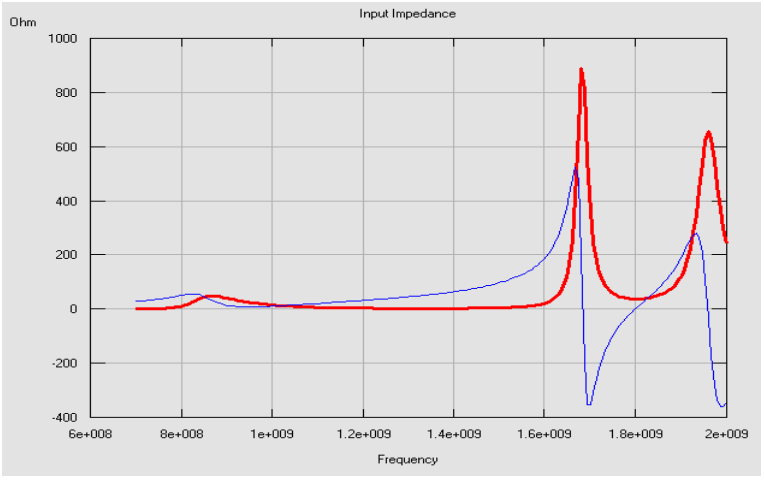

Fig 4.11c Input impedance curve (dark is real and light is imaginary part)

(d) Radiation pattern: At 900MHz the pattern is omndirectional and resembles that of the half-wave dipole. At 1800MHz the pattern is somehow directive whose maximum pattern lies along the negative Z-axis and complex.

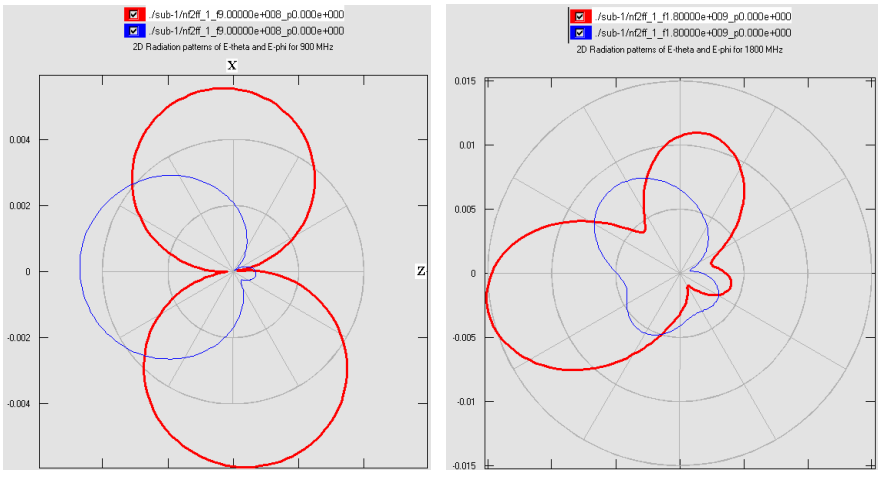

(i) (ii)

Fig 4.11d (i)&(iii), (ii)&(iv) are the 2D and 3D radiation patterns at 900MHz, 1800MHz, respectively.

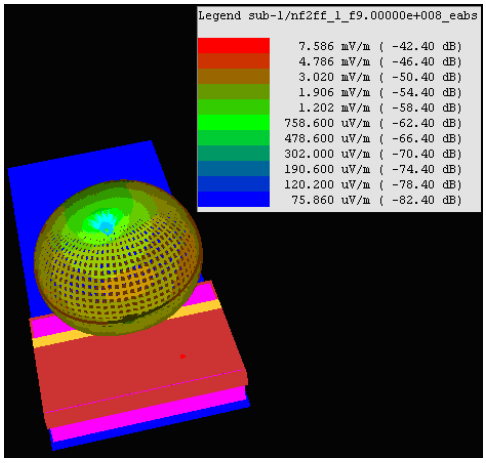

(iii)

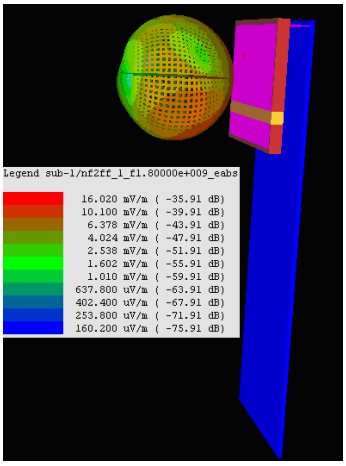

(iv)

Fig 4.11 (… Continued)

Remark: The antenna structure is simple, single layered and easy to implement. Like the the patch antenna loaded with shorting pins it is well matched at its input around the resonance frequencies. And also the radiation patterns are not affected by the shifting of the air gap.

4.3 Discussion

It can be seen from the simulation output that for all antenna structures put in to consideration the BW (impedance BW), the radiation pattern and the returnloss can be inferred so that one can measure the performance of the specific antenna relative to the standard performance of an antenna within the given band (GSM,DCS,PCS,IMT or Bluetooth bands). In the design, simulation and performance comparison of the above ten antennas one challenge in the design process is not put into consideration, material challenge (form factor). If a designer needs his integrated mobile phone to have good aesthetic value, he has to withstand this challenge. That is, different form factors have different requirements on antenna shape and placement. I took a probe fed planar dualband patch antenna in different forms (by varying only the shape of the casing): standard monoblock form and rectangular form, as shown if fig 4.12.

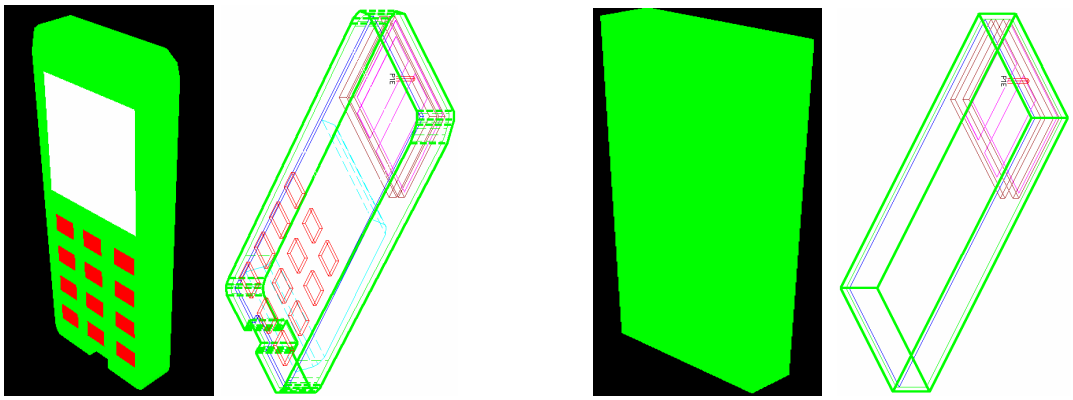

(a) (b)

Fig 4.12 (a) Standard monoblock form and (b) Rectangular form

The same antenna structure is used for both cases. But due the difference in their form factors they have slightly different outputs intheir S_{11} (which determines their BW, bands of operation, radiation pattern etc..).

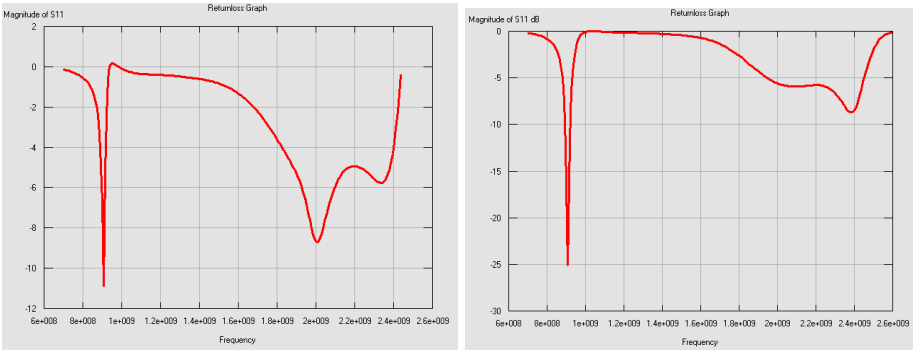

(a) (b)

Fig 4.13 Returnloss of the (a) monoblock form (b) recatangular form

For $RL \leq -5dB$ the standard monoblock operates around GSM900 and IMT2000 but the rectangular form operates around GSM900,IMT2000 and Bluetooth bands.

This chapter presented a review of the different approaches that have been used to produce dual band response. Irrespective of the disadvantages (complexity of the integrated structure and fabrication process incase of multiresonator antennas) all the antennas designed, simulated and analyzed above can be put in to practice depending on their performance.

CHAPTER 5

CONCLUSIONS AND FUTURE WORKS

5.1 CONCLUSIONS AND RECOMMENDATIONS

In this thesis work different dualband patch antennas for mobile phones are designed, simulated and their performance is compared with the regulatory standard performance measurements. From the results it can be seen that for an antenna to operate at dual frequencies (or more) the parameters that play vital role are: the number of layers (along with the shape of the patches and number of ports or feeds), the materials to be loaded (pins, notches, airgaps, stubs and slots), the dimension of the patch(s), the position of the feed(s), the relative permittivity of the substrate, the relative permittivity of the casing, the form factor and placement of the antenna.

One of the difficulty in the simulation process was getting the exact location of a feed. This is because the exact location (which the designer is convinced with) around some promising region is found by trial and error. This makes the design and simulation process difficult. Another difficulty is that the SAR values of each antenna can not be quantitatively measured here as it is done practically with another laboratory set up.

After withstanding the above difficulties it is possible to see that patch loaded with adjustable air gap (controllable $0.33cm$ air gap) and pin loaded patch antenna have better performance compared to the rests as their performance measures are close to thr regulatory standards in all bands. The reflected power for both antennas is 12.25%, $|\Gamma|^2 x100\%$ and the transmitted power is 87.75%, $|T|^2 x100\%$,i.e, $VSWR \leq 2$. And also the antennas are suitable for integrated mobile phone since their structures are simle and single layered. The table below shows the perdentage reflected and transmitted power at each antenna. The value of $VSWR$ for the given antenna is measured for RL where all the bands of operations exist.

Antenna	$RL(dB)\left(=20\log\lvert\Gamma\rvert\right)$	$VSWR\left(=\frac{1+\lvert\Gamma\rvert}{1-\lvert\Gamma\rvert}\right)$	$\lvert\Gamma\rvert^2 x100\%$	$\lvert T\rvert^2 x100\%$
A	<-7	2.64	19.95	80.05
B	<-4.5	4.41	39.69	60.31
C	<-5	3.55	31.36	68.64
D	<-5.5	3.26	28.09	71.91
E	<-5	3.55	31.36	68.64
F	<-9	2.08	12.25	87.75
G	<-7	2.64	19.95	80.05
H	<-7	2.64	19.95	80.05
I	<-7	2.64	19.95	80.05
J	<-9	2.08	12.25	87.75

In conclusion, this thesis had met the objective of investigation of performance different dual band patch antennas for mobile phones. Since a significant amount of work had been accomplished, it provided a sense of achievement despite the fact that there are still important areas that reqire further work.

5.2 RECOMMENDATIONS FOR FUTURE WORKS

These include:

1. Now a days the mobile phones are sophisticated and highly miniaturized. This is the direct consequence of the antenna's efficiency and size. This shows further research work is required to compromise the antenna size with the size of an integrated mobile phone.
2. Doing the prototype of each antenna simulated and measuring their SAR levels.
3. Examining each antenna to meet the regulatory standard SAR level.
4. Broadbanding those simulated antennas which are having narrow bands.
5. Investigating performance of arrays of different kinds of dual band patch antennas for mobile phones.
6. Investigating performance of the patch antennas by varrying their feeds.
7. Since the use of vertical loading, the alignment of stacked elements and using multiple resonators complicates fabrication and designing process and also adjustable air gaps at high frequency are too difficult to control and use of stubs to the overall antenna size, then there is need for a new antenna configuration which is small, easy to design and fabricate, and for which an accurate theoretical prediction of the final resonance frequency can be made. Most importantly, it should be easy to integrate with passive and active devices, i.e. compatible with MIC and MMIC technology.

References

[1] Balanis, C.A., Antenna Theory: Analysis and Design, John Wiley & Sons, Inc,.1997.

[2] C. A. Balanis, Advanced Engineering Electromagnetics. New York: John Wiley and Sons, 1989.

[3] Kumar, G. and Ray, K.P., Broadband Microstrip Antennas, Artech House, Inc, 2003.

[4] D. M. Pozar, "A Microstrip Antenna Aperture Coupled to a Microstrip Line", Electronics Letters, Vol. 21, pp. 49-50, January 17, 1985.

[5] Garg, R., Bhartia, P., Bahl, I., Ittipiboon, A., Microstrip Antenna Design Handbook, Artech House, Inc, 2001.

[6] Stutzman, W.L. and Thiele, G.A., Antenna Theory and Design, John Wiley & Sons, Inc, 1998.

[7] Qian, Y., et al., "A Microstrip Patch Antenna using novel photonic bandgap structures", Microwave J., Vol 42, Jan 1999, pp. 66-76.

[8] JR James & P S Hall, Handbook of Microstrip Antennas, Peter Peregrinus Ltd.,1989.

[9] K. R. Carver and J. W. Mink, "Microstrip Antenna Technology," IEEE Transactions on Antennas and Propagation, Vol. 29, No. 1, pp. 2-24, January 1981.

[10] A. Reineix and B. Jecko, "Analysis of Microstrip Patch Antennas Using Finite Difference Time Domain Method," IEEE Transactions on Antennas and

Propagation, Vol. 37, No. 11, pp. 1361-1369, November 1989.

[11] P. A. Tirkas and C. A. Balanis, “Finite-Difference Time-Domain Method for Antenna Radiation,” IEEE Transactions on Antennas and Propagation, Vol. 40, No. 3, pp. 334-340, March 1992.

[12] G.F. Pedersen and J. Bach Andersen, "Integrated antennas for hand-held telephones with low absorption", IEEE Vehicular Technology Conf., pp. 1537-1540, Mar. 1994

[13] "Jumping on the band wagon", Mobile Europe, vol. 9, No. 3, Mar. 1999, pp. 31-32.

[14] M. Martínez-Vázquez, M. Geissler, D. Heberling and D. Sánchez-Hernández,"Recent developments in antenna design for personal communications handsets at the IMST", COST 260 Meeting on Smart Antennas, Rennes, Oct. 2000.

[15] CHANG, E., LONG, S. A., and RICHARDS, W.F.: 'Experimental investigations of electrically thick rectangular microstrip antennas', IEEE Trans, 1986, AP-34,(6).

[16] KUMAR G., and GUPTA, K. C.: 'Non-radiating edge and four edges gap coupled multiple resonator broad band microstrip antennas', IEEE Trans, 1985, AP-33, pp. 173-177.

[17] SCHAUBERT, D. H., FARRAR, F. G., SMDORIS, A., and HAYES, S. T.: 'Microstrip Antennas with Frequency Agility and Polarization Diversity', IEEE Trans., AP=29, No. 1, Jan 1981, pp. 118-123.

[18] LONG, S. A., and WALTON, M. D.:'A Dual-Frequency Stacked Circular-Disc Antenna', IEEE Trans., AP=27, No.2, March 1979, pp. 270-273.

[19] BENNEGUEEOUCHE, J., DAMMO, J.P., and PAPIERNIK, A.: 'Original multilayer microstrip disc antenna dual frequency band operation theory and experiment', IEE Proc. H, vol= I40 No.6. Dec 1993, pp. 441-445.

[20] LEE. R. Q., LEE, K.F., and BOBINCHAK, J.:' Characteristics of a two-layer electromagnetically coupled rectangular patch antenna ', Electron. Lett., 23,(20), 1987, pp. 1070-1072.

[21] LEE, R. Q.. and LEE, K.F.:' Gain enhancement of microstrip antennas with overlaying parasitic directors ', Electron. Lett.,24, (11), 1988, pp. 656-658.

[22] DAMIANO, J.P., BEMVEGUEOUCHE, J., and PAPIERNLK, A.:' Study of multilayer microstrip antennas with radiating elements of various geometry', IEE Proc. Vol=137, pt.H, No.3, June 1990, pp. 163- 170.

[23] BHATNAGAR., P. S., DANIEL, J.P., MAHDJOUBI, K., and TERRET, C.: 'Experimental study on stacked triangular microstrip antennas'. Electron. Lett.. 22, (16), 1986, pp. 864-865.

[24] BHATNAGAR., P. S., DANIEL, J.P., MAHDJOUBI, K., and TERRET, C.:' Displaced mutilayer triangular elements widen antenna bandwidth ', Electron. Lett., 24, (15), 1988, pp. 962-964.

[25] LEE, C. S., NALBANDIAN, V , and SCHWERMG, F.: 'Planar Dual-Band Microstrip Antenna', IEEE Trans., Ap=43, No.8, August 1995, pp. 892-897.

[26] CROQ, F., and POZAR, D. M.: 'Multifrequency Operation of Microstrip Antennas Using Aperture Coupled Paralle1 Resonators', IEEE Trans., AP=40, No. 11, Nov. 1992, pp. 1367- 1374.

[27] YAZIDI, M. E., HIMDI, M., and DANIEL, J. P.: 'Aperture coupled microstrip antenna for dual frequency operation', Electronics letters, Vol. 29 No. 17, August 1993, pp. 1506-1508.

[28] MACI, S., GENTILI, G. Bq PIAZZESI, P., and SALAVADOR, C.: 'Dual-band slot-loaded patch antenna', IEE Proc.. Microw. A&P, Vol 142, No.3, June 1995, pp. 225-232.

[29] ZHONG, S. S., and LO, Y. T..: 'Single Element Rectangular Microstrip Antenna For Dual Frequency Operation', Electronics Letters, Vol. 19, No. 19, April l983,pp. 298-300.

[30] RICHARDS, W. F.,and DAVIDSON, S. E.: 'Dual-Band Reactively Loaded Microstrip Antenna', IEEE Trans., AP=33, NO,5, May 1985, pp. 556-561.

[31] WANG, B. F., and LO, Y. T.: 'Microstrip Antennas for Dual Frequency Operation', IEEE Trans., AP=32, No.9, Sept. 1984, pp. 938-943

[32] SANCHEZ-HEWANDEZ, D. and ROBERTSON, D.I.: ' Triple band rnicrostrip parch antenna using a spur-line filter and a perturbation segment technique ', Electron. Lett., 29, (17),Aug. 1993, pp. 1565-1566

[33] AKANO, H., and VICKIEN, K.,: 'Dual-frequency Square Patch Antenna With Rectangular Notch', Electronics Letters, Vo1.25, No.6, August 1989, pp. 1067-1068.

[34] LEE, C. S., and NALBANDIAN, V.: 'Impedance Matching of a Dual-Frequency Microstrip Antenna with an Air Gap', IEEE Trans., AP=41, NO.5, May. 1993, pp. 680-682

[35] SANCHEZ-HERNANDEZ, D and ROBERTSON, D. I.:' Analysis and design of a dual band circularly polarized micostrip patch antennas', IEEE Trans., Ap=43, No.2, Feb. 1995, pp. 201-205

[36] SANCHEZ-HERNANDEZ,D.,PASSIOPOULOS, G. and ROBERTSON, D.I.:' Single fed dual band circularly polarised microstrip patch antennas', 26th EuMC Progue, Czsch Republic. Sept. 1996, pp. 273-276

[37] SANCHEZ-HERNANDEZ, D., PASSIOPOULOS, G., FERRANDO, M., DE LOS REYES. E., and ROBERTSON, D. 1.:' Dual band circularly polarised microstrip antennas with a single feed', Electron. Lett., 32, (25), Dec. 1996, pp. 2295-2298

[38] SANCHEZ-HERNANDEZ, D., WANG, Q. H., REZAZADEH, A. A., and ROBERTSON, D. I.: ‘ Millimeter wave dual band microstrip patch antennas using multilayer GaAs technology ', IEEE Trans., MTT=44, No. 9, Sept. 1996, pp. 1590-1593

[39] K. Hirisawa and M. Haneishi, Analysis, Design, and Measurement of small and Low-Profile Antennas, Artech House, Boston: 1992.

[40] IEEE Transactions on Antenna And Propagation, September 2005 Vol 53, No. 9 page 2812.

[41] EMPIRE (IMST GmbH)

[42] Jean-Francois Zurcher and Fred E.Gardiol: “Broad Band Patch Antennas”, Artech House Boston . London.

[43] David M.Pozar: “Microwave Enginnering”, 3ed, John Wiley & Sons, Inc., 2005.